Part VII
OBSERVING THE UNIVERSE
B. Jones

Observing the Universe

Bernard J.T. Jones
Theoretical Astrophysics Center (TAC)
and
Niels Bohr Institute,
Blegdamsvej 17, Copenhagen, Denmark
BJONES@NBIVAX.NBI.DK

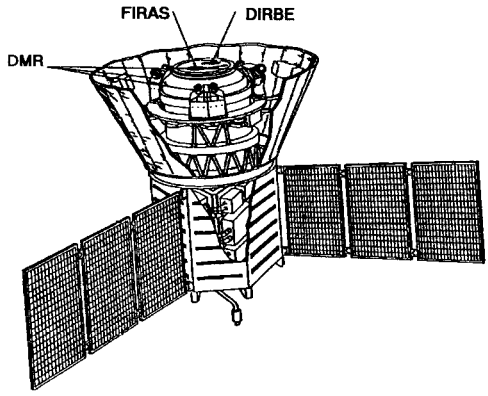

Figure 1: *The COBE satellite and its 3 experiments after Boggess et al., 1994).*

In the beginning of time there was nothing:
Neither sand, nor sea, nor cooling surf;
There was no Earth, nor upper heaven,
No blade of grass - Only the Great Void.

Völuspá (The Sybil's Prophecy)
(Icelandic Eddic Poem)

[0]Proceedings of the VII Brazilian Summer School of Cosmology and Gravitation (Rio de Janeiro, August 1993)

Summary

In this series of lectures I adopt the point of view that we make observations in order to map the structure of the Universe, rather than simply to determine its size, age and density. Since the discovery of the Cosmic Relict Radiation in 1965 and the establishment of the Hot Big Bang Theory, theorists have been building models for the origin and evolution of cosmic structure on scales from galaxies to the largest superclusters of galaxies and beyond. We are now in a position to confront those models with observation and it is this I wish to discuss.

The ability to tackle these issues observationally has come as a consequence of key developments in instrumentation, the establishment of numerous 4-meter class telescopes and the launching of key satellite-borne experiments like IRAS, COBE and now the Hubble Space Telescope. This has resulted in an abundance of data probing to enormous distances and looking back to very early times. The question is what to make of it all.

We are helped in this task by the ability to run ever more powerful computer simulations of the evolving Universe. This in turn opens up new avenues of research, which in turn stimulates more observational projects. It is this aspect of the subject that I wish to present: what do we expect on the basis of our models and how do we go about measuring it?

Observational Cosmology is no longer simply a search for two numbers that will fix the size and age of the Universe. Cosmology is today one of the fastest expanding branches of physics with a future that can look well into the next century. It is my hope that these lectures will show that while we have made substantial progress in our understanding of cosmic structure, there is still a long way to go and there are many exciting discoveries ahead.

1 Introduction

1.1 The Scope of the Present Review

Since the discovery of the cosmic microwave background radiation in 1965, Cosmology has become a major branch of physics in its own right. The issues that were

discussed prior to that time are no less interesting now than they were then, but the focus of the subject has changed considerably during the past three decades. We are, of course, still interested in describing the parameters of the cosmological models derived from Einstein's theory of General Relativity that best fit the Universe as a whole. But while these parameters (the "deceleration parameter", the "cosmological constant", and so on) are important, the focus of attention has moved towards understanding the details of the *structure* that is found in the Universe on various scales.

This structure manifests itself in the form of galaxies, clusters of galaxies and still larger aggregations of luminous material. The last 40 years have seen tremendous progress in acquiring data about these structures. This data comes from all wavebands, from the radio to the X- ray regions of the electromagnetic spectrum. When all this data is put together we get a remarkably coherent view of the evolution of our Universe. It is this view that I wish to describe in this article.

It is perhaps true to say that contemporary Cosmology is driven by observational data rather than by theories, as in the past. Today we have the capability of subjecting many theories and ideas to the test of direct observation. However, while Cosmology is today a branch of the physical sciences, it is rather special in that we have only one instance of the Universe to study and we cannot perform experiments on it! We can only build models and compare the results with observations. This means that models for the Universe play a central role in understanding cosmology and interpreting data.

It is impossible to cover all but a part of observational cosmology in a short series of lectures. The choice of the subject matter is biased by my own interest and by the fact that the participants in the school generally have a mathematical physics background, rather than an astronomy background. The lectures lean heavily towards those aspects of observational cosmology that are closely related to theoretical models of the Universe.

1.2 Books, Reviews and Papers

There are now a number of excellent up-to-date texts discussing cosmology, the "Bible" of the subject being Peebles' latest book *Principles of Physical Cosmology* (Peebles, 1993). That book is the 700-page successor to the earlier edition *Physical Cosmology* (Peebles, 1971), which is still worth a read despite its great age. Kolb

and Turner's excellent book, *The Early Universe* (Kolb and Turner, 1990) focuses more on the physics of the earliest phases of the cosmic expansion.

Peebles' *Large Scale Structure of the Universe* (Peebles, 1980) is a more technical treatise focusing on the origin and evolution of large scale cosmic structures and is essential reading for anyone proposing to research this field. The recently published book *Structure Formation in the Universe* by Padmanabhan (1993) is an excellent overview of the subject.

The large number of Summer and Winter Schools that focus on various aspects of cosmology often provide excellent reviews. In particular I would mention *Observational and Physical Cosmology* (Sanchez et al., 1992), *New Insights into the Universe* (Martinez et al., 1992) and the Summer School held in Edinburgh in 1989 *Physics of the Early Universe* (Peacock et al., 1990)).

This is not intended as a Review Article, and so I will not be exhaustive in citing all papers relevant to a given issue; that would make the Bibliography impossibly long and not that useful to a person needing an introduction to the subject. So I have tried to focus on citing early articles to give ideas their appropriate historical credit, and some of the more recent papers through which a reader can get into the literature.

1.3 Abbreviations, Prejudices etc.

Throughout this article I shall use a distance scale corresponding to a present value of the Hubble constant $H_0 = 100h$ km.s^{-1}Mpc^{-1} and the reader can substitute her/his own favourite value for h. I will stick as close to the so-called "standard model" as possible, which means I will have relatively little to say about the infamous yet entirely useful Cosmological Constant.

I shall endeavour to use "Universe" whenever I mean the place where we live, and "universe" for a model of the Universe. Similarly, "the Galaxy" is the "galaxy" where we are situated. I shall try to avoid abbreviations, but the following bits of jargon are frequently encountered and may slip into the text: "CDM" for "Cold Dark Matter", "HDM" for "Hot Dark Matter", "LSSU" for Peebles' book "The Large Scale Structure of the Universe", "MWB" for "Microwave Background" and "CBR" for the "Cosmic Background Radiation". Generally MWB and CBR are used interchangeably, despite the fact that there are many background radiations

that are not in the microwave band (such as the X-ray background, but that would be an "XRB" !). I will studiously avoid "GA" for "Great Attractor". Perhaps the most important abbreviation is "FLRW" for the names Friedmann, Lemaitre, Robertson and Walker - the discoverers of the metric that solves Einstein's Equations and describes the Universe in which we live over most of its history. This is frequently and unfortunately abbreviated to "FRW" or even just "RW".

As a prejudice I will do my best to avoid using General Relativity except where necessary. The standard cosmological model is homogeneous and isotropic and there are perfectly adequate Newtonian analogues which I can use for almost all purposes. General Relativity is essential for deriving results that concern light propagation and there I will confine myself to quoting results without proof, providing motivation wherever possible. Observational astronomy has its own peculiar jargon, the worst aspect of which is perhaps the notion of measuring brightness in magnitudes. There is a short Appendix describing briefly this somewhat idiosyncratic way in which optical astronomers measure the apparent and intrinsic brightness of astronomical objects.

Finally, I have borrowed freely from many of the above mentioned Books and Reviews (including my own) and from the articles that have appeared in the literature.

Chapter 38

A Brief History

The discovery that our Universe is expanding, with the immediate interpretation that the Universe began a finite time in our past, must rank as one of the most startling and profound discoveries ever made. The development of large telescopes in the latter half of the nineteenth century coupled with the technological advances in photography enabled astronomers to look beyond our Solar System, and even beyond our Galaxy. At first, the debate was whether these faint nebulae did or did not lie beyond our own Milky Way. The story of the Shapely-Curtis debate, an interplay between scientific argument and personal prejudice, is beautifully told by Sandage in the *Hubble Atlas of Galaxies* (Sandage, 1961). The great debate took place in 1920, but it was not until 1925 that Hubble settled the issue once and for all (Hubble, 1925). Once it was established that these nebulae were extragalactic, and were probably at enormous hitherto uncontemplated distances, the way was opened up to probe the motions of the galaxies and so to map out the Universe.

1 Cosmic Expansion

The first published list of galaxy redshifts was that of Slipher (1915). Most of the velocities in the list were large and positive and this led astronomers of the time to add a so-called "K-term" to the solution for the motion of the Sun relative to distant stars and nebulae. Remember, at that time astronomers were not even sure whether these objects were extragalactic, so it would have been difficult to reach any profound conclusions.

Slipher expanded the list and the extended data set of 41 velocities was published by Eddington in §70 of his book *Mathematical Theory of Relativity* (Eddington, 1925). It is certainly significant that this section of Eddington's book is on "de Sitter's Spherical World", since this reflects the general scientific reaction to this data set. If these objects were to be outside our Galaxy, this was at the time the only available explanation of the recession phenomenon.[1] Eddington noted in his text the preponderance of positive (receding) velocities, but evidently hesitated to draw the correct conclusion. It was in fact Wirth (1922) who first suggested that this K-term might be a function of distance from the sun. Wirth came to this conclusion by noting that the galaxies of smaller diameter tended to have the greater radial velocities. Following up on this, Lundmark (1924) plotted a redshift magnitude diagram for this sample, but found no convincing trend.

By 1925 it was known that the galaxies were systems not unlike our own Galaxy, lying far beyond the limits of our own System. The quest for radial velocities of fainter galaxies was continued by Humason who provided the largest radial velocity known at the time (Humason, 1929). The paper immediately following Humason's in the journal was Hubble's (1929) confirmation of the existence of the a redshift-distance effect that now bears his name. Hubble did not however conclude that the effect was due to a general expansion of the system of galaxies.

Astronomers at the time were still focused on notions of gravitational redshifts or the so-called "de Sitter effect" that had been derived as consequences of Einstein's General Relativity. Hubble was evidently unaware of the solutions of Friedman and Lemaitre and in his 1929 paper attributed the relationship to the "de Sitter effect". In the year before Hubble's "discovery", Robertson (1928) had already suggested that this was in fact a redshift-distance relationship and had provided a theoretical explanation for the phenomenon. We would certainly be justified in calling the relationship "Robertson's Law". Humason (1931) pushed the redshift-magnitude relation to far greater depths, but it was not until the famous paper of Humason (1936) that the relationship was referred to as the Hubble Diagram.[2]

Taken with Hubble's earlier realization that the Universe was homoge-

[1]It is perhaps surprising that nobody seems to have suggested that the expansion might be the result of a vast Galactic Explosion in the recent past. Much later, in the 1960's, the Quasars were found to have very large redshifts. This gave rise to the *redshift controversy* in which one suggestion for the origin of the large Quasar redshifts was a vast Galactic Explosion.

[2]The discussion about whether redshifts were indeed of cosmological origin raged on into the early 1970's. Although few today doubt the interpretation in terms of cosmic expansion it is nevertheless important to find observational evidence for this notion. See section 5.

nous and isotropic on the largest scales his telescopes could probe, this led to the logical conclusion that the Universe was "born" only a finite time in our past. This must rank as one of the most dramatic conclusions in the history of science.

It was so startling a discovery that there was some reticence in embracing it within the framework of modern physics, and indeed several theories were put forward to avoid this "natural" conclusion. The argument that ensued was a remarkable battle between two theories: the "Big Bang Theory" which expressed a creationist view of the Universe and the "Steady State theory" which denied that view by postulating that matter was continually being created in the space between the galaxies.

As more data was acquired, evidence was presented supporting first one side and then the other. The tendency was certainly for the data to support increasingly the creationist view that the Universe did begin a finite time in our past, but it was not until 1965 that the issue was finally resolved beyond all possible doubt with the discovery by Penzias and Wilson of the radiation left over from the birth of the Universe: the Cosmic Microwave background Radiation.

In order to appreciate fully the role played by observational astronomy in this quest for understanding, it is worthwhile recalling a few highlights of that debate.

2 Big Bang vs. Steady State

Only fifty years ago we saw the Universe only through the visible light radiated by the stars in galaxies. By present standards, astronomers then saw only a small neighbourhood of the Universe, yet they were able to discover the cosmic expansion and establish models of the Universe in terms of Einstein's Theory of Relativity. The Universe looked homogeneous and isotropic on the very largest scales, and seemed to conform to some models formulated earlier by Friedmann and by Lemaitre.

The fact of the cosmic expansion led to the natural conclusion that the Universe began a finite time in our past - the Universe began with a "Big Bang". A number of cosmologists finding this philosophically displeasing put forward alternatives that sought to avoid this singularity. There were attempts to avoid the

singularity both within the context of Einstein's theory[3], and by suitably modifying the theory. Among the latter approaches was the significant "Steady State" theory of Hoyle (1948) and Bondi and Gold (1948).

The Steady State theory avoided the singularity by postulating creation of matter at just the right rate to compensate the decrease in the density of the Universe due to the expansion. The theory thus substituted continuous creation (by some unexplained process) for instantaneous creation (by an equally unexplained process). The beauty of the Steady State theory was that it required that the Universe looked the same from all places and at all times. The theory also made specific predictions about the relationship between the steady state expansion rate and the amount of material in the Universe.

These two divergent views of the Universe polarised the cosmological and philosophical communities and it was not until the early 1950's that observational data was brought to bear on deciding the issue. Whereas the galaxy data in the optical wavebands could offer no strong reason to support either view, it was the data from the new radio telescopes that provided the hint that the Steady State theory faced a serious problem. This new data, taken at face value, was claimed to show that distant radio sources were more numerous than nearby ones. The Universe could thus not be in a steady state.

The interpretation of the radio source counts was a controversy that raged for over a decade. The issue was still being argued when in the early 1960's distant objects known as "quasars"(QSO's for short) were first identified. These were the most distant objects known at that time and as more of these were discovered it became evident that they too seemed to be more numerous in the past. However, QSO's were a mystery - it was entirely conceivable at that time that the radial velocities of these objects did not reflect their true distances and so their discovery was not a decisive factor in establishing the Big Bang theory as the most likely model describing the Universe.

The breakthrough came in 1965 with the announcement by Penzias and Wilson (1965) of the discovery of a Cosmic Microwave Background Radiation field which was interpreted by Dicke, Peebles, Roll and Wilkinson (1965) as being the relict radiation left over from the Big Bang.

At that point in time, all argument stopped. The hot Big Bang the-

[3]We now know that all solutions of the classical Einstein equations for cosmological models containing "physical" matter have a singularity

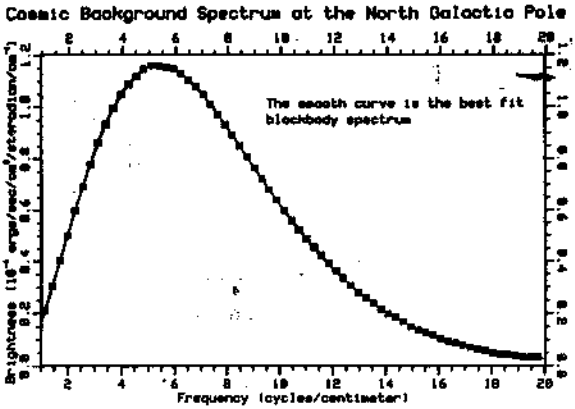

Figure 1: *The spectrum of the Cosmic Microwave Background Radiation based on only 9 minutes of data. The points are the actual measurements.*

ory had been experimentally established as the correct interpretation of the cosmic expansion discovered 30 years earlier by Hubble. Today, no serious cosmologist would doubt this interpretation. Cosmology made the transition from philosophy to become one of the paradigms of modern physics. Physical Cosmology was born.

3 The Renaissance in Cosmology

The discovery by Penzias and Wilson in 1965 of the relict radiation marked a turning point in Cosmology as a branch of the physical sciences. Not only did it establish once and for all that the Universe did begin with a hot big bang, but it has in addition provided a mechanism for probing those earlier moments of cosmic history which otherwise would have been inaccessible to observation. The Cosmic Microwave Background carries information to us from a time when the Universe was merely a million years of age. Its accurate Planckian Spectrum (see figure 1)) and large scale isotropy establishes the notion that the Universe was in the past very closely homogeneous and isotropic, and that the Universe had a hot singular origin. We shall see that there is currently no viable alternative explanation other than that this is the left over radiation from a hot big bang.

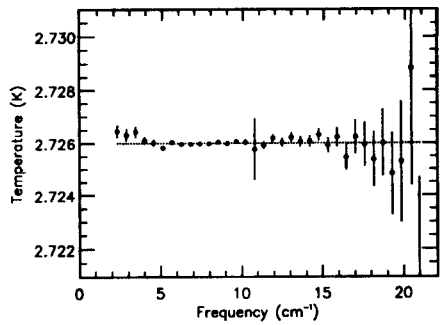

Figure 2: *FIRAS measurement of Cosmic Microwave Background Temperature. This yields a temperature of* 2.736 ± 0.010 *(from Mather et al., 1993)*

The COBE satellite was launched on November 18th., 1989 into an almost polar Earth orbit with an altitude of some 900 km. It carried on board several experiments working at far infrared and microwave wavelengths, these experiments were labelled "DMR", "FIRAS" and "DIRBE". These abbreviations stand for *Differential Microwave Radiometer*, *Far InfraRed Absolute Spectrophotometer* and *Diffuse InfraRed Background Experiment*.

The temperature of the Cosmic Microwave Background Radiation has now been determined very accurately by the FIRAS experiment on board the COBE space craft. Figure 2 shows temperatures measured at various frequencies by FIRAS. The best fit temperature for the FIRAS data is (Mather et al., 1994)

$$T = 2.736 \pm 0.010 \quad 95\% \text{ confidence level} \tag{1}$$

This is one probably the most accurately determined number in cosmology today. Whereas we do not know the cosmic mass density to within a factor of 10, we do know the radiation field density to a fraction of a percent!

COBE's other great achievement was to detect for the first time very small amplitude anisotropies in the angular distribution of the microwave background radiation temperature. The anisotropies detected revealed the existence of structures on very large scale - on the order of a gigaparsec - at a time when the Universe was a mere million years old. The discovery of these fluctuations with

approximately the expected amplitude is remarkable confirmation both of our underlying cosmological model and the idea we have to explain the origin of cosmic structures.

Chapter 39

Cosmology - a quick overview

1 Looking into the distance is looking into the past

The finite speed of light means that as we look to ever greater distances, we are also looking further into the past. This phenomenon allows us direct access to the past history of the Universe and so allows us to test directly hypotheses about the evolution of cosmic structure. With large optical telescopes we can see back to the time when galaxies and clusters of galaxies were forming, and with microwave detectors we can see back to a time long before that when the Universe was almost homogeneous.

The present age of the Universe is thought to be somewhere in the range 10-20 billions years. Galaxies formed when the universe was only a few billion years old, and the microwave receivers are seeing back to a time when the Universe was merely a few million years old. We have direct evidence for the nature of the Universe over a considerable fraction of its history.

There is another important phenomenon that is associated with the fact that we are looking into the past: this is the "red shift" of the light from distant objects. Historically, it was noticed that the spectral lines in the spectra of the more distant galaxies were shifted towards longer wavelengths relative to the same lines in the spectra of their nearer counterparts. The redshift was interpreted by Hubble as being due to the Doppler Shift and he concluded from his data that the more

distant objects were receding from us at greater speeds than the nearby ones, thus giving rise to a greater red-ward shift of the spectral lines.

An astronomer observing a spectral line having a wavelength λ_0 in the laboratory would observe the same line in the spectrum of a distant galaxy at a wavelength λ_{obs}. The "redshift" z of the galaxy is then defined as

$$z = \frac{\lambda_{obs}}{\lambda_0} - 1. \tag{1}$$

For small z ($z \ll 1$) this is interpreted as being due a recession velocity

$$V = cz \tag{2}$$

and Hubble's observation that the more distant galaxies displayed the greater redshifts is expressed as

$$V = cz = H_0 D \tag{3}$$

where D is the distance to the galaxy. The constant of proportionality H_0 measures the local expansion rate of the universe.

H_0 is called the "Hubble Constant" and is traditionally measured in units of $\mathrm{km.\,s^{-1}Mpc^{-1}}$ since distances are measured in Megaparsecs and velocities are measured in kilometres per second. This is not a particularly convenient unit of measurement, it is more useful to give the inverse Hubble constant, H_0^{-1}, in units of time. For small z, the "look-back time" is approximately $t_{lookback} \approx z/H_0$.

2 The Universe was more Homogeneous in the Past

Today, the Universe we see is homogenous and isotropic on the largest scales, but is far from homogenous on scales smaller that clusters of galaxies. We have direct evidence for this from observations of the distribution of galaxies to the limits that our telescopes can see, and more recently from observations of the microwave background radiation which tell us what the Universe was like on large scales when it was only a million years old.

We can see and study galaxies out to a redshift of 0.5 - 1.0, which represents a substantial fraction of the past history of the Universe. Over that lookback time, the distribution of galaxies in the Universe is certainly no more lumpy than it is today, and the evidence is that it was in fact less lumpy.

We can see quasars to much greater distances than galaxies and they do not seem to be strongly clustered. However, they do not provide unambiguous evidence for the large scale homogeneity of the Universe since we do not really know how these objects are related to galaxies or clusters of galaxies.

On the basis of our understanding of the origin of the light elements we know that the Universe was probably homogeneous on very small scales at the time when these elements were formed: a few minutes after the big bang. Of course this is a model dependent statement and it is conceivable that we might be able to construct inhomogeneous models that produce the correct element abundances.

3 Cosmological Models

It is thought that for most of its history the evolution of the universe has been controlled by the force of gravity. This means that models for the evolution of the Universe are to be found among the solutions to the Einstein Field equations. Observation indicates that over most of its lifetime the Universe has been homogeneous and isotropic on the largest scales, and thus it is to be expected that the class of homogeneous and isotropic solutions of the Einstein Equations discovered by Friedman and Lemaitre provide the appropriate description of the Universe in the large[1].

In order to know which of these Friedman-Lemaitre solutions is the one describing the Universe we live in, we have to know the equation of state describing the material in the Universe. This is a question of cosmic physics that was largely resolved by the discovery of the cosmic microwave background radiation in 1965. This discovery fixes the amount of radiation present in the Universe at present and at all times in the past. Curiously, we do not know the amount of baryonic matter in the Universe - we can only know the amount *luminous* baryonic matter and have to infer the total amount from indirect observations. This is the main uncertainty in fixing the appropriate Friedman-Lemaitre model.

[1]It is interesting to note that there was hardly any observational evidence for homogeneity and isotropy at the time these solutions were proposed!

Can we be sure that we are in fact using the right equations and that we have the correct physics? Could we have made some basic assumption that would invalidate our picture[2] ? Clearly, we can never be certain. It is important to bear in mind that we are seeking the simplest cosmological theories that are consistent with the observed data. It may well be possible to construct quite complex models that agree with what we see, but these would have relatively little aethsetic appeal in the face of a simpler model that does the same thing.

Since we have no other Universe to study other than the one in which we live, can do no more than ask that our models be well motivated by existing physical theories. In this sense we can never be sure that we know the "truth" about our Universe - we can only be assured that we are capable of understanding what we see. If our simple models make predictions that are subsequently verified by observation, then so much the better. So, in a sense, our models for the Universe are supposed to fit the facts and cause us to make further observations to validate the model.

4 The Standard Model

This is not the place to review the details of the evolutionary history of the so-called Standard Model for the Universe. It is however essential to give an overview of the key features of this history in order to see the observations in context. What should be emphasised is that we are no longer talking about evidence for the hot big bang, that is now on such a firm footing that it is hard to imagine any sensible alternative. We are now at the stage of filling in the details: seeking to explain the details of the model by putting forward theories for the evolution of the chemical elements, the formation of galaxies and other phenomena with observable consequences.

In the so-called "Standard Model" the Universe has for all its history been homogeneous and isotropic on the largest scales. The model is therefore described mathematically by one of the simplest exact solutions to the Einstein Equations: the Friedman- Lemaitre Solution.

The evidence of the relict radiation left over from the Big Bang and our understanding of the nucleosynthesis of the light elements tells us that the Universe was hotter in the past than now. We therefore talk of the "Hot Big Bang" theory

[2]We might wonder for example whether magnetic fields could be playing a key role, or more fundamentally, whether there is another long-range force of which we have no knowledge.

for the Universe.

This relict radiation carries information from a time in the past when the Universe was less than a million years old to the present. We see this radiation as the "Cosmic Microwave Background Radiation", and by examining its properties, its spectrum and its angular distribution, we can get direct evidence of the state of the Universe at that early time. The microwave background radiation is therefore a primary tool for understanding the evolution of our Universe.

5 The Success of the Standard Model

The successes of the standard model described above can be listed as follows:

a) The Universe is observed to be homogeneous and isotropic on the largest scales.

b) The expansion follows a linear velocity - distance law (the "Hubble Law") out to reasonably large distances.

c) The microwave background radiation field was predicted as the relict radiation left over from a hot big bang.

d) The spectrum of the microwave background radiation is accurately Planckian.

e) The microwave background radiation is isotropic to almost one part in a million.

f) The oldest known stellar systems are no older than the inferred age of the Universe.

g) The hot big bang explains the origin of the elements Helium and Deuterium.

Taken at face value, (b) indicates that the Universe was denser in the past than it is now. (a) says that the Universe is homogeneous and isotropic now and (e) tells us that this was so in the distant past. The mere existence of the radiation, observation (c), and its Planckian spectrum, observation (d), tells us

that the universe was hotter and denser in the past than now. It is impossible to understand the microwave background radiation in any other terms. We are inevitably led to the conclusion that the Universe expanded homogeneously and isotropically from a hot and dense state a finite time in our past.

The key piece of evidence that the Universe was denser in the past than now lies in the observed spectrum of the microwave background radiation: it is accurately Planckian. It is almost impossible to understand the accurately Planckian nature of a radiation field of this intensity without invoking the idea that the radiation field was once in thermodynamic equilibrium with matter at a high temperature and certainly at a far higher density than today.

Observation (f) about the ages confirms that picture: we should certainly see no systems older than the inferred age of the Universe, and it is a nice coincidence that the ages attributed to the oldest systems are consistent with this view of the Universe. Of course, this "confirmation" is predicated on the assumption that we understand the formation of galaxies and their stars. It is therefore not surprising that the formation of galaxies is one of the key problems of modern theoretical cosmology.

To avoid this conclusion that the Universe started with a Hot Big Bang, we would have to adopt a "Continuous Matter Creation" theory in which matter is continually being created to fill up the gaps left by the cosmic expansion. It would be difficult to account for the existence of the microwave background radiation and its spectrum in such a model. However, observation (f) would be surprising in a Continuous Creation theory where there is no reason for objects not to be indefinitely old.

One of the primary observational supports for the hot big bang theory is the explanation of the observed abundances of the light elements ^{4}He and D. These elements, along with ^{3}He, and ^{7}Li are synthesised in the first minutes of the big bang, and it is possible to make rather precise calculations of the expected primordial abundances of these elements in various cosmological models. The observed Helium abundance is very close the primordial abundance. This is fortunate since most of the helium in the Universe is thought to have originated in the big bang - the only suggestions for alternative sites of formation of this quantity of Helium are rather exotic. Thus the Helium abundance provides a direct and unambiguous test of our cosmological paradigm. The evidence from Deuterium is less direct since it is a rather fragile element that is easily destroyed in stars and converted to ^{3}He. Proper interpretation of the Deuterium abundance requires models for Galactic evolution,

Event		T (Kelvin)	t (seconds)
Planck Time	Start of classical era	10^{32}	10^{-43}
GUT phase transition	Baryongenesis	10^{29}	10^{-37}
Nucleosynthesis	He, D, Li formed	10^{9}	10^{2}
Recombination	End of Fireball	10^{3}	10^{13}
First Stars and Galaxies	H_2 formed	10^{2}	10^{15}
Clusters of Galaxies, QSO's		10^{1}	10^{17}
Here we are		3	10^{18}

Table 1: Approximate Calendar of Events

but when this is done we can estimate the primordial nucleosynthesis contribution to the Deuterium abundance.

6 Calendar of Events

The history of the Universe is characterised by a hot big bang some 10^{10} years in our past, followed by an expansion during which the material in the Universe cools down to its present value. Several events and eras are distinguished during this history, these are summarized in Table 1.

The content of the Universe at any instant of time is determined by the temperature and density. At early times it is dominated by exotic particle species, but within a few minutes after the big bang we have a mixture of hot baryons and photons at temperatures of billions of degrees. The temperatures then are so high that the baryonic material is ionised. It remains so until over a million years have elapsed and then we have the so- called "recombination" event[3] after which the material in the Universe is almost neutral.

The period before the decoupling of matter and radiation is referred to as the "fireball phase" It is a period where the radiation pressure dominates the

[3]This is an unfortunate name in the sense that the Universe is becoming neutral for the first time in its history. We can alternatively talk of the "decoupling epoch"

equation of state of the material. During the early part of the fireball phase the radiation component is so dense that it even dominates the gravitational deceleration of the cosmic expansion.

The period after decoupling is referred to as the "neutral period" of expansion, and it is during this time that an inhomogeneities in density can grow under the influence of gravity to form the first bound systems: galaxies and stars.

Chapter 40

Observational Cosmology

Observational cosmology was once regarded as "the Search for Two Numbers". These two numbers: the Hubble Constant H_0 (the value for the present rate of expansion of the Universe) and the deceleration parameter, q_0 (the rate at which this expansion is slowing down due to the influence of gravity) are indeed important descriptors of the overall scale and content of the Universe, but they are only one part of contemporary observational cosmology.

We see structure in the Universe on all scales and have much to learn about the nature and evolution of that structure. There are many projects today mapping that structure on all scales. An interesting by-product of studying that structure is to constrain the parameters H_0 and q_0.

This is perhaps the place to mention what some may regard as the "third" number describing the Universe: Einstein's Cosmological Constant. Einstein's theory of General Relativity in its simplest form provides a fine description of gravitational physics, having satisfied all the tests to which it has been subjected so far. However, the equations themselves may not be the "ultimate" description: there may be extra terms in the equations that we are unable to measure. The cosmological constant is one such term, and, as its name implies, the test for the presence (or otherwise) of this term in the Einstein equations should ultimately come from observations of the Universe on the largest observable scales. Today we can impose some rather weak upper limits on the size of this term.

Name	Description	Reference
Zwicky	Bright Galaxies $m < 15.5$ (No redshifts)	Zwicky (1957-61)
Lick	Counts of Galaxies in small cells down to $m \sim 18$	Shane and Wirtanen (1967)
Uppsala	Diameter selected galaxies from ESO SKy Survey	Nilson (1973)
APM	2 million galaxies on the southern sky UK Schmidt survey	Maddox et al (1990)
Abell	Rich Galaxy clusters in Northern Hemisphere	Abell (1958)
ACO	Rich Galaxy clusters in Southern Hemisphere	Abell et al., 1989)

Table 1: *Galaxy and Cluster Surveys having no redshifts. The list is far from exhaustive and is merely intended as a guide to some major catalogues.*

1 Projected Sky Surveys

Creating catalogues of the sky positions of astronomical objects has been a principal goal of astronomers over many centuries (even millennia). However, the first catalogues specifically devoted to extragalactic objects did not come until the "Reference Catalog of Bright Galaxies" of de Vaucouleurs and de Vaucouleurs (1964) and the "Zwicky Catalogue" compiled at Caltech on the basis of Palomar Sky Survey plates by Zwicky (1961). It was in fact the Palomar Sky Survey that gave rise to the first systematic view that the distribution of galaxies was clustered and gave rise to the identification and classification of galaxy clusters by Abell (1958).

The surveys of the distribution of galaxies on the sky lead to a deeper un-

derstanding of the fact discovered by Hubble, Shapely and others that galaxies were clustered. The quantification of this clustering in terms of the clustering correlation functions has enabled us to speculate on the origin of clustering. Since that time, there have been numerous surveys of the sky at a variety of wavelengths, giving rise to a diversity of catalogues that were later to serve as the basis for three-dimensional redshift surveys.

Currently, the largest catalogue of optically selected objects is the "APM Survey" (Maddox et al., 1990) which is based on digitalized scans of the UK Schmidt survey of the southern sky. This catalogue contains some 2 million galaxies down to the around magnitude 20. The largest catalogues of infrared selected galaxies are based the IRAS catalogue of objects found in the survey undertaken by the IRAS satellite. This catalogue has a great advantage in providing uniform all-sky coverage, including galaxies rather closer to the plane of the Milky Way than optical surveys can reach. However, it is biased by not including elliptical galaxies (these are not strong infrared sources), and it must be noted that only a small fraction of non-elliptical galaxies are IRAS galaxies. The absence of ellipticals means that rich galaxy clusters are not well represented in the catalog.

2 Redshift Surveys

Redshift surveys have been the primary source of information about the large scale structure of the Universe, and it will not be long before the number of galaxies having measured redshifts is 100,000. The redshift surveys must start with a catalogue of objects selected according to some criterion: the galaxies may be selected from an optical catalogue, from the optical identifications of, say, an infrared catalogue, or even from optical identifications of objects in catalogues of X-ray or radio sources. For a long time the "CfA Redshift Catalogue" (also known as "ZCAT") compiled by Huchra et al., (1983) was the principle redshift catalogue used in the analysis of large scale spatial structure. This catalogue was simply a compilation of redshifts that existed in the literature, and was far from homogeneous either in terms of the selection of objects or their distribution on the sky. It was used because it was generally available.

It was not until the work of de Lapparent et al. (1986) (the "CfA" or "de Lapparent Slice") that we had enough redshifts in a sufficiently deep survey that we could properly see the large scale structure of the Universe. The slice was just

Name	Description	Reference
RC2	Second Reference Catalog of Bright Galaxies $m < 13$	de Vaucouleurs et al. (1976)
RSA	Revised Shapely-Ames Catalogue of nearby Galaxies	Sandage and Tammann (1981)
ZCAT	North Zwicky Center for Astrophysics Redshift Survey	Huchra et al. (1983)
Seven Samurai	Sample of $\sim$ 400 Elliptical Galaxies	Lynden-Bell et al. (1988) Dressler et al. (1991)
SSRS	Southern Sky Redshift Survey (Diameter Selected)	da Costa et al. (1991)
CfA Slice	de Lapparent's Survey of a strip of sky centered on Coma cluster.	de Lapparent et al. (1986)
Pencil Beam	Redshift survey in Deep Narrow-Angle cones	Broadhurst et al. (1990)
QDOT	Redshift survey of galaxies selected from IRAS catalog. 1 galaxy in 6 has a redshift	Saunders et al. (1991)
IRAS	Redshift Survey of Galaxies selected from IRAS database. Full sky coverage except Galactic Plane	Strauss et al. (1992)
DARS	Durham-Stromlo Redshift survey of small area of sky down to $m_J = 16.8$	Metcalf et al. (1989)
Stromlo-APM	Redshift Survey of 1 in 20 Galaxies taken from APM survey with $b_J \leq 17.15$.	Loveday et al. (1992)

Table 2: *Galaxy Redshift Surveys. The list is far from exhaustive, in some cases the data has been made publically available by the authors.*

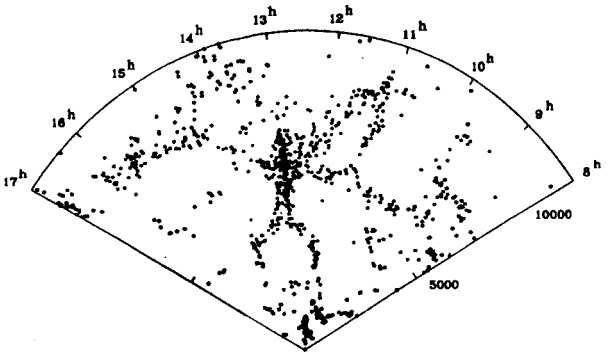

Figure 1: *The* **de Lapparent Slice***: a redshift survey of a 6° wide band of sky including the Coma cluster and other rich clusters. This picture revealed the bubble-like structure of the Universe for the first time. (After de Lapparent et al. 1985).*

that: a band of sky containing at its center the Coma Cluster (see figure 1). What this survey revealed for the first time was the filamentary and bubble-like structure in the distribution of galaxies.[1] Further slices were added to this first slice (Geller and Huchra, 1989) revealing an even larger structure: the "Great Wall". The data for the first slice is publicly available, but not the data from the subsequent slices.

For some time redshift surveys were restricted to small areas of sky (the Durham Deep Redshift Survey (Metcalf et al., 1989; Hale- Sutton et al., 1989), or even "pencil beams" (Broadhurst et al., 1990). More recently we have been able to get redshift samples covering large solid angles. An APM "Bright Galaxy Catalogue" containing all galaxies brighter than $b_J < 16.5$ was constructed from the APM catalogue and a subsample of 1787 of these had their redshifts measured (Loveday et al., 1992a,b). The IRASbased galaxy catalogues cover the whole sky (including areas hitherto obscured by the Milky Way) and have been the subject of numerous redshift studies starting with Strauss et al. (1990) and Lawrance et al. (1991), and more recently by Fisher et al. (1993). The IRAS based catalogues are however sparse galaxy samples in the sense that only a small fraction of all galaxies

[1]This structure was predicted by Zel'dovich and his group on the basis of their "pancake" model of structure formation. However, despite this amazing picture, the Pancake Theory fell into disfavour on various other grounds. (No one criticism was responsible for the demise of this theory.)

are represented in the catalogue.

3 Cosmography: Mapping the Universe

Modern Observational Cosmology has moved away from this traditionalist approach of trying to describe the Universe in terms of a parametrised Friedmann-Lemaitre cosmological model. We now have the capability of observing the Universe in many wavebands spanning most of the electromagnetic spectrum and the sky has been surveyed and mapped in most wavebands. Whereas in 1956 there were on the order of 100 redshifts for galaxies, with the maximum around 0.46, today we have tens of thousands of redshifts of galaxies, radio sources and quasars going almost to a redshift of 5.

The early view of the Universe was essentially a two-dimensional one: we saw the distribution of galaxies projected on the sky. Mapping the Universe in redshift space has provided a third dimension, albeit one that is slightly confused by a mix of radial velocities due to the overall cosmic expansion, and "peculiar" velocities induced in the motions of galaxies by fluctuations in the gravitational field (the clustering). Exploring the relationship between the velocity distribution and the observed inhomogeneity in the galaxy distribution has provided a vital tool in this evolving picture and is today one of the center-pieces of observational and theoretical cosmology.

It is now possible, under some fairly general assumptions, to use these redshift surveys to reconstruct a three-dimensional picture of the Universe. Not only can we provide a plausible map of the three-dimensional space distribution of galaxies, but we can also estimate the components of the galaxy peculiar velocities transverse to our line of sight.

New tools appear to study the Universe. Not only do we cover diverse wavebands, but we can study cosmic structures through their influence on the light that passes through them from more distant galaxies. These "gravitational lenses" are potentially a powerful way to probe the distribution of all gravitating matter, luminous and nonluminous.

4 The Microwave Background Radiation

The Cosmic Microwave Background Radiation not only provides the key evidence supporting our picture of the Universe, it also provides us with a tool to explore the details of the initial conditions for galaxy formation. When we look at the Cosmic Microwave Background Radiation we are looking back at the Universe when it was on the order of a million years old. At that time there were no stars or galaxies as we know them now, nor even any large scale structures. All that we could see then are the embryonic precursors of the present structures.

These embryonic structures nevertheless leave a detectable imprint on the angular distribution of Cosmic Microwave Background Radiation. The radiation field has some very low amplitude structure which we can use to probe the nature of the inhomogeneity of the Universe at those early times. The effect is very small and roughly consistent with our naive theories of how the structure today must have looked at recombination. Exploring the anisotropy of the radiation field will be one of the most powerful tools we have for understanding the details of the birth of cosmic structure.

That program started with the COBE satellite which first successfully detected these anisotropies on angular scales of several degrees. These scales correspond to structures far larger than any we have as yet detected by direct observation of the galaxy distribution. Subsequent experiments, both ground based and balloon borne, will probe this structure down to smaller angular scales, looking directly at the precursors of galaxies and galaxy clusters.

5 Telescopes and Satellites

Progress in understanding our Universe has been strongly linked to the development of telescopes and their detectors. When Hubble had free use of the largest telescopes on Earth, the 100″ in the 1930's and the 200″ in the 1950's, he made substantial advances in mapping the Universe. He established the extragalactic distance scale (Lundmark, 19xx, Hubble, 19xx), the expansion of the universe (Slipher, 19xx, Hubble, 19xx) and noted both the large scale homogeneity and isotropy of the universe. He also noted departures from this homogeneity - he discovered the clustering of galaxies, describing the counts in cells distribution as being approximately lognor-

mal. The 1950's saw the appearance of larger redshift surveys (Humason, Mayall and Sandage) and the start of the program to fix the scale of the Universe.

In these early days of observational cosmology the primary detector was the photographic plate. Deep photographs or spectra were acquired with exposures lasting many hours (or even days). The primary limitation on our ability to probe the Universe came from the limitation in our ability to detect photons.

Today there are many "4-meter" class telescopes. These are equipped with extremely sensitive detectors that essentially measure a single photon! (The 200″ Hale telescope with such equipment is still one of the most powerful telescopes on Earth, despite its great age.) The move towards the end of this century is towards building 8 and 10-meter telescopes: we have the 10m KECK telescope sited on Hawaii already working, and the European Southern Observatory (ESO) VLT, an array of 8m telescopes, is due to start work in the mid-1990's.

From the ground we are limited to wavelengths transmitted by the atmosphere and those images are degraded by atmospheric turbulence. Although in the infrared we can try to work in some narrow bands where the atmosphere is less opaque or we can try to correct for atmospheric instability by using active optics, the best solution is to put telescopes high in the atmosphere (borne aloft by balloons) or in space. This allows us access to wavebands not accessible from the ground (Ultra-violet, Infrared, X-rays), and even in the visual waveband we have far higher image resolution than can be achieved from Earth.

The COBE satellite started a new direction in observational cosmology by providing direct evidence for the conditions at the time of recombination before any substantial cosmic structures had formed. Eventually there will be a "COBE II" that will explore the whole sky with greater sensitivity and higher angular resolution than COBE itself, but in the meantime most of the data on the structure of the Cosmic Background Radiation field will come from balloon-borne equipment, or telescopes placed at the South Pole. Such experiments as have been performed already have added substantially to the first evidence provided by COBE by going to higher angular resolutions and greater sensitivity.

Space Observatories are not limited to the optical wavebands: they can usefully cover all wavebands from the radio wavelengths to hard X-rays and even gamma rays. In this article the focus is on cosmology and large scale structure, rather than specific classes of objects. To date the impact of the COBE and IRAS satellites has been outstanding and we will soon have results from the important

ROSAT satellite that will surely affect our view on how galaxy clusters have evolved. We are now starting to get data from the Hubble Space Telescope which will give us a direct view of galaxy evolution in the relatively recent past.

as the Universe expands. We have normalized all lengths relative to their present day value and so the present value of $a(t)$ is $a(t_0) = 1$.

The Einstein equations (or their Newtonian equivalent) in the simple case of homogeneous and isotropic dust models give the differential equation for the scale factor in terms of the total mass density ρ:

$$\frac{1}{a}\frac{d^2a}{dt^2} = -\frac{4\pi G}{3}\rho \tag{2}$$

This is supplemented by an equation expressing the conservation of matter:

$$\frac{d\rho}{dt} + 3\frac{\dot{a}}{a}\rho = 0 \tag{3}$$

which is equivalent to

$$\rho(t) = \rho_0 a^{-3} \tag{4}$$

Note that equation (2) is not valid if there is any substantial pressure due to the matter in the universe, and in that case we would also need to modify equation (3. However, for simplicity we shall only discuss the Universe at the present time and in its recent past when equations (2)-(4) are thought to be a good approximation.

The *Hubble Parameter* is defined as

$$H = \frac{\dot{a}}{a} = \frac{\dot{l}}{l} \tag{5}$$

and is a function of time. H describes the rate of expansion of the Universe and has units of inverse time. It is experimentally measured as a velocity increment per unit distance since it describes the expansion through the relationship between velocity and distance: $\dot{l} = Hl$, or in more familiar notation $v = Hr$.

We define the *redshift* to a galaxy at distance l to be

$$1 + z = \frac{1}{a} \tag{6}$$

When we look at a distant galaxy we are looking at it as it was in the past (because of the finite light travel time). At the time we are seeing it, the scale factor $a(t)$ was smaller than the present value ($a_0 = 1$). It can easily be shown that the recession velocity we measure from the shift in the spectral lines is just cz, in other words, the quantities z appearing in equations (1) and (6) are the same thing.

1.2 Important quantities: H_0, Ω_0, ρ_c

At this point it is convenient to introduce some fundamental definitions. Hubble's expansion law states that the recession velocity of a galaxy is proportional to its distance from the observer, in other words $\dot{l}_0 \propto l_0$. The constant of proportionality (the cosmic expansion rate) is the present value of the Hubble parameter:

$$H_0 = \frac{\dot{l}_0}{l_0} = \frac{\dot{a}_0}{a_0} \tag{7}$$

H_0, the present value of the Hubble Parameter, is usually called "Hubble's Constant".

There is an important value of the density, ρ_c, that can be derived from the Hubble parameter (the Hubble parameter has dimensions $[\text{time}]^{-1}$). This is the density such that a uniform self-gravitating sphere of density ρ_c isotropically expanding at rate H has equal kinetic and gravitational potential energies:

$$\rho_c = \frac{3H^2}{8\pi G} \tag{8}$$

Since H is a function of time, then so is ρ_c.

We can measure the density of the Universe in terms of ρ_c by introducing the *density parameter* Ω:

$$\Omega = \frac{\rho}{\rho_c} \tag{9}$$

Note that Ω also depends on time and we shall denote the present day value of Ω by Ω_0. There may be a mixture of different type of matter in the universe that make up the total density ρ. We may think, for example, of baryons, photons and perhaps some exotic elementary particles. Each of these individually has a density that can be normalized relative to ρ_c, thus each species has its own Ω. We will, for example, denote the contribution of Baryonic material to the total cosmic density by Ω_B.

The density ρ_c has a special significance. A universe whose density is $\rho_c(t)$ when its expansion rate is H is referred to as an *Einstein de Sitter* universe. This model clearly has $\Omega = 1$ at all times. The expansion rate of such a universe is

fixed by the density. Model universes that are denser than $\rho_c = 3H^2/8\pi G$ when their expansion rate is H will stop expanding and contract down to a future singularity. Models that are less dense will expand forever. The $\Omega = 1$ universe is a limiting case dividing two classes of behaviour and that is why the parametrization of the density in terms of ρ_c is so useful. The behaviour of the various model universes as a function of Ω can be seen by looking at the dynamical equation for the expansion factor $a(t)$.

Equations (2) and (4) for $a(t)$ can be shown to integrate to

$$\left(\frac{\dot{a}}{a}\right)^2 = \Omega_0 H_0^2 a^{-3} - H_0^2(\Omega_0 - 1)a^{-2} \tag{10}$$

The integration constants have been derived using the boundary conditions that $a(t) \to 0$ as $t \to 0$, $(\dot{a}/a)_0 = H_0$ and that the present density of matter is $\rho_0 = \Omega_0 \rho_c$. We can recall that the first term on the right hand side comes from the gravitational effect of the cosmic mass distribution, while the second term appeared as a constant of integration whose value was determined by the initial conditions for the expansion. This second term is referred to as the "curvature term" because of the way it arises in the cosmological solution to the Einstein equations.

The standard textbooks referred to above give the solutions of this equation for general values of Ω_0. It is sufficient here to note that the cases $\Omega = 0, 1$ simplify the right hand side of this equation and the solution is then particularly simple

$$\begin{aligned} a(t) &\propto t^{\frac{2}{3}} \qquad \Omega_0 = 1 \\ a(t) &\propto t \qquad \Omega_0 = 0 \end{aligned} \tag{11}$$

In the case $\Omega_0 = 0$ the scale factor grows linearly with time and we describe this as undecelerrated expansion: the first term on the right of equation (10), the gravitational term, has no effect.

Equation (10) gives the Hubble expansion rate as a function of time, and replacing the scale factors with redshifts it can be written as

$$H^2 = \left(\frac{\dot{a}}{a}\right)^2 = H_0^2 \left[\Omega_0(1+z)^3 + (\Omega_0 - 1)(1+z)^2\right]. \tag{12}$$

The terms on the right hand side are of equal magnitude at a redshift

$$1 + z_\dagger = |\Omega_0^{-1} - 1| \tag{13}$$

This is the redshift at which an open ($\Omega < 1$) universe makes the transition to undecelerrated expansion.

Associated with the curvature term in equation (12) is a length scale

$$R_\dagger = cH_0^{-1}|1 - \Omega_0|^{-\frac{1}{2}}(1+z)^{-1} \tag{14}$$

$cH_0^{-1}|1 - \Omega_0|^{-\frac{1}{2}}$ can be called "the (present) curvature radius" of the model. In the case $\Omega_0 = 1$ the curvature radius is infinite and we speak of the "flat model universe". On the other hand if $\Omega_0 << 1$ this term will today make the dominant contribution to the expansion rate.

1.3 The Hubble Parameter h

Determining the Hubble constant, H_0, requires that we have a way of getting the distance to galaxies independently of their redshifts. The history of determining the extragalactic distance scale is in itself a fascinating subject (Rowan-Robinson, 1986) and even today there is considerable uncertainty. There seems to be two distinct bodies of opinion, one clustering its estimates of H_0 around 50 km. s^{-1}Mpc^{-1} and the other around 80 km. s^{-1}Mpc^{-1}, the lastest results from the Hubble Space telescope favouring the lower value (Saha et al. 1994). We shall absorb this ignorance into a "Hubble parameter" h defined so that

$$H_0 = 100h \text{ km. s}^{-1}\text{Mpc}^{-1} \tag{15}$$

So all distances quoted will contain the quantity h, and the reader is invited to substitute her/his favourite value.

It is probably safer in practise to use radial velocity to express distances. This reflects the Hubble law and so when we say a galaxy is at a distance of $30h^{-1}$ Mpc. we could equally well say it is at a distance of 3000 km. s^{-1}. This is fine, but it may look a bit strange to say that a void has a diameter of 5000 km. s^{-1}, or to say that the galaxy clustering correlation function drops to unity on a scale of 500 km. s^{-1}.

The present value of the Hubble Constant, H_0, and the density parameter, Ω_0, together determine the present age of the universe. In the case of an $\Omega_0 < 1$ universe:

$$t_0 = \frac{1}{H_0}\left[\frac{1}{(1-\Omega_0)} - \frac{2}{\Omega_0}\frac{1}{(1-\Omega_0)^{3/2}}\cosh^{-1}\left(\frac{2}{\Omega_0}-1\right)\right], \ \Omega_0 < 1. \qquad (16)$$

There are two important limits of this equation: $\Omega_0 = 0$ and $\Omega_0 = 1$:

$$\begin{aligned} t_0 &\rightarrow H_0^{-1}, \ \Omega_0 \rightarrow 0, \\ &\rightarrow \tfrac{2}{3}H_0^{-1}, \ \Omega_0 \rightarrow 1. \end{aligned}$$

It is certain that there should not be any objects older than this in the Universe, so determining ages is an important way of constraining the values of H_0 and Ω_0. It seems that the oldest known stellar systems for which we can determine ages have ages in excess of 16 Gyr. (Sandage and Cacciari, 1990). If we accept this value, then we see that an $\Omega_0 = 1$ universe is always too young unless H_0 is considerably lower than any of the values so far put forward. An open universe with $\Omega_0 < 0.1$ can work provided H_0 is at the lower end of the suggested range of values.

What are we to make of this? That neither age determinations of star clusters nor the extragalactic distance scale can be relied on, with the latter probably being the most uncertain. Introducing a cosmological constant would of course help.

A useful equation relates the age of the Universe $t(z)$ at a given redshift z given the *present* cosmological parameters Ω, H_0:

$$H_0 t(z) = \int_z^\infty \frac{dz}{(1+z)^2\sqrt{1+\Omega z}} \qquad (17)$$

The cases $\Omega = 0, 1$ can of course be expressed analytically. This equation is important in calculating how many years after the Big Bang we see a galaxy, QSO or whatever, and given the present age of the Universe t_0 what the lookback time to that object is. A useful fitting formula for the *lookback time* to a redshift z in a Universe characterised by present Hubble constant H_0 and density parameter Ω is

$$t_{lookback} \simeq \frac{H_0^{-1}}{\epsilon}\left[1-(1+z)^{-\epsilon}\right]$$

$$\epsilon = 1 + \frac{1}{2}\Omega^{0.6}$$

The formula is correct for the two cases $\Omega_0 = 0, 1$.

1.4 q_0, Ω_0 and Λ

The central task of classical cosmology was to determine the cosmic expansion rate, H_0 and the *deceleration parameter* q_0:

$$H_0 = \frac{\dot{a}_0}{a_0}, \qquad q_0 = -H_0^{-2}\frac{1}{a_0}\left(\frac{d^2a}{dt^2}\right)_0 \tag{18}$$

H_0 was seen as the slope of the velocity-distance relationship and q_0 as the deviation from the linear Hubble law, its curvature, due to the gravitational deceleration of the cosmic expansion.

It is easy to see from equation (2) that the deceleration parameter q_0 and the density parameter Ω_0 are essentially the same thing:

$$\Omega_0 = 2q_0 \tag{19}$$

However, this is only true under circumstances where equation (2) is true, and in particular if the cosmological constant $\Lambda = 0$.

If we allow the cosmological constant into the equations, equation (2) becomes

$$\frac{1}{a}\frac{d^2a}{dt^2} = -\frac{4\pi G}{3}\rho + \frac{\Lambda}{3} \tag{20}$$

Substituting equations (2)and the definition of Ω (equations (8) and (9)) into this last equation we get

$$\begin{aligned} q_0 &= \tfrac{1}{2}\Omega_0 + \lambda \\ \lambda &= \Lambda/3H_0^2. \end{aligned} \tag{21}$$

This relationship between Ω_0 and q_0 holds only as long as equations (2) or (20) are valid; that is, provided there is no cosmic pressure. The Einstein de Sitter universe has $q_0 = \frac{1}{2}$ (since $\Lambda = 0$ and $\Omega_0 = 1$).

1.5 Dark Matter

The luminous matter itself accounts for only $\Omega_{lum} \sim 0.005h^2$ (Faber and Gallagher, 1979). This was discovered long ago to be insufficient to account for either the flat rotation curves of disk galaxies (the dark massive halo problem, Rubin (1988)), or for the velocity dispersions of groups and clusters of galaxies (the virial mass discrepancy problem, Zwicky (1933)). It later became apparent from cosmic nucleosynthesis arguments that the baryonic density of the universe was substantially higher than the density inferred from the luminous material.

Cosmic nucleosynthesis sets strong bounds on the amount of baryonic material in the Universe (Boesgard and Steigman, 1985; Pagel 1991a,b). Standard Big Bang nucleosynthesis implies that

$$0.011 < \Omega_B h^2 < 0.026 \tag{22}$$

where Ω_B is the contribution of baryons to the total mass density. (See chapter 4 of the Kolb and Turner (1990) book for an excellent discussion of this). There is a need already here to have ten times as much mass in the baryonic dark matter as is accounted by the luminous mass in galaxies. There is "dark (nonluminous) baryonic material" in some form or other, perhaps warm gas, or even very low luminosity stars. The amount of baryonic dark matter inferred from nucleosynthesis appears to be just about enough to explain the cluster virial mass discrepancy problem in most clusters of galaxies. However, this would not be sufficient to make $\Omega_0 = 1$. The question as to whether $\Omega_0 \neq 1$ is a central issue of cosmology which would take an entire review all by itself.

Direct determinations of Ω_0 are frustrated by the fact that Ω_0 describes the quantity of gravitating matter in the universe, whereas we only see the luminous material which is but a fraction of the total mass density. If the luminosity density were everywhere proportional to the mass density, this would not prove a problem since it would only be necessary to discover what the scaling factor is. However, it is evident that the mass and light are distributed differently on different scales and some other hypothesis is needed.

The simplest hypothesis of this kind is that the *fluctuations* in mass density about the mean are proportional to the *fluctuations* in light density. The constant of proportionality is referred to as the *biasing parameter* and it is denoted by the symbol b. We shall encounter this frequently in what follows (see section 5).

Note that the constancy of the biasing parameter is merely a simplifying hypothesis, the actual situation could be far more complicated.

1.6 The Standard CDM Model

If there is a "standard model" in cosmology which serves as a reference point to test our understanding, it is the so-called "CDM Model". The model is motivated by the wish to have an Einstein de Sitter Universe ($\Omega = 1.0$) and yet have only a fraction of the total mass density, Ω_B, consistent with the data (cf equation (22) in the form of baryonic material. There are many candidates for what constitutes the missing non-baryonic material: but in the CDM model it is postulated that this is a massive non-interacting particle such as the axion. Since the dark matter dominates the mass density, it is the dominant source of fluctuations in the gravitational potential: after the recombination of the the cosmic plasma, the baryons fall into the dark matter potential wells to form galaxies and clusters of galaxies.

The motivation for the standard CDM model comes from the theory of cosmic inflation which, in its simplest forms, requires that $\Omega = 1.00....$ The inflationary theory also makes predictions about the nature and amplitude of the fluctuations that give rise to cosmic structure. The models therefore has the advantage of being well specified. See Kolb and Turner for details.

The detailed consequences of the CDM model were explored in a series of papers by Davis, Efstathiou, Frenk and White ("DEFW") in the late 1980's (see for example Frenk et al., 1990). These papers used numerical simulations to explore the model and so allow detailed comparison with observational data on large scale structure. There is a growing opinion that these models do not produce enough large scale structure, though that problem could be fixed at the cost of producing problems in the details of the small scale galaxy formation process. Whatever the long term outcome however, the work be DEFW forms one of the conerstones of modern cosmology.

2 Photons

2.1 The redshift

Why should a photon travelling across a homogeneous and isotropic universe from a distant galaxy towards us suffer a redshift? Why is that redshift related to the expansion factor between emission and reception? The short answer is "because solving for the motion of photons in the FRW metric shows that there is a redshift".

The following description is a little more informative and shows how to attribute the redshift to the fact that the galaxy from which the photon was emitted was moving relative to the observer who detects it. This relative motion of source and observer is of course a consequence of the cosmic expansion. When looking at the relative motion, we have to remember that the observer receives the photon at a time later than the time at which it was emitted.

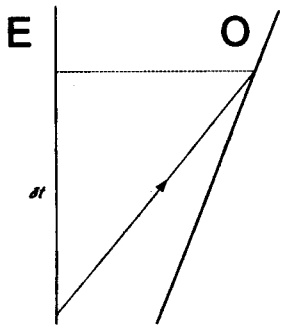

Figure 1: *The cosmological redshift*

Consider two neighbouring observers, O and E whose world lines are depicted in the space-time diagram in figure 1. The photon travels from E, reaching O a time δt later. The photon has travelled a distance $c\delta t$ and so, according to Hubble's Law, if the expansion rate is denoted by $H = \dot{a}/a$ the relative velocity of O and E is just $\delta v = c\delta t(\dot{a}/a)$. The Doppler shift due to the motion of O relative to E results in a shift in frequency

$$\delta\nu = \nu(t + \delta t) - \nu(t) = -\nu\frac{v}{c} = -\nu\delta t\frac{\dot{a}}{a}. \tag{23}$$

This leads immediately to

$$\nu(t) \propto a^{-1} \tag{24}$$

describing the shift in frequency with the expansion factor $a(t)$. If we define the *redshift* z such that $1+z$ is the relative frequency shift between emission and reception, we have

$$1 + z = \frac{\nu_E}{\nu_O} = \frac{\lambda_O}{\lambda_E} = \frac{a_0}{a(t)} \tag{25}$$

where $a(t)$ is the scale factor of the time of emission, and a_0 is the present (observer) scale factor.

2.2 Temperatures

Consider a distribution of photons, and for simplicity suppose that the directions of motion of the photons are randomly and isotropically distributed. Suppose further that the number of photons per unit frequency is given by the function $\eta(\nu)$. We define the *thermodynamic temperature* of this set of photons by the equation

$$kT_\gamma = \frac{1}{4}h\frac{\int \nu^4\eta(\nu)[1+\eta(\nu)]d\nu}{\int \nu^3\eta(\nu)d\nu}. \tag{26}$$

This somewhat intimidating equation describes the temperature of a distribution of test electrons in equilibrium with the radiation field. For the specific case where the photon distribution is the *Planck Law*

$$\eta(\nu) = \frac{1}{e^{\frac{h\nu}{kT_0}} - 1} \tag{27}$$

and it can be verified by direct substitution and integration that

$$T_\gamma = T_0. \tag{28}$$

In other words, the temperature T_0 appearing in the Planck Law (27) is just equilibrium temperature of the radiation field.[1] A well known result seen from a slightly different point of view.

[1] We shall see later, in section 3.1, why this particular distribution arises in a plasma of photons and electrons.

During some phases of the cosmic expansion cosmic background photons are neither created nor destroyed. They are simply scattered if there are any free electrons around, and redshifted by the cosmic expansion. The frequencies change like $\nu \propto (1+z)$, and so from equation (27) the temperature assigned to the Photon distribution must change like

$$T_0 \propto (1+z) \tag{29}$$

If physical processes intervene to change $\eta(\nu)$, or to create photons, the Planck Law is not preserved and this result is no longer necessarily true.

2.3 Photon density

The spatial density of photons in a Planckian distribution at temperature T_0 is

$$n_\gamma = \frac{8\pi}{c^3} \int \frac{\nu^2 d\nu}{e^{\frac{h\nu}{kT_0}} - 1} \tag{30}$$

(This follows because there are $\nu^2 d\nu d\Omega/c^3$ modes of a given polarisation per unit volume moving into a solid angle $d\Omega$. There are 4π steradians in a sphere and there are 2 polarisations). Doing the integral and putting in the numbers we have

$$n_\gamma = 60.4 \left(\frac{kT_0}{hc}\right)^3 \sim 400 \text{ cm.}^{-3} \tag{31}$$

if we use $T = 2.736$ K. We notice that

$$n_\gamma \propto T_0^3 \propto (1+z)^3 \tag{32}$$

and so since a coexpanding volume scales as $(1+z)^{-3}$, the number of photons per unit co-expanding volume is conserved with the expansion. This is of course just as it should be since scattering neither creates nor destroys photons.

Since the number of baryons in a co-expanding volume is also conserved ($n_B \propto (1+z)^{-3}$), the photon to baryon ratio is a constant:

$$\frac{n_\gamma}{n_B} \simeq 3.5 \times 10^7 (\Omega h^2)^{-1} \tag{33}$$

There are far more photons in any volume than there are baryons!

3 The Expansion

Let us focus attention on a particular spherical volume of radius R, expanding with the Universe. If the volume contains baryonic particles having density n_B, then at times when the baryon number is conserved we must have

$$n_B \propto R^{-3} \tag{34}$$

at all times. (The assumption of homogeneity tells us that particles can neither leave nor enter this volume).

The present baryonic density of the Universe is known only approximately - we have relatively poor estimates of how many baryons we cannot see. We represent our ignorance of this quantity by writing

$$n_B(\text{today}) = 2 \times 10^{-5} \Omega_B h^2 \text{cm.}^{-3} \tag{35}$$

where Ω is called the "cosmic baryon density parameter".

If the volume contains radiation the situation is little different since at times when photons are neither being created nor destroyed the number of photons in the volume also remains constant and the photon number density n_γ falls off as

$$n_\gamma \propto R^{-3}. \tag{36}$$

In principle, we can measure n_b and n_γ at the present day. To do that we need the relationship between the photon number density and the temperature of the radiation field:

$$n_\gamma = \frac{8\pi}{c^3} \int \frac{\nu^2 d\nu}{e^{h\nu/kT_0} - 1} = 60.4 \left(\frac{kT_0}{hc} \right)^3 \tag{37}$$

(Note that $n_\gamma \propto T^3 \propto (1+z)^3$ and so the number of photons per unit coexpanding volume is indeed conserved). Using the radiation field temperature $T = 2.736K$ determined from the COBE satellite data we find

$$n_\gamma = 400 \quad \text{cm.}^{-3} \tag{38}$$

We note that today the ratio of photons to baryons is

$$s = \frac{n_\gamma}{n_B} = 3.5 \times 10^7 (\Omega_B h^2)^{-1} \tag{39}$$

From the point of view of numbers, the photons are the dominant species of particle, vastly outnumbering the baryons.

The parameter s is a constant of nature and is of great importance to cosmology - if the value of s had been different the Universe today might look rather different. Once we know Ω we will have the value of s, or alternatively we might be able to determine s from other phenomena and so determine Ω_B indirectly. s is not a fundamental constant in the same way that the fine structure constant is - it is not a part of any physical laws. In principle s should be explained as a consequence of some fundamental theory of the Big Bang or the physical processes that take place shortly thereafter.

3.1 The FireBall Phase

Once the light elements have formed at redshift $z \sim 10^9$ the Universe expands and cools until it becomes largely neutral at a redshift $z \sim 10^3$. The cosmic plasma during this period of time is characterised by being completely ionised, and the pressure is dominated by Compton scattering of the cosmic background photons off the free electrons:

$$p = \frac{1}{3} a T^4 + n_B k T \tag{40}$$

The first term is the radiation pressure (a is the radiation constant) and the second is the gas pressure (k is the Boltzmann constant). The ratio of these terms is $aT^3/3kn_B$ and during this period is independent of time and large: it is on the order of the number of photons per baryon, which we saw in equation (33) was $\sim 10^8$.

The scattering time for photons is

$$t_{Compton} = \sigma_T n_e c \tag{41}$$

where

$$\sigma_T = \frac{8\pi}{3}\left(\frac{e^2}{m_e c^2}\right)^2 = 6.65 \times 10^{-26} \text{ cm.}^2 \tag{42}$$

is the Thomson cross section and n_e is the free electron number density.[2] During the fireball phase the ionisation is complete and so this timescale is very short in comparison with the cosmic expansion timescale.

In general, the spectrum of the photons is governed two processes: the Compton scattering between electrons and photons and the free-free absorption and emission of photons by electron pair scattering (Bremsstrahlung). The equation describing this process is the Kompaneets equation, which we can write down symbolically as

$$\frac{\partial \eta}{\partial t} = \left(\frac{\partial \eta}{\partial t}\right)_{Compton} + \left(\frac{\partial \eta}{\partial t}\right)_{Bremsstrahlung} \tag{43}$$

In equilibrium, these process balance to produce the Planck spectrum (27. In the fireball phase of the Universe these processes are very rapid when compared with the cosmic expansion timescale. This means that the photons and electrons can rapidly come into thermal equilibrium and can relax rapidly towards the Planck distribution. The fireball provides the *mechanism* for establishing the accurately Planckian distribution of the microwave background radiation that is observed today (cf. figure 1).

The best data on the accuracy of the Planck Law comes from the COBE satellite (see figure 2). However, we can combine the best data over all wavelengths at which the background radiation field has been measured to verify the Planck law over a longer baseline in frequency (figure 2). Combining data from different experiments is of course dangerous since they have different systematic errors. The limits on the distortion parameters have been calculated for this data set.

This is a very important point: the accuracy of the Planckian fit to the data demands that the Universe was far denser in the past than it is now. Any

[2]The Thomson cross section describes the scattering of light off electrons in the limit where the wavelength of the light is longer than the Compton wavelength $h/m_e c$ of the electron. At higher frequencies the cross section falls below the Thomson cross-section because of quantum effects, and then we speak of *Compton Scattering*. The usage of the names "Compton" and "Thomson" Scattering is frequently mixed up and Peebles (1993) has even resorted to calling the process Compton-Thomson Scattering!

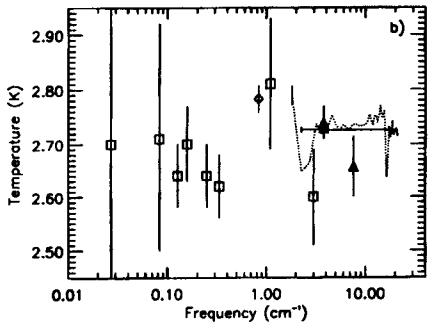

Figure 2: *Measurement of Cosmic Microwave Background Temperature made by a number of experiments covering a broad range of frequencies. The dotted line corresponds to the FIRAS data. (From Mather et al., 1993)*

theory of the Universe that sought to revive ideas that the Universe did not start from a hot dense phase would have to face the problem of explaining why the cosmic background radiation is so accurately Planckian.

The rate of free-free absorption and emission can be calculated to be

$$t_{ff} \simeq 1.4 \times 10^{24} (\Omega_B h^2) T^{-5/2} \text{ s.} \tag{44}$$

and so the Planck law must be established during periods when this is less than the cosmic expansion timescale, t_{exp}. This happens when $t < 10^{20} T^{-2}$ s., of when

$$T_{PlanckLaw} > 2 \times 10^8 \text{ K} \tag{45}$$

If for some reason the spectrum of the radiation were perturbed substantially after that time, we would see today deviations from the Planck spectrum. This argument can be turned around and we can use the observed accuracy with which the Planck law fits the data to constrain the thermal history of the Universe.

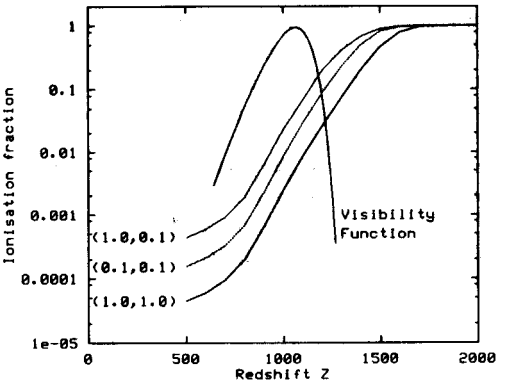

Figure 3: *Recombination of the primeval plasma in various cosmological models, the curves are labelled with the values of* (Ω_T, Ω_B). *Also shown is the "visibility function" - the contribution to the optical depth seen from the present day. (After Jones and Wyse, 1985).*

3.2 Recombination

The recombination of the primeval plasma is an important process, since the manner in which the recombination takes place largely determines what we see when we study the cosmic microwave background radiation in detail. Basically, as we look back into the past using the microwave background radiation, we are looking into a fog of electrons. Unless there has been a re-ionisation of the cosmic plasma since the recombination, the free electron density is so low that we can see back to a redshift of around $z_{\tau=1} \simeq 1000$. At that point, the Universe is still fairly neutral with an ionisation of a few parts in a thousand. As an ionised gas cools down the particles, ions and electrons, in the gas slow down. Eventually the gas becomes neutral since collisions between ions or between electrons and ions can no longer maintain the level of ionisation. In a simple hydrogen plasma this neutralisation would occur when the temperature falls to around 10^4K. It is therefore not surprising that the Universe should recombine. However, the process is somewhat more complicated than this because the photons in the cosmic radiation field vastly outnumber the baryons. Even below 10^4K there are enough energetic photons around to maintain the level of ionisation close to unity until the temperature has dropped further to around 4000 K. At that point the Universe rapidly becomes almost neutral.

The ionisation histories for several cosmological models are shown in figure (3 (Jones and Wyse, 1985). The ionisation never drops to zero and the residual ionisation depends on both the total Ω_T and the baryonic Ω_B for the model. For a given Ω_T, the residual ionisation is simply proportional to Ω_B.

Also shown in this figure is the *visibility function* describing how far back a present day observer can see: in other words where the last scattering surface is. The optical depth of the universe to Thomson scattering between the present day and a redshift z at which the age of the Universe was t is:

$$\tau(t) = \int_{t_0}^{t} \sigma_T n_e(t) c dt \tag{46}$$

where σ_T is the Thomson cross section and $n_e(t)$ is the ionisation history as a function of time. If we take the simplest case where the ionisation is unity at all times, then $n_e(t) = n_c \Omega_B (1+z)^3$, where n_c denotes the present Einstein de Sitter density.

Converting time to redshift, we find that in the general case when the ionisation history is $x_e(z)$:

$$\tau(z) = \sigma_T (n_c \Omega_B) c (\Omega_T h^2)^{-\frac{1}{2}} 3.806 \times 10^{17} \int_0^z s^{\frac{1}{2}} x_e(s) ds \tag{47}$$

Here n_c is the Einstein de Sitter critical density, and so $n_c \Omega_B$ is the present day baryonic density in the model.

Consider the case where there is no re-ionisation of the cosmic plasma since the recombination time. The probability that a photon is received from an interval of redshift dz is then

$$P(z)dz \propto e^{-\tau(z)} \frac{d\tau}{dz} dz \tag{48}$$

This is called the *visibility function* and is illustrated in figure (3). It is interesting that the visibility function is almost totally independent of either Ω_T or Ω_B. The lack of Ω_B dependence comes from the fact that the residual ionisation is inversely proportional to Ω_B, thus effectively cancelling the Ω_B term in front of the integral in (47). The visibility function also lies well into the post-recombination era and is fairly narrow. It has its maximum at $z_m \simeq 1067$ and is well approximated by a Gaussian of redshift width $\sigma_\tau \simeq 80$.

So when the COBE satellite looks at the last scattering surface, it is essentially looking back to a narrow band of redshifts around $z \sim 1000$, at which time the Universe is almost neutral.

3.3 The Post Recombination Era

The post-recombination era is the time up to the present when the evolution of the Universe, and the structure within it, is controlled by the force of gravity. The pressure is due to the thermal motions of the particles, and has negligible influence on motions on cosmic scales. Thus we believe that the structure we see today has grown out of the gravitational amplification of small amplitude inhomogeneities that were present during the fireball phase. The observation of inhomogeneities on the last scattering surface by the COBE satellite provides direct support for this notion: the observed inhomogeneities have rather small amplitude, but the amplitude is nevertheless large enough to account for the present observed structure.[3]

The fact that gravitation is the dominant force means that we can model the Universe using a computer to solve for the relative motions of particles moving under their mutual gravitational attraction. While this is a time consuming process, it is very straightforward and has played a major role in our understanding of the evolution of large scale cosmic structure.

[3]As we shall see later, the scale of the inhomogeneities observed by COBE is considerably larger than the scales where we can observe and measure large scale structure, so a hypothesis is needed relating the inhomogeneities on various scales. This is the hypothetical *Power Spectrum* of inhomogeneities.

Chapter 42

Classical Tests

Once large telescopes became available and photographic plates became sensitive enough to take pictures and spectra of fainter galaxies, the quest to discover the parameters of the cosmological model that best describes our Universe was on. The idea was to use the galaxies as tracers of the cosmic mass density and to use them to map the Universe in depth. On local scales the Universe looks Euclidean, but the hope was that going to large redshifts (approaching unity) would yield the parameter values. It is perhaps disappointing in retrospect that many decades of effort have not really brought us definitive values for these parameters.

This failure is not that surprising: the Universe has been evolving even in the relatively recent past and the intrinsic properties of the galaxies differ with look-back time, or distance. Without understanding that evolution we cannot hope to easily untangle the mixed effects of geometry and galaxy evolution. However, the situation is not hopeless since there are possibilities of better understanding galaxy evolution, and this is the purpose of much ongoing research.

1 Number - Redshift counts

A redshift survey covering some part of the sky consists of giving the redshift to all objects of a given type in the survey region. If the objects did not change with time and were distributed the same way at all distances, then in a universe with Euclidean Geometry, the number of objects seen per unit redshift interval would be

proportional to the volume and the number of objects per interval of redshift dz would simply increase with redshift (ie. distance) as z^2dz.

The geometry of the Universe is not Euclidean, and since galaxies evolve with time their local number density, $n_g(z)$ is not independent of redshift. It is in fact possible to write down in closed form the formula for the number of objects seen in each redshift interval dz, taking account of the geometry of the Friedmann Universe and of the fact that the number of sources evolves with time. The number of sources dN_g per unit redshift dz and per unit solid angle $d\Omega$ is

$$\frac{dN_g}{dzd\Omega} = n_g(z)(cH_0^{-1})^3 z^2 \frac{\left[\frac{1}{2}\Omega_0 z + (\frac{1}{2}\Omega_0 - 1)(\sqrt{1+\Omega_0 z} - 1)\right]^2}{(\frac{1}{2}\Omega)^4 z^2 (1+z)^3 \sqrt{1+\Omega_0 z}} \tag{1}$$

(Here, the $d\Omega$ on the left hand side represents an element of solid angle, and is not to be confused with the density parameter!) The small $z \ll 1$ limit is the first part of this formula:

$$\frac{dN}{d\Omega} = n_g(z)(cH_0^{-1})^3 z^2 dz \quad z \ll 1 \tag{2}$$

This can easily be verified by considering the (Euclidean) volume of a spherical cap of depth dz at a distance $D = H_0^{-1}cz$.

It was felt originally that this would provide a good way of measuring the density parameter Ω_0. However, this relationship has not yet provided a satisfactory basis for getting at the value of Ω_0. The paper of Loh and Spillar (1986) is an interesting attempt to exploit this relationship. They used a galaxy survey to determine approximate redshifts for ~ 1000 galaxies out to a redshift of $z \sim 1$. On the basis of this survey, they look at the redshift-volume relationship and conclude that $\Omega_0 = 0.9 \pm 0.3$ if $\Lambda = 0$. Caditz and Petrosian (1989) however, argued that the luminosity function history assumed by Loh and Spillar is not consistent with their data. Taking this into account, Caditz and Petrosian derive $\Omega_0 \approx 0.2$ with considerable uncertainty due to such things as incompleteness of the sample. Yoshii and Takahara (1989) make a detailed model for the luminosity evolution based on merger driven evolution and discuss the problems associated with such methods of getting at Ω_0.

Whereas applying this equation to real data is relatively straightforward in theory, in practise it is not so easy. The Universe consists of objects of diverse

types and so identifying the counterparts of local objects at great distances can be very difficult. This is made more difficult still because of the effect of the cosmological redshift on the light we detect from objects at different distances. A given detector measures the light coming from the bluer wavelength part of the spectrum of the more distant objects. It is perhaps for this reason that the QSO's have not yielded any significant estimators for the density parameter Ω_0, despite the existence of large numbers of redshifts.

There is hope, however, that this relationship may prove useful when applied to deep redshift surveys of galaxies or extremely distant clusters of galaxies. The unknown evolution of these objects is the central problem to be tackled, so if nothing else this line of research will tell us about galaxy and cluster evolution.

2 Angular Diameters

2.1 The general formula

The angular diameter subtended by a face-on galaxy of (proper) diameter L located oriented perpendicular to the line of sight at redshift z is given by the formula

$$\theta = \frac{L}{zcH_0^{-1}} \left[\frac{\frac{1}{4}z\Omega_0^2(1+z)^2}{\frac{1}{2}\Omega_0 z + (\frac{1}{2}\Omega_0 - 1)(\sqrt{1+\Omega_0 z} - 1)} \right]. \qquad (3)$$

Ω_0 is the current value of the density parameter. At small $z \ll 1$ this is simply

$$\theta = \frac{L}{zcH_0^{-1}} \left[1 + z(\Omega_0 + \frac{3}{2}) + O(z^2) \right] \qquad z \ll 1. \qquad (4)$$

This makes perfect sense since $zc = V$ is the recession velocity of the galaxy and VH_0^{-1} is therefore its Hubble distance, D. The angular diameter in the small z limit reduces to L/D.

2.2 Large redshifts

The angular diameter equation (3) cannot be derived from any simple trick with Newtonian theory - it is a consequence of General Relativity. Indeed, the equation

has some bizarre properties. If $\Omega_0 = 1$ the function $\theta(z)$ has a minimum at $z_m = 5/4$. Galaxies of a fixed proper diameter subtend larger angular size as their distances increase beyond that redshift[1]. For large $z \gg 1$ equation (3) reduces to

$$\theta \simeq \frac{Lz}{2cH_0^{-1}} \qquad z \gg 1. \tag{5}$$

which increases with z for fixed L.

We notice another curious and useful result from this asymptotic formula: a measuring rod whose proper length expands with the Universe has fixed angular diameter at very high redshift. The angular subtended by a rod of length $d = d_0(1+z)^{-1}$ is just

$$\theta(d_0) \simeq \frac{1}{2}\Omega_0 \left(\frac{d_0}{cH_0^{-1}}\right) \quad \text{radians} \qquad z \gg 1. \tag{6}$$

A useful special case of this is the angle subtended by a co- expanding rod of present day length 1 Mpc.:

$$\theta(1\text{Mpc.}) \simeq \frac{1}{2}\Omega_0 h \quad \text{arcmin.} \tag{7}$$

and this is independent of redshift.

2.3 Other important scales

A region that "came within its horizon" at a redshift z has a scale today of

$$l_H \simeq 2cH_0^{-1}(\Omega z)^{-\frac{1}{2}} \tag{8}$$

and so, using the previous formula, subtends an angle

[1]This is often "explained" as being a consequence of the focusing of the cone of light rays containing the object by the material internal to the cone. It is alternatively possible to see this as being a consequence of the fact that owing to the expansion the object was closer to us than it is now, and so the object would have looked bigger.

$$\theta_H(z) \simeq \left(\frac{\Omega_0}{z}\right) \qquad \text{radian} \tag{9}$$

Thus in an $\Omega_0 = 1$ universe, a causally connected region at recombination ($z_r = 1000$) subtends and angle of $\sim 2°$.

Another interesting scale in open universe ($\Omega_0 < 1$) is the curvature scale $R_\dagger$ defined above in equation (14). At great redshifts $z \gg \Omega_0^{-1}$ this scale subtends an angle

$$\theta_\dagger \sim \frac{1}{2}\Omega_0(1-\Omega_0)^{-\frac{1}{2}} \quad \text{radians} \tag{10}$$

If $\Omega_0 = 0.1 - 0.2$ this is just in the range of angular scales measured by the COBE satellite.

3 The Magnitude-Redshift Relation

Hubble's expansion law was a relationship between the apparent magnitude m of a galaxy and its redshift z. We can, in a given FriedmannLemaitre cosmological model calculate what this relationship ought to be for galaxies of intrinsic luminosity L. It can be shown that the apparent brightness l is related to the intrinsic luminosity L by

$$l = \frac{L}{4\pi}\left(\frac{H_0}{c}\right)^2 \left[\frac{(\frac{1}{2}\Omega_0)^2}{\frac{1}{2}\Omega_0 z + (\frac{1}{2}\Omega_0 - 1)\sqrt{(1+\Omega_0 z)}}\right]^2 \tag{11}$$

and for not too distant galaxies ($z < 1$), this simplifies to

$$l = \frac{L}{4\pi}\left(\frac{H_0}{cz}\right)^2 \left[1 + (\frac{1}{2}\Omega_0 - 1)z + \ldots\right] \tag{12}$$

This expression is also exact in the limits $\Omega_0 = 0$ and $\Omega_0 = 1$. The first terms are simply the standard r^{-2} inverse square law, the correction due to the Ω_0 term is due to the deceleration of the expansion.

Astronomers measure brightness on a logarithmic scale known as the *magnitude* scale[2]. So, up to a calibration constant that depends on the spectral band being used, the magnitude of an object of luminosity l is

$$m = -2.5 \log_{10} l + constant. \tag{13}$$

Galaxy brightness is quoted in magnitudes, and faint objects have large positive values of m (galaxies down to magnitude 20 to 21 can be identified on a UK Schmidt plate). The same magnitude scale can be used to measure the intrinsic luminosity L. We do this in a slightly round-about way by referring to the brightness the object would have were it situated at a distance of 10 parsecs; we call this the *absolute magnitude*, M of the object. Since the apparent brightness falls off inversely as the square of the distance, the apparent magnitude m of an object of absolute magnitude M at a distance of $D_{\rm Mpc}$ Mpc. is simply

$$m = M + 25 + 5 \log_{10} D_{\rm Mpc} \tag{14}$$

(thus if $D = 10{\rm pc} = 10^{-5}$ Mpc., we have $M - m = 0$). The quantity $m - M$ is called the *distance modulus* and is measured in magnitudes.

In terms of magnitudes, equation 11 becomes

$$m = 5 \log \left[\frac{4}{\Omega_0^2} \left(\frac{1}{2}\Omega_0 z + (\frac{1}{2}\Omega_0 - 1)[\sqrt{(1 + \Omega_0 z)} - 1] \right) \right] + constant \tag{15}$$

where the constant depends on the type of object selected and the spectral pass band of the observations. In practise, we do not attempt to calculate the constant, but merely fit a curve through the data points leaving the normalization arbitrary.

In astronomical units and at modest redshifts ($z < 1$) this is

$$m = M + 25 - 5 \log_{10} H_0 + 5 \log_{10} cz + 1.086(1 - q_0)z + \ldots, \tag{16}$$

where m is the apparent magnitude of a galaxy of absolute magnitude M seen at a redshift z. (Technically, these are the luminosities or magnitudes integrated over the whole spectrum of the emitted light. If the measurements are done in a restricted spectral band, then other terms come into this relationship, these are the

[2]See Appendix A

so-called K-correction terms). This expresses the Hubble Law directly in terms of a magnitude-redshift relationship.

Note that any intrinsic evolution of the quantity L (or the absolute magnitude M) will introduce non-geometric effects into the relationship and so confuse the determination of Ω_0. We can approximate this by assuming that the luminosity evolves as

$$L(t) = L_0[1 + \alpha(t - t_0)] \tag{17}$$

when expressed as a function of lookback time $t - t_0$. Relating lookback time to redshift then yields

$$l = \frac{L}{4\pi}\left(\frac{H_0}{cz}\right)^2 \left[1 + (q_0 - 1)z - \alpha H_0^{-1} z + \ldots\right]. \tag{18}$$

showing an extra linear dependence on z. Thus if this relationship is used to measure Ω_0, the (unknown) evolutionary correction biases Ω_0 downward by αH_0^{-1}.

Unfortunately, the program of measuring the curvature of the Hubble Law directly has not provided any strong constraints on Ω_0. This is largely because the curvature of the relationship is influenced by non geometric effects (galaxy luminosities evolve with time in an unknown way) and because there is considerable scatter in the magnitude-redshift diagram. Indeed, the tendency today is to use the Hubble diagram and the number-magnitude relationship together to determine the evolutionary history of galaxies! (See Guideroni and Rocca- Volmerange, 1990; Rocca-Volmerange and Guideroni, 1990).

4 Number - Magnitude counts

It was the evolution of the number counts with distance that provided the first clue for an evolutionary universe, as opposed to a Steady State universe. The number magnitude relationship provides an alternative probe of cosmological models and galaxy evolution and has generated a great deal of interest since we can now survey galaxies down to extremely faint magnitudes in many wavebands. In recent years we have seen faint galaxy counts by Tyson (1988) and by Jones et al. (1991) and Metcalf et al. (1991). The latter surveys penetrate to B-magnitudes $B < 25$. The

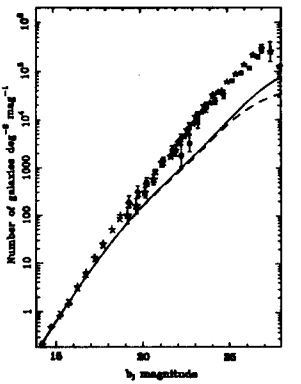

Figure 1: *b-magnitude counts compiled by Glazebrook et al. (1994). from various authors. The curves show the predicted counts in two no-evolution cosmological model having* $\Omega = 0.1, 1.0$.

interpretation of such counts and the galaxy evolution models that are used have been discussed by Koo (1990) and by Guideroni and Rocca- Volmerange (1990). The B-band data and the expectations from cosmological models in which the galaxies do not evolve in time is shown in figure (1) taken from the recent study of Glazebrook et al. (1994). It seems that the present data in the R and B bands can be largely understood in terms of current models of galactic evolution.

However, Cowie (1991) and more recently Glazebrook et al. (1994) have presented some infrared K-band counts of galaxies which confuse the situation somewhat by appearing to be consistent with cosmological models in which galaxies do not evolve. '(Alternatively we could demand a non-zero cosmological constant).

5 Surface Brightness tests

It is important to test our claim that the redshift in the spectra of galaxies is due the Doppler Effect in an expanding Universe and not simply a consequence of some other effect such as the so-called *tired light* effect in which photons redshift as they travel across the Universe, losing energy by some as yet unknown process. The possibility of testing this directly has been known for a long time (Tolman, 1930):

the surface brightness of objects would fall off as $(1+z)^{-4}$ in an expanding Universe, but only as $(1+z)^{-1}$ if there were no expansion.[3] In terms of observable quantities this test amounts to fitting either of the two curves

$$\mu(z) = 10\log(1+z) + constant, \quad \text{FRW Universe}$$
$$\mu(z) = 2.5\log(1+z) + constant \quad \text{Einstein Static Universe}$$

to measurements of the surface brightness μ of a sample of standard objects.

This simple test is unfortunately not quite as straightforward as one would like. The first problem is to find "standard objects" whose intrinsic surface brightness is the same. But even to measure the surface brightness requires that we define some intrinsic diameter that can be recognised at all distances for these standard objects. Even after doing that we have the problems of correcting for the fact of observing different wavebands at different redshifts, and of taking account of any evolutionary effects!

The attempt to select standard objects and define their proper "metric size" goes back many years. Brightest cluster galaxies have been frequently used for this purpose on the grounds that they are likely to be standard objects. The use of the "Petrosian Radius" (Petrosian, 1977) for this purpose has been discussed at length by Sandage and Perelmutter (1991). Since it is thought that these galaxies might have been built from the merging of other objects in the general cluster potential we should worry about possible evolutionary effects.

Another approach is not try to identify and use a "standard" galaxy, but rather to use all galaxies of a given type (such as luminous early-type galaxies), making corrections for the intrinsic variations of the properties of the galaxies with, say, luminosity. This is possible because it now seems that the properties of such galaxies define a so-called "fundamental plane". The basic proposition to do this is due to Kjærgaard et al. (1993).

[3]For an excellent review of testing the expansion hypothesis see Moles (1991) who discusses the Einstein Static Universe from this point of view.

Chapter 43

Galaxy Clustering

1 The Galaxy Distribution

It is usual to make the assumption that the distribution of luminous matter in the Universe reflects the distribution of matter in general, both luminous and nonluminous. If this were not the case, then understanding the nature of the Universe would be extremely difficult: if we could not trace the matter distribution by virtue of its luminosity we would have to infer it indirectly. We could in this worst-case scenario, attempt to trace the gravitational field of the matter by virtue of the velocity fields it drives, or by virtue of its gravitational lensing effects on the appearance and distribution of background objects. However, in interpreting such observations, we are always be biased by the fact that we are still using the luminous material as a probe.

There are good reasons to begin with the assumption that light traces mass. However, we do not have to go as far in this assumption as to say they are directly proportional on all scales. We can reasonably hope that our data will eventually reveal the relationship between the light and mass distributions, if there is indeed such a relationship.

We are able via observations to map out two aspects of the galaxy distribution: its density and its velocity field. Because our best-guess distances are based on the Hubble Law, which makes use of the velocities, these two aspects of the galaxy distribution are somewhat intertwined and have to be separated. This can be done on the basis of simple models relating densities and velocities, or by

measuring the galaxy distances by some means other than the redshift. We shall discuss this important are of research later.

2 Two-Point Correlation Function

The two-point clustering correlation function has been the mainstay of clustering studies for over 20 years. Its importance in cosmology has been fully discussed by Peebles (*LSSU*: 1980). The 2-point correlation function as used in astrophysics describes one way in which the actual distribution of galaxies deviates from a simple Poisson distribution. There are other descriptors like three point correlation functions, topological genus and so on.

There are two sorts of 2-point function. One describing the clustering as projected on the sky, thus describing the angular distribution of galaxies in a typical galaxy catalogue. This is called the *angular 2-point correlation function* and is generally denoted by $w(\theta)$. The other describes the clustering in space and is called *the spatial 2-point correlation function.* We frequently omit the word "spatial". The (spatial) 2-point correlation function is generally denoted by $\xi(r)$.

In order to provide a mathematical definition of the correlation function we will only consider the spatial 2-point function, the definition of the angular function follows similarly.

Consider a given galaxy in a homogeneous Poisson-distributed sample of galaxies, then the probability of finding another galaxy in a small element of volume δV at a distance $\mathbf{r}$ would be $\delta P = n\delta V$, where n is the mean number density of galaxies. If the sample is clustered then the probability will be different and will be expressible as

$$\delta P = n[1 + \xi(\mathbf{r})]\delta V \tag{1}$$

for some function $\xi(\mathbf{r})$ satisfying the conditions

$$\begin{aligned} &\xi(\mathbf{r}) \geq -1, \\ &\xi(\mathbf{r}) \to 0, \qquad |\mathbf{r}| \to 0 \end{aligned} \tag{2}$$

The first condition is essential since probabilities are positive, and the second is required in order that a mean density exist for the sample.

It is customary to make the assumption that the two point function is isotropic: it depends only on the distance between two points and not the direction of the line joining them:

$$\xi(\mathbf{r}) = \xi(r) \tag{3}$$

This is a reasonable but untested hypothesis.[1]

2.1 Calculating correlation functions

In practice, the correlation function is estimated simply by counting the number of pairs within volumes around galaxies in the sample, and comparing that with the number that would be expected on the basis of a Poisson distributed sample having the same total population. There are subtleties however due to the fact that galaxies lying near the boundary of the sample volume have their neighbours censored by the bounding volume.

One method discussed by Rivolo (1986) is to use the estimator

$$1 + \xi(r) = \frac{1}{N} \sum_{i=1}^{N} \frac{N_i(r)}{nV_i(r)} \tag{4}$$

where N is the total number of galaxies in the sample and n is their number density. $N_i(r)$ is the number of galaxies lying in a shell of thickness δr from the ith galaxy, and $V_i(r)$ is the volume of the shell lying within the sample volume. (So $N_i(r)$ is being compared with $nV_i(r)$, the Poisson-expected number lying in the shell). Note that n is usually taken to be the sample mean, but if there is an alternative (and better) way of estimating the mean density, the alternative should be used.

An alternative strategy to calculating $\xi(r)$ for a catalogue of N_G galaxies is to put down N_R points at random in the survey volume and compare the number of pairs of galaxies $n_{GG}(r)$ having separation r with the number of pairs $n_{RG}(r)$ consisting of a random point and a galaxy, separated by the same r:

$$1 + \xi(r) = \frac{n_{GG}(r)}{n_{GR}(r)} \frac{N_R}{N_G} \tag{5}$$

[1] Note that we are talking about *Statistical Isotropy*, so this equation implies nothing about the overall pattern of clustering.

(Davies et al. 1988).

The two point correlation function for the distribution of galaxies has a roughly power law behaviour on scales $R < 10h^{-1}$ Mpc., with a slope of -1.77:

$$\xi(r) = \left(\frac{r}{r_0}\right)^{-1.77}, \qquad r < 10h^{-1} \text{ Mpc.}$$
$$r_0 \sim 5h^{-1} \text{ Mpc.} \tag{6}$$

This is frequently referred to as "the 1.8 power law" and was discovered independently by Totsuji and Kihara (1969) and Peebles (1974).

What happens beyond $10h^{-1}$ Mpc. is somewhat contentious. It certainly falls below the power law behaviour, but it is not even clear whether it falls to negative values at any scale where it is measurable. What is notable is that the two-point correlation function is of negligible amplitude on those scales ($R \sim 20h^{-1}$ Mpc.) where the structure revealed in the redshift surveys (de Lapparent, Geller and Huchra, 1986) is most dramatic (see figure 1). (If there were enough galaxies that we could determine the values of $\xi(r)$ on these scales, its precise shape would indeed contain information about the large scale clustering. We are however constrained by sample discreteness.)

It should be remarked that the low amplitude of the two-point function on these large scales is consistent with the fact that the universe, if smoothed over such scales, would show little structure. We see the structure by virtue of what is happening on the small scales and in particular how the small scale structures relate to one another. The inadequacy of the 2-point function in describing what is seen on the largest scales has motivated people to look at other ways of describing the large scale structure.

2.2 A couple of examples

As a first simple illustration to see how the two-point correlation function works consider a "Swiss Cheese" model in which inhomogeneities are generated in a uniform distribution of points by shrinking a randomly placed sphere of radius R_0 to radius $R < R_0$ (see figure 1). Suppose the original sphere of radius R_0 contained N points. In order to estimate the number of pairs of points having separation s, consider a sphere of radius s placed randomly within the (shrunken) sphere of

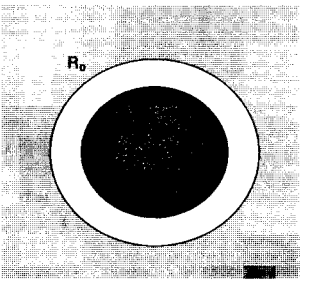

Figure 1: *Swiss Cheese model: a single cluster made by shrinking the matter in a sphere of radius R_0 to radius R.*

radius R. The number of particles within this sphere is $N(s/R)^3$ (the ratio of the volumes). The number of pairs is thus $\sim N^2(s/R)^6$. The volume of radius R can hold $(R/s)^3$ such spheres, and so the number of pairs having separation $s < R$ is $\sim (R/s)^3.N^2(S/R)^6 \sim N^2(s/R)^3$. If these particles had been distributed in the original sphere of radius R_0, the number of pairs would have been $\sim N^2(s/R_0)^3$, by the same argument. By definition, the two-point correlation function for the Swiss Cheese is then

$$1 + \xi(s) \sim \frac{N^2(s/R)^3}{N^2(s/R_0)^3} \sim \frac{R_0^3}{R^3}, \quad s < R, \quad \text{Swiss cheese} \tag{7}$$

This elementary example shows that $\xi(r)$ measures density enhancement. By extending the calculation further, it is easy to see that on scales $s > R$ where we removed particles, $\xi(r)$ goes negative.

Now let us go to a more realistic example. Consider an ensemble of nonoverlapping spheres having a range of sizes r that depend on the cluster occupancy n (see figure 2). Suppose further that the number density of clusters of occupancy n is n_{cl} and that

$$n_{cl} = An^{-\beta} \qquad r = Bn^{\alpha} \tag{8}$$

If each sphere of particles is regarded as a cluster, these relations describe the cluster population: we have so many spheres of occupancy n and radius r. For this model it can be shown using arguments similar to the Swiss Cheese example that

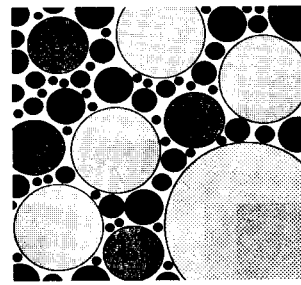

Figure 2: *Clusters of different sizes having different populations, n. Both the cluster population and the cluster radius have power law dependence on n*

$$\xi(s) \propto s^{\frac{2-\beta}{\alpha}+1}, \tag{9}$$

with the conditions that $\beta > 0$ and $\beta > 2 - 3\alpha$ (so α has to be small or else β goes negative). This model illustrates that we can tune α and β in more than one way to get $\xi(s) \propto s^{-1.8}$. The two- point correlation function alone is not enough to characterise the details of the clustering.[2]

2.3 Clustering in Projection

The earliest measurements of the two pint galaxy correlation function were done using the projected positions of galaxies on the sky. The then-available all-sky catalogues, the de Vaucouleurs Catalog of Bright Galaxies and the Zwicky Catalogue, provided samples of a few thousand galaxies down to a modest depth, while the Lick Catalogue of Shane and Wirtanen (1967) provided a larger but less uniform sample going to greater depth (Seldner et al., 1977). The situation today has improved considerably because of the APM survey of Galaxies on UK Schnmidt plates covering the southern sky. The two-point correlation function $w(\theta)$ obtained at various depths in that catalogue is shown in figure 3. The left hand panel shows the measured $w(\theta)$ for each depth. The right hand panel renormalises these to the same

[2]This model is a simple fractal. It is not rich enough in structure to mimic the real clustering in the Universe (Martinez and Jones, 1990).

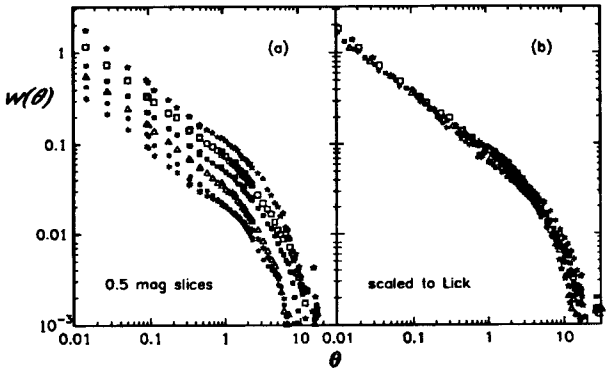

Figure 3: *The sky-projected 2-dimensional galaxy-galaxy correlation function for the APM catalogue. The left panel shows the correlations as a function of sample depth, and these are renormalised and superposed in the right hand panel. (After Efstathiou et al., 1992).*

effective depth using the assumption that the Universe is homogeneous (cf. equation (12)). The remarkable fit of these curves on top of one another is convincing evidence for the homogeneity of the Universe out to the maximum depth of the catalogue.

$w(\theta)$ shows the famous power law behaviour on small angular scales:

$$w(\theta) \propto \theta^{1-\gamma}, \quad \gamma \approx 1.75 \tag{10}$$

with a break away from this power law on larger angular scales. The nature of this break is very important since it reflects the existence and properties of clustering on large scales ($> 20h^{-1}$ Mpc.). This determination of the projected two-point correlation function is of considerable importance since it clearly shows a considerable amount of structure at large angular scales: more in fact than can be tolerated by the standard CDM model.

2.4 Limber's Formula and Depth Scaling

A sky projected catalogue is created by selecting objects from a statistically homogeneous and isotropic spatial distribution of galaxies according to some rule: we might for example choose all galaxies that are brighter than some apparent magnitude. There is then a precise mathematical relationship between the spatial correlation function $\xi(r)$ of the underlying galaxy distribution and the angular correlation function $w(\theta)$ of a galaxy catalogue drawn from that distribution according to the given selection procedure. This relationship is called *Limber's Formula* after its discoverer Limber (1958). We do not need to go into the details of this rather complex formula here[3], it is described in great detail in Peebles' two books *LSSU* (§§50-52) and *PCII* (equations 7.30 *et seq.*). Note that in general we can measure $w(\theta)$ rather easily and we wish to get at $\xi(r)$: thus we have to solve an inverse problem (Fall and Tremaine, 1977).

The selection function plays a key role in this relationship. For a catalogue that is selected according to apparent brightness this function expresses the probability that a galaxy at a given distance will be bright enough to be included in the catalogue. This in turn is controlled by the galaxy luminosity function that tells us how many galaxies there are of a given apparent brightness. Thus deducing the spatial two-point correlation function from the projected function using Limber's equation requires that the intrinsic brightness of the galaxies be independent of their location, and that we have a known universal luminosity function for the sample.

We can make a consistency check on these hypotheses by looking at the scaling properties of the projected two-point function. If we select subsamples of different limiting brightness from our catalogue we should find that samples of different depth obey the scaling relation

$$w(\theta) = D^{-1} w(D\theta) \tag{12}$$

[3]For completeness, Limber's Formula in the simple case $\Omega = 1$ is

$$w(\theta) = \frac{\int_0^\infty dy y^4 \psi(y)^2 \int_{-\infty}^{\infty} du \xi(\sqrt{(u^2 + (xy)^2)})}{\left[\int_0^\infty dy y^2 \psi(y)\right]^2} \tag{11}$$

(*LSSU* §51). The selection function $\psi(u)$ is the probability that a galaxy at distance u will be in the catalogue, and is simply an integral over the luminosity function. ($\psi(u)$ can usefully be normalized so that the numerator is unity.)

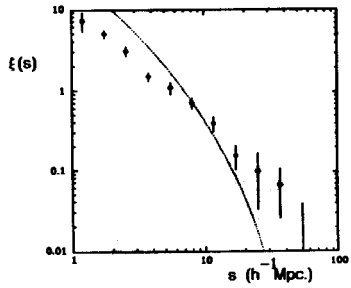

Figure 4: *The 3-dimensional galaxy-galaxy correlation function for the Stromlo-APM catalogue. The dotted line is the prediction of a standard CDM model, normalised appropriately at* $8h^{-1}$ Mpc., *the lack of large scale clustering is evident. This could be solved by "tilting" the initial spectrum of fluctuations in the model. (After Loveday et al., 1992).*

This equation is hardly surprising: it simply says that a deeper sample will look identical to a shallow sample, except that all the angular scales will be rescaled by the ratio of the distances of the samples. This scaling relation is thus a direct test of the homogeneity of the clustering in the Universe out to the maximum depth of the catalogue.

2.5 Clustering from redshift surveys

Redshift surveys are clearly a good way at measuring the clustering correlation function in three dimensions, the redshift does after all give an estimator of the distance to each object within the sample. However, the situation is not quite that simple. Firstly, redshift surveys rarely have more than a few thousand objects, so the error bars are not as small as we might like. Secondly, and more importantly, the redshift does not represent the distance accurately: there is a component of peculiar velocity which is correlated with the very density fluctuations that we are trying to characterise. When we deproject a sky-projected survey, we make assumptions about the statistical isotropy of the peculiar velocity field. But the issue of the radial component of the peculiar velocity is not relevant.

We can turn this argument around and argue that it is important to compare the deprojected 2-dimensional correlation function with the 3-dimensional

correlation function as this will give us a direct handle on the peculiar velocity field.

2.6 Cluster-cluster correlation function

The clusters of galaxies trace out the distribution of luminous matter in the Universe, and it is through these that we identify and catalogue galaxy clusters. It might be thought then that the clusters would follow the same clustering pattern as the galaxies that define them. However, this is not so: the clusters of galaxies as catalogued by Abell (1958) and by Abell, Corwin and Olowin (1989) show a correlation function that has almost the same slope as the correlation function of galaxies, but a considerably greater amplitude. This fact was discovered independently by Klypin and Khopylov (1983) and Bahcall and Soneira (1983)). For the Edinburgh-Milano cluster redshift survey (Collins et al., 1992)

$$\xi_{cc}(r) = \left(\frac{r}{16.4 \pm 4.0 h^{-1} \text{ Mpc.}} \right)^{-2.1 \pm 0.3} \tag{13}$$

Another survey of clusters identified in the APM catalogue of galaxies by Dalton et al. (1992) shows a slightly lower normalization. Figure 5 summarises the results

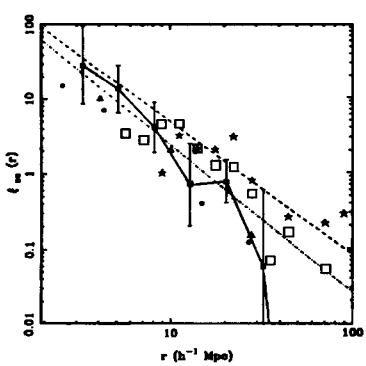

Figure 5: *The cluster-cluster correlation function for a variety of samples. The points connected by straight line segments are from the Edinburgh-Milan cluster survey* (after Collins et al., 1993).

from a variety of surveys (each denoted by a different symbols) and the dashed line

represents the fit to the rich cluster-cluster correlation function found originally by Bahcall and Soneria (1983). What is evident from the correlation function shown in figure 5 for clusters in the Milano-Edinburgh survey, is that the amplitude of the cluster-cluster function is some 3-4 times the amplitude of the galaxy-galaxy function.

Some part of the scatter in the figure is due to the fact that the cluster samples are based on clusters identified by different criteria. Comparing the clustering correlation function for clusters of different richness shows a trend: richer galaxy clusters are more correlated than poorer ones (see Bahcall and West, 1992).

There has been much discussion about how to explain this result, and whether or not the numerical simulations show this. When running a numerical model with a given set of initial conditions it is necessary to evolve the model until both the velocity dispersions of the objects in the model and the clustering amplitude are correct (if possible!). The velocity dispersion depends on the mass density fluctuation amplitude: as this grows the peculiar velocities also grow. Fortunately there is a free parameter which allows us to adjust the amount of clustering we see at the time when the velocity dispersion is correct - the *bias parameter b*. This parameter fixes the ratio of the mass density and light fluctuations (see section 5 and essentially determines which of the particles in the simulation are to be regarded as luminous from the point of view of identifying and measuring clustering.

Typically, to explain the level of cluster-cluster correlation needs a bias parameter $b = 2.0 - 2.5$ in the standard CDM model. Of course, the outstanding question remains as to what such a value for the bias parameter would mean in terms of the physical processes responsible for galaxy formation.

2.7 The two-power-law model

There has been much discussion of the notion that the clustering of galaxies should be discussed not in terms of the 2-point correlation function $\xi(r)$, but in terms of the quantity $1 + \xi(r)$ (Guzzo et al., 1991). The proposed fit (taking redshift space distortion into account) is

$$1 + \xi(r) \propto \begin{cases} r^{-\gamma_1} & \gamma_1 \simeq 1.8, \ r < 3.5h^{-1} \text{ Mpc.} \\ r^{-\gamma_2} & \gamma_2 \simeq 0.8, \ 3.5h^{-1} \text{ Mpc.} < \mathrm{r} < 20\mathrm{h}^{-1} \text{ Mpc.} \end{cases} \tag{14}$$

This simple equation can always be regarded as a reasonable fitting formula for $\xi(r)$. The question really is whether there is any physical basis for preferring the quantity $1+\xi(r)$ and so for believing that this form has any real significance. In the linear regime where $\xi(r) < 1$ it is clear that we should be looking at the *fluctuations* in the density, not the density field itself, and so $\xi(r)$ is the quantity that makes physical sense. In that case the power law fit to $1+\xi(r)$ is simply fortuitous. In the nonlinear regime it hardly matters since we have no theory for strongly nonlinear evolution. Generally, we compare with N-body models and we can measure whatever quantity we like.

3 High Order Correlations

The two-point correlation function measures the clustering of galaxies taken two at a time. While this is an important descriptor of the deviation from a Poisson distribution it does not by any means contain all the information about the clustering - many different clustering models can have identical two-point correlation functions. The natural way of proceeding is then to go to higher order correlation functions or to find alternative descriptors of the clustering which are sensitive to particular features.

3.1 Some definitions

Let us consider a discrete distribution of points. If the density of points is $\bar{n}$, then the probability of finding a point inside a randomly placed volume element dV is just

$$dP_1 = \bar{n}dV \tag{15}$$

We can write the joint probability of finding a point in each of two randomly selected volume elements dV_1 and dV_2 having separation R_{12} as

$$dP_2 = \bar{n}^2[1+\xi_2(r_{12})]dV_1dV_2 \tag{16}$$

The function $\xi_2(r)$ is called the two point correlation function. This is identical to the function defined in equation (1): it follows by combining equations (15) and (1) to get the probability of finding points in *two* randomly chosen volume elements.

The definition of the 3-point function follows similarly, but with an important subtlety: the 3-point function is defined as an excess probability of finding a given configuration of three points, over and above our expectations based on the 1- and 2- point functions. Thus we write the probability of finding three particles in a triangle whose sides are r_{12}, r_{23} and r_{31} as

$$dP_3 = \bar{n}^3[1 + \xi_2(r_{12}) + \xi_2(r_{23}) + \xi_2(r_{31}) + \xi_3(\mathbf{r}_1, \mathbf{r}_2, \mathbf{r}_3)]dV_1 dV_2 dV_3 \qquad (17)$$

The 2-point terms represent the contribution from the pairwise distribution. In a statistically homogeneous clustered distribution of points, the 3-point function ξ_3 depends on the shape of the triangle as well as its size. The shape of the triangle is generally parametrised by two variable such as an angle and the ratio of the lengths of the sides defining that angle.

Going to four point functions, we use a definition that involves four points and we must be careful to remove the direct contributions from the 2- and 3- point functions. This then involves a combinatorial problem in counting all the relevant pairs and triples.

3.2 Scaling Relations

When the three point function was measured, it was realised that there is a relationship between the 2-point and 3-point functions. If we consider a triangle of three galaxies placed at points $\mathbf{r}_1, \mathbf{r}_2, \mathbf{r}_3$ and denote the distance between the vertices i, j of the triangle by r_{ij}, then

$$\xi_3(\mathbf{r}_1, \mathbf{r}_2, \mathbf{r}_3) = Q[\xi_2(r_{12})\xi_2(r_{23}) + \xi_2(r_{23})\xi_2(r_{31}) + \xi_2(r_{31})\xi_2(r_{12})] \qquad (18)$$

and for all shapes of triangles tested within a given survey Q has the same value. The value of Q is however less certain and estimates from different surveys cover a considerable range

$$Q \simeq 0.6 - 1.0 \qquad (19)$$

The fit appears to be valid on scales of up to a few megaparsecs ($r < 2h^{-1}$ Mpc.) where the 2-point function certainly has a power law form, and there is evidence that it is still valid over considerably larger scales where the clustering is linear.

It will be noticed that equation (18) contains only products of pairs of two-point functions. By virtue of the definition (17) it could not contain terms linear in ξ_2, but it might have contained a term proportional to $\xi_2(r_{12})\xi_2(r_{23})\xi_2(r_{31})$. The evidence is that there is no such contribution. If there were such a contribution it would dominate over the products of pairs of ξ_2 functions on the smallest scales.

There is evidence that the 4-point function can also be expressed as a sum of products of 2-point functions taken three at a time, and this has lead to the suggestion that in general the J-point function can be written as

$$\xi_J(\mathbf{r}_1, ..., \mathbf{r}_J) = \sum_{graphs} Q_\alpha^{(J)} \sum_{ab} \prod^{J-1} \xi_2(r_{ab}) \tag{20}$$

This somewhat unwieldy notation is simply a way of denoting the sum over all pairs of points, counted in an appropriate way. The first sum over all graphs refers to the graphs that can made up from all the sets of $J-1$ edges connecting the J points. The product refers to the product of the values of the 2-point functions for that particular graph. The coefficients Q^J are to be determined from the data, and perhaps from some theory.

We see simple power law scaling for the 2-point function ($\xi_2(r) \propto r^{-\gamma}$) and for the 3-point function ($\xi_3(r) \propto r^{-2\gamma}$) for a given shape of triangle. Given the hierarchy expressed through equation (20) it is not unreasonable to expect this scaling behaviour to continue on to all order of correlation functions with:

$$\xi_J(r_1, ..., r_J) = \lambda^{(J-1)\gamma} \xi_J(\lambda r_1, ..., \lambda r_J). \tag{21}$$

It is important to notice that the power of the scale factor that appears, $(J-1)\gamma$, tells us that the hierarchy is determined by one scaling index: γ. The consequences of such a scaling hierarchy have been extensively analyzed by Balian and Schaeffer (1989).

4 Counts in Cells

In the previous section, we saw that the clustering is to be described by a hierarchy of correlation functions. On small scales where the 2-point correlation function is large, the high order correlation functions dominate the character of the clustering.

We do not know these, and cannot reliably calculate them. Moreover, if we knew what they were it would not help much with getting an intuitive grasp of how the clustering should look.

This leads us to consider other measures of the clustering that directly attack the question of the appearance of the galaxy distribution, and the hope is that such descriptors are somehow linked to the dynamical processes that caused the clustering. This is hardly the place to delve into this complex subject, so I shall focus on one such measure: the counts-in-cells distribution.

4.1 Counts and Moments

To be specific, let us focus attention on a distribution of particles having a density n. Suppose that we analyze counts in a the sample volume that is divided into M cubic cells of equal size l and volume $V = l^3$. If the cells are simply labelled by and index i, we can attach an occupation number N_i to the ith cell and compute the mean and variance of N_i:

$$\bar{N} = \frac{1}{M}\sum_{i=1}^{M} N_i$$
$$\mathrm{var}(N) = \frac{1}{M-1}\sum_{i=1}^{M}(n_i - \bar{N})^2 \qquad (22)$$

The variance of the counts in the cells is directly related to the 2-point correlation function for the sample

$$\mathrm{var}(N) = \bar{N}[1 + \bar{N}\bar{\xi}_2(V)] \qquad (23)$$

where

$$\bar{\xi}_2(V) \equiv \sigma_V^2 = \frac{1}{V^2}\int_V \xi(r_{12})dV_1 dV_2 \qquad (24)$$

Thus we can use the counts in cells to estimate this integral over the correlation

function. [4] To this end we note that the expectation value of $\bar{N}$ is

$$< \bar{N} >= nV \tag{26}$$

and the quantity

$$S = \frac{1}{M-1}\sum_{i=1}^{M}(n_i - \bar{N})^2 - \bar{N} \tag{27}$$

has expectation value

$$< S >= n^2V^2\sigma_V^2 \tag{28}$$

(This follows from equations (23) and (22)).

We can generalize this procedure to the higher moments of the cell counts and the averages over the higher order correlation functions. If we write

$$\bar{\xi}_J(V) = \frac{1}{V^J}\int_V \xi_J(\mathbf{r}_1, ..., \mathbf{r}_J)d\mathbf{r}_1...d\mathbf{r}_J \tag{29}$$

then it can be shown that these are related to the moments $< (\Delta n)^J >$ by the hierarchy of equations

$$\begin{aligned} < n > &= \bar{N} \\ < (\Delta n)^2 > &= \bar{N}^2\bar{\xi}_2 + \bar{N} \\ < (\Delta n)^3 > &= \bar{N}^3\bar{\xi}_3 + 3\bar{N}^2\bar{\xi}_2 + \bar{N} \\ < (\Delta n)^4 > &= \bar{N}^4\bar{\xi}_4 + 6\bar{N}^3\bar{\xi}_3 + 7\bar{N}^2\bar{\xi}_2 + \bar{N} + 3 < (\Delta n)^2 >^2 \end{aligned} \tag{30}$$

(Peebles, *LSSU*). In principle these equations can be used to test the scaling of the various order correlation functions and their possible scaling relationships.

---

[4] Since $\xi(r)$ is related to the Power Spectrum, we can equally write this as an integral over the Power Spectrum $P(k)$:

$$\sigma^2(l) = \frac{1}{2\pi^2}\int_0^\infty P(k)W_V(kl)k^2dk, \tag{25}$$

the function $W_V(x)$ being the window function corresponding the choice of volume V.

In practise we have to take care of selection functions when using magnitude limited samples, and we have to take care of the sample boundaries. There are also considerable problems in interpreting this in redshift space where the deviations from uniform Hubble flow are correlated with the density fluctuations. Determining the correlation functions from these cell counts is not entirely straightforward!

4.2 Scaling the variance

Measuring the two-point correlation function on large scales is difficult because the amplitude is small and there is a technical (though not insuperable) problem in determining the normalisation relative to which the "excess" counts are measured. Another way of looking at the large scale structure is to use the variance of the counts in cells as just described. The results for the APM bright galaxy survey are

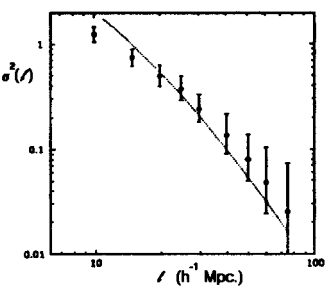

Figure 6: *The variance of counts in cells as a function of cell size for the Stromlo-APM catalogue (after Loveday et al., 1992).*

shown in figure 6 (this is formally equivalent to the spatial 2-point function from the same survey show in figure 4). The counts on scales in excess of $30 - 50h^{-1}$ Mpc. are clearly in the so-called linear regime, the variance is substantially smaller than unity. Thus it is straightforward to compare the predictions of N-body models based on a given input power spectrum $P(k)$ using equation (25).

In making this comparison, we need a spectral shape, an amplitude and a bias parameter. Given the spectral shape, the COBE observation of large scale fluctuations fixes the amplitude, and since it is generally believed that the spectrum has the classical Harrison-Zel'dovich form on these large scales that leaves only one free fitting parameter: the bias b.

4.3 Higher Moments

The volume averaged higher order correlation functions (equation (29)) have been the subject of several recent investigations, both theoretical (eg. Bernardeau, 1992) and observational (eg. Gaztanaga, 1994). In the simple scaling hierarchy, the quantities $Q_J = \xi_J/\xi_2^{J-1}$ are of importance since they should be independent of scale. The analogous quantities for the averaged correlation functions (29) are

$$S_J(V) = \frac{\bar{\xi}_J}{\bar{\xi}_2^{J-1}} \qquad J > 2 \tag{31}$$

The volume is usually taken as a sphere, weighting all points within the sphere equally (ie: a "top-hat window"). This equation has been the subject of numerous tests, from the point of view both of the observed galaxy distribution and N-Body simulations. The quantities S_J can be calculated analytically within the quasi-nonlinear gravitational instability picture (Bernardeau, 1992).

The case $J = 3$ is called the *skewness ratio* of the distribution:

$$S_3(V) = \frac{\bar{\xi}_3(V)}{\bar{\xi}_2^2(V)} = \frac{< \delta(\mathbf{x}; V)^3 >}{\delta(\mathbf{x}; V)^{2^2}} \tag{32}$$

where

$$\delta(\mathbf{x}; V) = \frac{1}{V} \int \delta(\mathbf{x} + \mathbf{r}) W_V(\mathbf{r}) d\mathbf{r} \tag{33}$$

is the quasi-linear regime density fluctuation field smoothed over the window V. Looked at this way, we see that $S_3(V)$ is a measure of the *skewness* of the density fluctuations relative to their variance. For a power law power spectrum of Gaussian initial fluctuations, quasi-linear perturbation theory yields

$$S_3(R) = \frac{34}{7} - (n + 3), \quad \mathcal{P}(k) \propto k^n \tag{34}$$

and this is independent of scale (Juskiewicz and Bouchet, 1991). It is not scale independent for a general spectrum such as a CDM initial spectrum, and so some care has to be taken when making comparisons between theory and observation.

Gaztanaga (1994) has made an extensive analysis of the distribution of galaxies in the APM survey, and is able to deproject the results to obtain estimates of S_J for values of $J = 1, ..., 9$, covering a range of length scales from $0.5h^{-1}$ Mpc. to $\sim 10h^{-1}$ Mpc. depending on the value of J. On the largest scales ($R > 7h^{-1}$ Mpc.:

$$\begin{aligned} S_3^{APM} &= 3.16 \pm 0.14 \\ S_4^{APM} &= 20.6 \pm 2.6 \\ S_5^{APM} &= 180 \pm 34 \end{aligned} \tag{35}$$

The value of S_3 fits equation (34) for $n = -1$ which seems appropriate for this range of scales, and the values of S_3 and S_4 are consistent with numerical models for the same $n = -1$. This is at least encouraging for the gravitational instability picture for structure formation. The results are remarkable in particular because they make no assumptions about how the light distribution traces the mass distribution. The theoretical estimates of the S_J are based simply on gravitational instability and so the relationship (34) that is derived concerns the mass distribution. Yet what is measured from the APM survey concerns the luminosity distribution.

In N-Body models the scaling relation (31) can be tested for a variety of initial conditions. This has been undertaken by Lucchin et al. (1993) for scale-free Gaussian initial conditions having power spectra $\mathcal{P}(k) \propto k^n$ with $n = -3, ..., +1$, for the moments up to $J = 5$. For the cases $n = -1, 0, +1$ where the analysis is most reliable, they do indeed find scaling laws of the form $\bar{\xi}_J \propto \bar{\xi}_2^p$ in close agreement with equation (31). However, there do seem to be small but systematic deviations in that their measured scaling slope: p is manifestly different from $J - 1$.

4.4 The lognormal and other distributions

Looking at the moments of the cell count distribution is interesting because of their close relationship with the higher order correlation functions. However, it still remains to discover what the actual distribution of cell counts is on various scales. There is certainly enough data in the large sky- projected catalogues to get at the distribution projected on the sky, but this falls somewhat short of determining the true spatial distribution.

There have been several suggestions on this point. Historically, Hubble (1934) suggested that the projected galaxy counts followed the *lognormal distribution*

$$P_{LN}(N) = \frac{1}{\sqrt{2\pi}\sigma N} \exp\left[-\frac{(\log N - \overline{\log N})^2}{2\sigma^2}\right] \tag{36}$$

where the variance σ is

$$\sigma^2 = 2(\log \bar{N} - \overline{\log N}) \tag{37}$$

Arguments were first given by Coles and Jones (1991) why one might expect such a distribution on the basis of a pseudo- nonlinear theory. The underlying driving force behind this model is that the peculiar velocity distribution remains remarkably Gaussian even during the nonlinear phases of evolution. Why that should be so remains rather a mystery. In any case, the subsequent attempts to verify this both in terms of the data and in terms of theoretical models of large scale clustering have proved surprisingly successful considering the simplicity of the distribution (Kofman et al., 1994).

Jones et al. (1993) derived the lognormal distribution for the strongly nonlinear regime on the basis of the measured scaling properties of the moments of the galaxy distribution and presented some scaling rules for the parameters of the distribution as a function of cell size. These predictions have not yet been verified in any detail.

Saslaw and Hamilton (1984) have argued for a distribution function

$$P_{SH}(N) = \frac{\bar{N}(1-\beta)}{N!}\left[\bar{N}(1-\beta) + N\beta\right]^{N-1} e^{-[\bar{N}(1-\beta)+N\beta]} \tag{38}$$

I have called their b parameter β in order to avoid confusion with the bias parameter. This parameter is interpreted as being the ratio of gravitational correlation energy to the kinetic energy in peculiar motions. It appears that this distribution fits the particle distribution in N-body models rather well, provided β is scale-dependent, and it also seems to fit well with the data in projected galaxy catalogues (Sheth et al., 1994).

Chapter 44

Deviations from the Standard Model

1 Modelling the Universe

1.1 Gravitation as the Dominant Force

We believe that for most of its history the Universe has been dominated on large scales by the force of gravity. Gravitation has been the force responsible for organising the material into the large structures we see, and into the galaxies and clusters of galaxies. The details of galaxy formation, however, are more complex because it is obvious that complex gas-dynamical processes have played a key role: we see gas and stars in galaxies today.

So, as long as we restrict out attention to scales larger than galaxies we should be able to generate models for the origin of the large scale structure we see today using only the theory of gravitation.

This raises two questions: (a) do we have to use Einstein's Theory of General Relativity, or can we get away with Newtonian gravitation? and (b) can we solve the problem on a computer? The first question is one of complexity: Einstein's equations are difficult enough to handle even in the case of homogeneous cosmological models. What hope could we have of dealing with inhomogeneous models? The

second question faces the fact that the basic equations, whether Newtonian or Einsteinian, are likely to be very difficult to handle and so the computer may be an essential tool.

First, as regards Einstein's theory there is no doubt that we should use this theory if at all possible. However, there are formidable difficulties in using this approach even on a computer and so we should be gratified that most problems can be attacked with the simpler Newtonian theory of gravitation. The conditions under which Newtonian theory should provide a good approximation to the evolution of a self-gravitating system like the Universe are relatively clear.

1.2 N-Body Simulations

Although it is in principle possible to model the Universe as an expanding gas using the equations of gadynamics, the demands on computer time to do that are generally too great to warrant this approach. Hence it has been customary to exploit the fact that the Universe is dominated by the force of gravity and replace the continuous mass distribution by a "gas" of self-gravitating particles. The hope is that this will represent a good approximation at least to the formation of large scale structure, and that at some future time we can modify the particle interactions to mimic gasdynamic behaviour on smaller scales. Modelling the Universe on a computer is not at all a recent idea, it goes back to the early work of Aarseth in the mid-1970's.

One of the key problems facing attempts to model the Universe numerically is to make the link between the idealised point masses in the model and the objects we see - the galaxies. Ideally we should like to improve our models, painting more physics on top of the simple selfgravitating agglomeration of particles. However, that physics does not come cheaply since it involves at least adding gas dynamical processes to the simulations and to go the whole way would involve adding some model for the star formation process too. Failing that we introduce the convenient notion of "biasing" in order to relate the mass and the light distributions in our models (see section 5).

It is customary to follow the evolution of N-Body models in *comoving coordinates*: a coordinate system that expands with the background universe.

$$\mathbf{x} = \frac{\mathbf{r}}{a(t)} \tag{1}$$

where $a(t)$ is the scale factor at time t for the chosen cosmological model (equation (10). In these coordinates the overall size of the simulation appears constant, the expansion has been taken out, but can easily be put back just by multiplying all length scales by $a(t)$. In such coordinates, the momentum of a particle and its rate of change can be written

$$\begin{aligned} \mathbf{p} &= ma^2\dot{\mathbf{x}} \\ \frac{d\mathbf{p}}{dt} &= -m\nabla\varphi. \end{aligned} \tag{2}$$

where m is the particle mass and φ is the fluctuating part of the gravitational potential, given by Poisson's equation in the comoving coordinate system:

$$\begin{aligned} \nabla^2\varphi &= 4\pi G a^2[\rho(\mathbf{x}) - \bar{\rho}(t)] = 4\pi G\bar{\rho}(t)a^2\delta(\mathbf{x},t) \\ \delta(\mathbf{x},t) &= \frac{\rho(\mathbf{x},t)}{\bar{\rho}(t)} - 1. \end{aligned} \tag{3}$$

In this equation, G is the gravitational constant as usual, and $\bar{\rho}$ is the mean density of the universe.

The problem boils down to how to solve the Poisson equation. The earliest attempts to do this took the direct approach and find the force on a given particle as the sum of the forces exerted by all other particles. With N particles this meant that the computing time increased as N^2 and this provided an important limitation on the number of particles that could usefully be used.

One way to improve on the direct interaction approach is to use the hierarchical "Tree Algorithms" (Barnes and Hut, 1986). These algorithms recognize that the contributions to the force on a given particle from the more distant particles can be approximated using multipole expansions. In order to systematise this, the particles are grouped into a hierarchy that has the structure of a tree. In this way the groups of particles making different contributions to the force can be rapidly identified. This results in a substantial improvement in performance for large numbers of particles and the speed of the method increases with $N \log N$ rather than N^2.

A simple alternative is to use a Fourier series to solve the Poisson equation, thereby benefitting from the use of the Fast Fourier Transform algorithm. The principle is simple: the Fourier transform of equation (3) is

$$\hat{\varphi}(\mathbf{k}) = -\frac{4\pi G\bar{\rho}a^2}{k^2}\hat{\delta}(\mathbf{k}) \tag{4}$$

where $\hat{u}$ denotes the Fourier transform of the function u. If a function is defined on N grid points, its Fourier transform can be calculated in $N \log N$ operations, and so the potential is computed in far fewer than the N^2 operations required in doing a direct double sum over all particles.

Implementing this is straightforward: we introduce a three dimensional mesh covering the density distribution and calculate the potential at the mesh points. We have to remember that the particles can lie anywhere within the mesh, but the potential is evaluated on the grid points. To do this[1] one writes equation (3) in terms of the particle representation of the simulated density field. Assume that the N particles are placed in a cubic box of side L, then

$$\begin{aligned} \nabla^2\phi \equiv 4\pi G n(\mathbf{x},t) = 4\pi G\left[\sum_{i=1}^{N} m\delta^{(3)}(\mathbf{x}-\mathbf{x}_i) - \frac{M}{L^3}\right], \qquad M = \sum_{i=1}^{N} m_i \\ \phi(\mathbf{x}) = a\varphi(\mathbf{x},t) \end{aligned} \tag{5}$$

One can then write the Fourier representation of the density field $n(\mathbf{x})$ and the potential $\phi(\mathbf{x})$ as

$$\begin{aligned} n(\mathbf{x}) &= \frac{1}{L^3}\sum_{k} n_{\mathbf{k}} e^{i\mathbf{k}.\mathbf{x}} \\ \phi(\mathbf{x}) &= \frac{1}{L^3}\sum_{k} \phi_{\mathbf{k}} e^{i\mathbf{k}.\mathbf{x}} \\ \mathbf{k} &= \frac{2\pi}{L}(q_1,q_2,q_3) \qquad q_i \in \mathbf{Z}+ \end{aligned} \tag{6}$$

The triples (q_1, q_2, q_3) are all triples of positive integers. The gravitational potential is then simply

$$\phi(\mathbf{x}) = -\frac{4\pi G}{L^3}\sum_{j=1}^{N}\sum_{\mathbf{k}\neq\mathbf{0}} \frac{m_j}{k^2} e^{i\mathbf{k}.(\mathbf{x}-\mathbf{x}_j)} \tag{7}$$

The term $\mathbf{k} \neq \mathbf{0}$ (the "DC component") is excluded since the mean density has been subtracted to create the fluctuating density field.

[1] Here I simply follow the paper by Hernquist et al., (1991)

This sum is easy to perform, and there are several sophisticated techniques that can make evaluating the sum more efficient (eg: Hernquist et al. 1991). Once the potential has been calculated the particles can then be moved for a short timestep and the process begun over again.

This kind of N-Body scheme is referred to as a "PM Code" (Particle-Mesh): the particles move around on the mesh used for providing the grid points at which the potential is calculated. Details in the potential and density field that are finer than the mesh are not resolved and this is the inherent limitation of this approach. There are various modifications to this simple PM scheme, combining the PM scheme on large scales with direct particle-particle interactions on the smaller scales ("P^3M), though the improvement comes with a price in paid in terms of computation time.

When assessing the relative merits of the various schemes for performing N-Body integrations it is important to bear in mind any differences in boundary conditions. By their very nature the Fourier methods have periodic boundary conditions. This means that the contributions from very large scales is neglected and also that the mean density of the box is the mean density of the Universe. Thus is not easy to model an overdense or underdense region with such a code. The direct particle codes generally have a vacuum outside of the boundary, and so the geometry of the simulations is spherical. Having vacuum on the outside of the simulation sphere is also unrealistic. It is also important to remember that in the direct particle methods the potential is often smoothed on small scales so as to avoid spending computational effort on close encounters. This "softening" of the potential can have serious effects on the small scale behaviour of the models.

The largest simulations to date are probably those of Gelb (1992) in which there are 256^3 particles.

2 Small Deviations

2.1 Linear Perturbations

We have already written down the definitions of the fluctuating component of the density field (equation 3):

$$\delta(\mathbf{x},t) = \frac{\rho(\mathbf{x},t)}{\bar{\rho}(t)} - 1. \tag{8}$$

Here, $\mathbf{x}$ represents spatial position in a coordinate system co-expanding with the background cosmological model, ie: $\mathbf{x} = \mathbf{r}/a(t)$ where $a(t)$ is the background scale factor. By doing perturbation theory we can derive an equation for the growth of $\delta(\mathbf{x},t)$. This growth rate depends on the equation of state of the matter, and in general on the scale of the perturbation[2]. In the simple case of a dust (zero pressure) Universe, which is appropriate to the situation after the epoch of recombination,

$$\ddot{\delta} + 2\frac{\dot{a}}{a}\dot{\delta} = 4\pi\bar{\rho}(t)\delta \qquad (|\delta| \ll 1) \tag{9}$$

The general solution of this takes the form

$$\delta(\mathbf{x},t) = A(\mathbf{x})D_1(t) + B(\mathbf{x})D_2(t) \tag{10}$$

where $D_1(t)$ and $D_2(t)$ are linearly independent functions that depend on the parameters of the cosmological model. In the specific case of an Einstein de Sitter Universe:

$$\delta(t) = At^{\frac{2}{3}} + Bt^{-1} \tag{11}$$

where A, B are independent of time, but depend on spatial position and are determined by the initial conditions. Note that this solution becomes unbounded both in the past and in the future, and so the approximation breaks down at these extremes.

It is generally argued (and with good reason) that the decaying B-term in equation (11) (or by convention the D_2 term in the general equation (10)) must be exactly zero, otherwise the Universe would not have been homogeneous in the past. This has some rather important implications.

2.2 Peculiar Velocity Fields

The gravitational effects of the density fluctuations will be associated with deviations from uniform Hubble flow. Recalling that the comoving coordinate $\mathbf{x}$ of a particle

[2]see Stefan Gottlöber's lectures in this volume for a detailed discussion

at position $\mathbf{r}$ is given by $\mathbf{r} = a(t)\mathbf{x}$, we can write the velocity of the particle as $\mathbf{u} = \dot{\mathbf{r}} = \dot{a}\mathbf{x} + a\dot{\mathbf{x}}$. Since the Hubble expansion at place $\mathbf{r}$ is $\mathbf{v}_H = (\dot{a}/a)\mathbf{r} = \dot{a}\mathbf{x}$ we see that the deviation from uniform Hubble expansion in these comoving $\mathbf{x}$-coordinates is just

$$\mathbf{v}(\mathbf{x}, t) = a(t)\dot{\mathbf{x}} \tag{12}$$

This fluctuating component of the velocity field is given by the continuity equation

$$\nabla.\mathbf{v} = -a(t)\frac{\partial \delta}{\partial t} = -a\frac{\dot{D}}{D}\delta \tag{13}$$

where we have written equation (10) as $\delta = A(\mathbf{x})D(t)$ for the no-growing-mode case.

If we assume that the fluctuating velocity field is irrotational, then it is the gradient of a velocity potential: $\mathbf{v} = -\nabla_{\mathbf{x}}\Phi$ and equation (13) is just the Poisson equation whose solution in this case can be written

$$\mathbf{v}(\mathbf{x}) = a\frac{f(\Omega)H}{4\pi}\int \frac{\mathbf{y} - \mathbf{x}}{|\mathbf{y} - \mathbf{x}|^3}\delta(\mathbf{y})d^3\mathbf{y} \tag{14}$$

The function $f(\Omega)$ depends on the cosmological model. What is interesting to note about this equation is that the velocity field is strongly correlated with the density fluctuations: indeed we can determine either one from the other. This can be used as a tool to map the Universe, an important point that we shall return to later.

2.3 Shear and Vorticity

The result expressed in equation (14) depends on a couple of assumptions: firstly that only the growing mode be present and secondly that the velocity field be irrotational. It is entirely reasonable to assume that the decaying mode perturbation is in fact zero, but what about the irrotational flow assumption?

Equation (13) is an equation for only one derivative of the velocity field. There are 9 derivatives $\partial v_i/\partial x_j$ and this equation merely states the value of the trace of this tensor (the so-called dilatation). Where do the other 8 derivatives come from? Looked at another way, if we write the velocity firled as the gradient of a potential, $\mathbf{v} = \nabla\Phi$, we can write equation 13) as

$$\nabla^2\Phi = -a\frac{\dot{D}}{D}\delta \tag{15}$$

and we have an equation for only one of the 9 independent components $\partial^2\Phi/\partial x_i\partial x_j$. How do we determine the other components?

In linear theory these other components are in fact determined by the boundary conditions at the initial time: they do not depend on the growth of the density perturbations and they merely follow the cosmic expansion, conserving angular momentum. In linear theory they are independent of the gravitational field because the gravitational force is derived from a potential. A consequence of this is the decay of primordial vorticity: any vorticity that existed say at the time of recombination would have been far greater in the past, thus violating the small perturbation assumptions upon which the model is predicated. Thus we assume there was no primordial vorticity for much the same reason that we assume there was no decaying mode in the perturbations. This was a subject of great debate in the late 1960's and early 1970's (Jones, 1976).

The situation with the shear is a little more complex since shear is generated by gravitational forces in the nonlinear regime: shear generation is a second order effect. So while we could easily argue that there is no primordial shear, we have to admit the possibility that shear is generated through gravitational tidal fields. This process is in fact thought to be the origin of galactic spin. However, it is not given by equation(14) which is an equation valid only in the linear regime.

3 Random Fields

The distribution of matter in the Unvierse does indeed show structure, but this structure is painted on an otherwise random density field. The question is how to best describe this situation: we need a mathematical description for a spatially random density distribution.

3.1 Specifying the Fluctuations

The cosmic density field at some time $\rho(\mathbf{x})$ can been decomposed into its mean value ρ_0, which is independent of position, plus a fluctuation:

$$\rho(\mathbf{x}) = \rho_0 + \delta\rho(\mathbf{x})$$
$$< \delta\rho(\mathbf{x}) > \; = 0 \tag{16}$$

The angular bracket here denotes the simple spatial average. The *relative density fluctuation* can then be defined as

$$\delta(\mathbf{x}) = \frac{\delta\rho(\mathbf{x})}{\rho_0} \tag{17}$$

which is a dimensionless random (scalar) function of position.[3] Specifying a random function of position is a technically difficult problem that is the subject of numerous texts, so here it will suffice to take a heuristic approach.

There are several ways of describing $\delta(\mathbf{x})$. One way is statistically: we can specify the joint probability $P(\delta_1, \delta_2, \ldots, \delta_N)$ of finding values $\delta_i = \delta(\mathbf{x}_i)$ of the density fluctuations at the points $\mathbf{x}_i, i = 1, ..., N$. This joint probability distribution may in turn be specified in terms of its statistical moments, one of which is the important *two-point correlation function* telling us how, on average, the density fluctuations at points a dsitance $\mathbf{r}$ apart are related:

$$C(\mathbf{r}) = \overline{\delta(\mathbf{x})\delta(\mathbf{x}+\mathbf{r})} \tag{18}$$

The overbar denotes the probability average. For a function $F(\delta_1, ..., \delta_N)$ defined at N points, this is given in terms of the joint probability distribution $P(\delta_1, ..., \delta_N)$ by

$$\overline{F} = \int F(\delta_1, ..., \delta_N) P(\delta_1, ..., \delta_N) d\delta_1 \ldots d\delta_N. \tag{19}$$

This probability average is an average over independent realizations of the random process $\delta(\mathbf{x})$. If the value of the probability distribution $P(\delta_1, ..., \delta_N)$ depends only on the relative configuration of the points, but not on their spatial location, the random process $\delta(\mathbf{x})$ is said to be spatially homogeneous. In this case we might be tempted to say that the probability average (19) is the same as the spatial average

$$\lim_{V\to\infty} \frac{1}{V} \int F(\delta(\mathbf{x}_1 + \mathbf{y}), ..., \delta(\mathbf{x}_N + \mathbf{y})) d^{(N)}\mathbf{y} \tag{20}$$

[3]Note that from the point of view of General Relativity $\delta(\mathbf{x})$ is not a proper scalar: it depends on the coordinate system being used. In particular we could use space-like hypersurfaces where $\delta(\mathbf{x}) = 0$ everywhere!

However, this conclusion depends on the existence of the limit and its not depending on the shape of the volume V: this is a very deep question rooted in ergodic theory.

The correlation function (18) must satisfy

$$\begin{aligned} \lim_{|\mathbf{r}|\to\infty} C(\mathbf{r}) &= 0 \\ C(\mathbf{r}) &= C(-\mathbf{r}) \\ C(\mathbf{r}) &\leq C(0) \end{aligned} \tag{21}$$

and in particular there must exist a positive function $\mathcal{P}(\mathbf{k})$ such that

$$C(\mathbf{r}) = \int \mathcal{P}(\mathbf{k}) e^{i\mathbf{k}.\mathbf{x}} d\mathbf{k}. \tag{22}$$

This function is called the *Spectral Density* or *Power Spectrum* of the random process $\delta(\mathbf{x})$. Obviously not all functions $C(\mathbf{r})$ can be correlation functions. If in addition

$$C(\mathbf{r}) = C(r) \tag{23}$$

the random process $\delta(\mathbf{x})$ is said to be isotropic.

3.2 Fourier representation

An alternative way of specifying a random field is via its Fourier representation. Essentially, we try to represent the random function as a sum of independent sine-waves in much the same way as we would represent an ordinary (non-stochastic) function in terms of its Fourier integral or a Fourier series. However, if the random field $\delta(\mathbf{x})$ is statistically homogeneous,the integral

$$\int |\delta(\mathbf{x})| d\mathbf{x} \tag{24}$$

taken over all of space need not be bounded and the usual Fourier representation will not work. This leads us to consider a function $\delta(\mathbf{x}, V)$ defined on a finite volume V such that

$$\delta(\mathbf{x}) = \delta(\mathbf{x}), \quad \mathbf{x} \in V$$

$$= 0, \qquad \mathbf{x} \notin V. \tag{25}$$

The Fourier integral of this function exists:

$$A(\mathbf{k}, V) = \frac{1}{2\pi^3} \int \delta(\mathbf{x}, V) e^{-i\mathbf{k}.\mathbf{x}} d\mathbf{x} \tag{26}$$

where the integral is taken over all space. The problems arise because the limit of this integral as $V \to \infty$ diverges. This means that strictly speaking we cannot write

$$\begin{aligned} a(\mathbf{k}) &= \frac{1}{2\pi^3} \int \delta(\mathbf{x}, V) e^{-i\mathbf{k}.\mathbf{x}} d\mathbf{x} \\ \delta(\mathbf{x}) &= \int e^{i\mathbf{k}.\mathbf{x}} a(\mathbf{k}) d\mathbf{k} \end{aligned} \tag{27}$$

as a Fourier transform pair, since the first of these integrals does not exist. Nevertheless, these two equations are commonly seen in the literature.[4] Note that the amplitudes $a(\mathbf{k})$ are complex numbers.

3.3 The Power Spectrum

The Fourier transform of the correlation function $C(\mathbf{r})$ must exist and it is positive (see equation (22) - if this were not the case the function $C(\mathbf{r})$ would not be the correlation function of a stationary random process). Let us allow ourselves to be less than rigorous and accept equations (27) as being meaningful. The function $a(\mathbf{k})$ is then a random function of position in $\mathbf{k}$ space, and we can talk about the

[4]It may be of interest to give the formally correct version of these equations. If we consider an elemental volume $d\mathbf{k}$ of $\mathbf{k}$-space we can define a quantity denoted as $dZ(\mathbf{k})$ by

$$dZ(\mathbf{k}) = \frac{1}{(2\pi)^3} \int \delta(\mathbf{x}) e^{-i\mathbf{k}.\mathbf{x}} \left(\frac{e^{-idk_1 x_1} - 1}{-ik_1} \right) \left(\frac{e^{-idk_2 x_2} - 1}{-ik_2} \right) \left(\frac{e^{-idk_3 x_3} - 1}{-ik_3} \right) d\mathbf{x}. \tag{28}$$

We have written this out relative to a specific choice of coordinate system in which $\mathbf{x}$ has coordinates (x_1, x_2, x_3). The inverse of this integral exists and can be written as:

$$\delta(\mathbf{x}) = \int e^{i\mathbf{k}.\mathbf{x}} dZ(\mathbf{k}) \tag{29}$$

where the integration is over all wavenumber space and the integral is to be regarded as a stochastic Fourier-Stieltjes integral. These equations are the formally correct versions of equations (27).

correlations between the amplitudes a at two different values of $\mathbf{k}$. It turns out that the amplitudes for different values of $\mathbf{k}$ are statistically independent, and so we can simply write

$$< a^*(\mathbf{k})a(\mathbf{k}') >= \mathcal{P}(\mathbf{k})\delta^{(3)}(\mathbf{k}-\mathbf{k}'). \tag{30}$$

(In this context, $\delta^{(3)}(\mathbf{x})$ is the Dirac delta function in three dimensions.) This is just the reason we do Fourier analysis of ordinary (non-stochastic) functions: the functions are resolved into independent components.

It is this statistical independence of the amplitudes for different wavenumbers that makes the Fourier representation of the density fluctuation field so useful: it means that the statistical properties of these amplitudes is described by a single function - their variance. It is an important theorem that the function $\mathcal{P}(\mathbf{k})$ in equation (30) is the same function appearing in the Fourier representation of the correlation function, equation (22): it is the spectral density, or power spectrum, of the process $\delta(\mathbf{x})$. [5]

We have seen that the mean square of the amplitudes is given as a function of frequency by the power spectrum. However, to do anything useful we need to specify their underlying statistical distribution. Certainly the most convenient assumption is that these amplitudes are selected from a Gaussian distribution whose variance is given by the power spectrum. Remember that the amplitudes are complex numbers (they arise out of a Fourier transform). The relationship between the real and imaginary part of the amplitude is called the *phase*. If we write the complex amplitude $a(\mathbf{k})$ in angular coordinates in the complex plane $a(\mathbf{k}) = |a(\mathbf{k})|e^{i\theta}$,

[5]Note that $\mathcal{P}(\mathbf{k})$ is indeed a density: it is the contribution of modes of wavenumber $\mathbf{k}$, per unit volume of wavenumber space, to the total variance of the random process $\delta(\mathbf{x})$. This can be seen by noting that equation (22) for zero lag $\mathbf{r}$ is just

$$\overline{\delta(\mathbf{x})\delta(\mathbf{x})} = \int \mathcal{P}(\mathbf{k})d\mathbf{k}. \tag{31}$$

The left hand side is the variance of the random process $\delta(\mathbf{x})$ and so we see that $\mathcal{P}(\mathbf{k})$ is the contribution to this variance from wavenumbers in the interval $[\mathbf{k}, \mathbf{k}+d\mathbf{k}]$. Note that $\mathcal{P}(\mathbf{k})d\mathbf{k}$ is dimensionless. If the power spectrum depends on the wavenumber k, and not on the direction of the vector $\mathbf{k}$, we can write

$$\mathcal{P}(k)d\mathbf{k} = 4\pi k^2\mathcal{P}(k)dk = 4\pi k^3\mathcal{P}(k)d\ln k. \tag{32}$$

So in the rather usual case when the power spectrum depends only on the magnitude of the wavevector, $4\pi k^3\mathcal{P}(k)$ is the contribution to the variance of the fluctuations per unit logarithmic interval of k.

then under the assumption that the real and imaginary parts of the amplitudes are Gaussian, the modulus $|a(\mathbf{k})|$ is Rayleigh- distributed and the phase θ is uniformly distributed.

3.4 $\xi(r)$, $\mathcal{P}(k)$, variances and so on.

The fact that the power spectrum and the correlation function are a Fourier transform pair means that we can talk in either language: it is generally a matter of taste. If the random process is homogeneous and isotropic:

$$\mathcal{P}(k) = \frac{1}{(2\pi)^3}\int \xi(r)e^{-i\mathbf{k}.\mathbf{r}}d^3\mathbf{r} = \frac{1}{2\pi^2}\int_0^\infty \xi(r)\frac{\sin kr}{kr}r^2dr \qquad (33)$$

The inverse form is easily calculated and is left as an exercise. The variance of the fluctuations per unit logarithmic interval of k (see equation (32) is then

$$\Delta^2(k) \equiv 4\pi\mathcal{P}(k) = \frac{2}{\pi}k^3\int_0^\infty \xi(r)\frac{\sin kr}{kr}r^2dr. \qquad (34)$$

If $\xi(r) \propto r^{-\gamma}$ then $\Delta(k) \propto k^\gamma$.

3.5 Normalization

In order to compare numerical models with the observed Universe, we have to stop the evolution of the numerical model at some appropriate time that can be regarded as "today". The variance of the galaxy counts on a scale of $8h^{-1}$ Mpc. is observed to be unity, and so if the galaxies really traced the mass distribution, we could use this observation to stop the N-Body model: "run until the variance of the density fluctuations on a scale of $8h^{-1}$ Mpc. reached unity". However, galaxies do not necessarily trace the mass, and so we need an assumption to relate the observed fluctuations in galaxy number density to the (unobservable) fluctuations in the mass density. For simplicity, I shall confine the rest of this section to a discussion of the case $\Omega = 1.0$.

The hypothesis that is generally adopted is that the variance in the fluctuations in the mass density are proportional to the *variance* of the fluctuations in the galaxy density. Symbolically:

$$\frac{\delta N}{N} = b\frac{\delta \rho}{\rho} \tag{35}$$

The constant of proportionality b is called the *bias factor*, we shall discuss the motivation for this model in more detail in section 5. Since on scales of $8h^{-1}$ Mpc. the lefthand side is unity, our models have to be stopped when

$$\left(\frac{\delta \rho}{\rho}\right)_{8h^{-1}\ \mathrm{Mpc.}} = \frac{1}{b}, \quad \Omega = 1 \tag{36}$$

We shall see how to specify the variance of the density fluctuations in terms of the power spectrum below (see equation (39) below). Although this is straightforward in principle, in practise the situation is a little more complicated. The normalisation is done using the power spectrum of the initial conditions scaled to the present using linear theory, rather than the power spectrum at a given time in the simulations.

4 The Spectrum of Fluctuations

4.1 Windows and Spectra

Physically, we can measure neither the value of the density fluctuations, $\delta(\mathbf{x})$, at a point nor the associated the Fourier amplitude $a(\mathbf{k})$. Because our instruments have finite resolution we always measure an average of $\delta(\mathbf{x})$ relative to some measurement window. In general physics problems, this measurement window has a response that varies as a function of distance from the point of measurement, the specific dependence being a characteristic of the measurement apparatus.

The simplest window function is the hard sphere with which we measure with equal weight all values of the field within a specific radius R, and nothing outside of that radius. This is the so-called *top hat* window. We can imagine putting spheres of radius R down at random places in the sample volume and recording the mass M enclosed in every sphere. There will be a mean mass $< M >$ for this sample and the variance of the mass is

$$\sigma_M^2 \equiv \left(\frac{\delta M}{M}\right)^2 = \left\langle \frac{(M - < M >)^2}{< M >^2} \right\rangle \tag{37}$$

It can be shown that this is expressible in terms of the power spectrum of the process $\delta(\mathbf{x})$ as

$$\left(\frac{\delta M}{M}\right)^2 = \int W^2(kR)\mathcal{P}(\mathbf{k})d\mathbf{k}. \tag{38}$$

where the window function W is given by

$$W(kR) = \frac{3}{(kR)^3}(\sin kR - kR\cos kR). \tag{39}$$

This window function is just the Fourier transform of a uniform spherical volume, appropriately normalised. $W(kR)$ is proportional to the Bessel Function $j_1(kR)$: it is positive until $K_0 \sim 2\pi/R$ and then oscillates. Hence the main contribution to the integral (38) comes from low frequency wavenumbers $k < 2\pi/R$. The higher frequencies all oscillate within the top-hat volume and so their contributions cancel.

If we take a simple power law power spectrum

$$\mathcal{P} \propto k^n \tag{40}$$

then it is clear that the integral (38) can be estimated as

$$\left(\frac{\delta M}{M}\right)^2 \sim R^{-(n+3)} \tag{41}$$

and expressing the mass contained in the top-hat as $M \propto R^3$ we have in the standard "sloppy" notation for the variance:

$$\left(\frac{\delta M}{M}\right) \sim M^{-\frac{n}{6}-\frac{1}{2}} \tag{42}$$

This is a useful way of thinking of the random density field associated with a power-law power spectrum of index n. The variance in the density fluctuations averaged over spheres containing a mas $\sim M$ falls of as $M^{-(n+3)/6}$. Note that in the special case $n = 0$ (*white noise* fluctuations) we have $\sigma_M \propto M^{-\frac{1}{2}}$, this corresponds to the familiar "$\sqrt{N}$" fluctuations.

4.2 The Harrison-Zel'dovich Spectrum

The power spectrum of density fluctuations in the Universe is determined by the physical processes that generated them - this is one of the outstanding problems concerning the physics of the earliest stages of the cosmic expansion. In the absence of any generally accepted theory, it is generally assumed that the power spectrum of the fluctuations depends only the magnitude of the wavevector k and not its direction, and furthermore we generally assume a power law form

$$\mathcal{P}(\mathbf{k}) \propto k^n \tag{43}$$

for some index n (the "spectral index". A special case of this is the *Harrison-Zel'dovich spectrum* which has the form

$$\mathcal{P}(k) \propto k \tag{44}$$

There are various reasons why such a simple power law form might be expected on the basis of inflation theories for the origin of primordial fluctuations. This form of the spectrum is distinguished physically by the fact that the potential fluctuations associated with such density perturbations all have the same amplitude, independent of the mass scale. In this sense, the Harrison-Zel'dovich spectrum is truly scale-independent and is characterised by one number: the amplitude of the potential fluctuations.

If we use the Harrison Zeldovich spectrum (44) in equation (42) for the mass fluctuations we find that

$$\frac{\delta M}{M} \propto M^{-2/3}, \quad \text{Harrison- Zel'dovich} \tag{45}$$

The fluctuation in the gravitational potential associated with this mass fluctuation is

$$\delta\phi \propto G\frac{\delta M}{R} \sim G.\frac{\delta M}{M}.\frac{M}{R} \sim G.M^{-2/3}.M^{2/3} \sim \text{constant} \tag{46}$$

independent of M. (The last step follows because $M \propto R^3$). The fluctuations in the gravitational potential in a density distribution described by the Harrison Zel'dovich ($n = +1$) power spectrum are independent of scale.

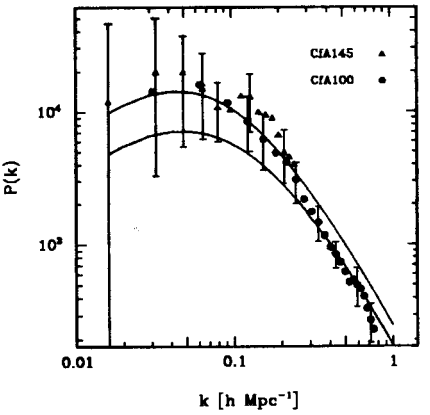

Figure 1: *Power Spectrum of galaxy clustering as determined from the CfA Redshift Survey. The two lines represent standard CDM models having different normalizations. No one model can fit the entire range of scales. (After Vogely et al., 1992)*

This is an important feature of the Harrison-Zel'dovich spectrum. This is the spectrum that is "predicted" by many (though not all) inflationary theories for the very early Universe. This scale independent amplitude must be a constant of nature that is to be determined from the theories. It determines the epoch at which structure in the Universe formed.[6]

4.3 The observed power spectrum

Comparing the Harrison Zel'dovich spectrum with observation is not that easy. Observing the $n = 1$ part of the spectrum involves going to enormous scales, and the only realistic hope here is to measure the spectrum on those scales via the spectrum of microwave background fluctuations. Determining the spectrum on smaller scales can be done from galaxy surveys: (figure 1) shows an example of this and the comparison with some models. To make this comparison it is necessary for the models

[6]Power law spectra have divergences either on large scales or on small scales if they extend over infinite range. The $n = 1$ spectrum has the unique property of doing violence to the geometry of space-time on both large and small scales!

to say something about the galaxy formation process in order to relate fluctuations in the galaxy distribution to fluctuations in the mass distribution (biasing). Hence it is only possible to check the Harrison Zeldovich spectrum for consistency on these scales.

Figure 1 shows the data and compares with tthe predictions of a standard Cold Dark Matter cosmological model. What is clear is that, relative to this model, there is a lot of power on large scales (small k). If the models are scaled to fit the small (nonlinear) scales, they have too little power on large scales. Conversely, if the fit is adjusted to the largest scales we have a problem on galaxy scales. The excess power in the projected two-point angular correlation function from the APM survey (Maddox et al., 1990) is further evidence for this. Most importantly, the quadrupole component of the Microwave Background anisotropy indicates more power on large scales than is consistent with a standard CDM model normalised to a scale of $8h^{-1}$ *Mpc*. The simplest way of dealing with this problem is to abandon the idea that $n = 1$ and make n somewhat lower. This is referred to as *tilting* the power spectrum.

However, given our ignorance of the galaxy formation process, it is arguable that the large scales should be fitted with the Harrison Zel'dovich spectrum and that we should not be too bothered about a factor two or so disagreement in the small scale amplitudes.

4.4 Evolution of the spectrum

Perturbations stop growing under the influence of gravitation when they enter the horizon during the fireball phase of the cosmic expansion. Moreover, the Harrison-Zel'dovich spectrum is such that all perturbations enter the horizon with the same amplitude. Thus the variance of the amplitude of the density fluctuations is scale independent for that range of scales such that the perturbations enter the horizon during the fireball phase.

What this means is that, for an initially Harrison Zel'dovich spectrum, the spectrum of fluctuations that emerges from the fireball at recombination has constant amplitude on small scales, and the primordial spectrum on large scales. This is described by a *Transfer Function* $T(k)$ which maps the primordial $\mathcal{P}(k) \propto k$ spectrum into the postrecombination spectrum:

$$k^3\mathcal{P}(k) = A\left(\frac{k}{k_0}\right)^4 T^2(k)$$
$$T^2(x) = \frac{1}{\left(1+[ax+(bx)^{3/2}+(cx)^2]^\nu\right)^{2/\nu}} \tag{47}$$

The value of the amplitude A is fixed by the normalisation of the present day fluctuations in mass density on scales of $8h^{-1}$ Mpc. (cf. equation (36)). The equation for $T(k)$ is a fitting formula and in the case of the standard Cold Dark Matter model with $\Omega_0 = 1$ the coefficients have the values

$$a = 6.4h^{-1}\ \text{Mpc.}\quad \text{b} = 3.0\text{h}^{-1}\ \text{Mpc.}\quad \text{c} = 1.7\text{h}^{-1}\ \text{Mpc.}\quad \nu = 1.13 \tag{48}$$

(Bond and Efstathiou, 1984; there are several other variants on this formula in the literature). The central issue about this formula is that for small scales (large k) $T^2(k) \propto k^{-4}$ and so $k^3\mathcal{P}(k) \sim$ *constant*, whereas on large scales (small k) $T^2(k) \sim 1$ and $\mathcal{P}(k) \sim k$ as per the Harrison Zel'dovich spectrum.

5 Biasing

5.1 Relating Mass and Light

We do not know the relationship between the distribution of light in the Universe as traced by luminous galaxies and the distribution of mass. It would be perverse indeed if they were not related: we would then have dark clusters and the peculiar motions of galaxies relative to the Hubble flow would not be related to the density field as determined from the galaxies themselves. Of course, we might eventually hope to check observationally for the existence of substantial amounts of nonluminous gravitating material: we might use gravitational lensing to do that.

Failing any direct link between the distributions of luminous matter and the mass distribution, we are forced to postulate a relationship that might be checked *a posteriori*. The conventional assumption is that the *fluctuations* in the light distribution are proportional to the *fluctuations* in the mass distribution. Symbolically:

$$b = \frac{\delta l/l}{\delta\rho/\rho}. \tag{49}$$

b is called "the bias parameter". Here l represents the luminosity density and ρ represents the mass density. In fact, our catalogues provide us with galaxy counts and we like to think about the mass distribution, so this last equation is frequently written

$$b = \frac{(\delta N/N)_{gal}}{(\delta M/M)} \tag{50}$$

where N is the galaxy number in a given volume and M is the mass in that volume. These last two equations are simply a rephrasing of equation (35).

5.2 Biasing mechanisms

There are many possible reasons why b might not be unity (see Dekel and Rees, 1987). Galaxy formation (the creation of luminous systems) may be a phenomenon that is nonlinearly related to the local density fluctuations, the efficiency of galaxy formation may depend on environment through nongravitational effects such as the photoionisation of the pregalactic intergalactic medium by QSO's, or other non-gravitational forces may control the galaxy formation process. Once we know more about the way in which galaxies formed we should be able to predict a value for b, but that seems to be some way off.

We have seen that N-Body models must be adjusted so that they give the correct mean deviation from the Hubble flow when the clustering in the model has grown to a level corresponding to what is observed (equation (36)). This adjustment is justified by the fact that the clustering in the model refers to the clustering in the mass distribution, not the clustering of the light distribution - the models have nothing to say about light. In order to make that link in these models we introduce a naive "light formation model" using a single scale-independent value of b such that when the model has the "correct" non-Hubble motions, it also has the "correct" amount of clustering on all scales.[7]

A simple recipe for applying biasing to N-Body models is *threshold biasing* in which only those density fluctuations having amplitudes greater than a certain threshold value on some scale will lead to the formation of luminous material. For

[7]It is not of course necessarily the case that there exists such a b in any given model. It is simply fortunate that for those models of cosmic structure evolution of primary interest we can in fact do this. Maybe galaxy formation is not so perverse after all!

convenience, this prescription is applied to the starting conditions in the N-Body model while the density fluctuations on all scales are still linear. This process is illustrated schematically in figure 2 where we show the distribution of density fluctuation amplitude along a line. The distribution has been smoothed to the scale on which the bias is to be applied, and the points of interest are the peaks where the density fluctuations rise above some threshold. These are the putative sites of formation of the galaxies which we will use to compute the galaxy clustering once the model has been evolved.

The threshold for this biasing is given in terms of the variance of the fluctuations, σ, in the starting conditions:

$$\delta_{bias} = b\sigma \tag{51}$$

This notion was introduced in a very important paper by Kaiser (1986)[8] who showed that in linear theory the clustering correlation function of the points above the threshold was simply related to the correlation function of the underlying random process by

$$\xi_{biased}(r) = e^{b^2\xi(r)} - 1, \quad \simeq b^2\xi(r) \qquad (b \gg 1) \tag{52}$$

The higher the threshold relative to the variance, the rarer is the galaxy formation process and the more clustered are the objects that form. Threshold biasing boosts the correlations.[9] This simple idea is certainly very attractive. Not only does it solve a problem in N-Body models by providing another free parameter which can be tuned to related velocity fields and clustering, but it has some rather nice consequences for galaxy formation. Elliptical galaxies are more clustered than spirals and are found mainly within rich clusters of galaxies. This might be explained by saying that different values of the bias threshold lead to different types of galaxy. Indeed, the suggested values for the standard CDM models were (Frenk et al., 1990)

$$b_{Spirals} = 1.5 \qquad b_{Ellipticals} = 2.0 \tag{53}$$

Since the higher threshold is more likely to be achieved where there is some underlying larger scale clustering (see figure 2) this suggested a natural reason why

[8]Kaiser, in this paper and in discussions leading up to it, was probably the first person to suggest the need for biasing and to make the idea explicit in terms of threshold biasing.

[9]A lot of work was done in the late 1980's discussing different biasing prescriptions ("peak biasing" for example). Many papers appeared on the statistics of thresholded density distributions and peaks in random fields, the "classical" paper being that of Bardeen et al. (1986), now known simply as "BBKS".

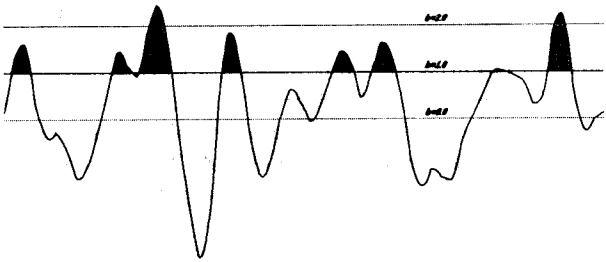

Figure 2: *Threshold biasing in a 1-dimensional random field*

ellipticals should be found more often in clusters than spirals. Of course, there is no *mechanism* here, but that is seen as a problem of the details of the galaxy formation process.

5.3 Measuring b (or $b/\Omega^{0.6}$)

In practise we would replace $\delta l/l$ by the variance of the luminosity distribution $\sigma_l(r)$ on some given scale and $\delta\rho/\rho$ by the variance of the mass density on the same scale, $\sigma_m(r)$:

$$b_r = \frac{\sigma_l(r)}{\sigma_m(r)}. \tag{54}$$

As a first approximation we could assume that b is a universal constant, though we would not be surprised if eventually it were found to be scale dependent. In a worse case we might envisage that b depends on position as well as scale.

From the point of view of observation we might be able to determine $\sigma_l(r)$ from galaxy counts and $\sigma_m(r)$ from the dynamics of the non-Hubble flow of the

galaxies. In this case we fix on some convenient scale where we can reasonably relate the non-Hubble flow to the local mass density. Conventionally we pick $8h^{-1}$ Mpc. for this scale since the variance of the luminosity density averaged over spheres of radius $8h^{-1}$ Mpc. thought to be about unity and therefore nominally in the so-called "linear regime".[10]

There is a subtle point here: the variance $\sigma_l(8h^{-1}$ Mpc.) refers to the variance in real space - not redshift space. So determining this requires a model of the distortion of the real space by the nonHubble redshifts. If we do the job statistically, we can apply the correction due to Kaiser (1987):

$$\sigma_z^2(r) \simeq \left(1 + \frac{2}{3}\frac{\Omega^{0.6}}{b_r} + \frac{1}{5}\frac{\Omega^{1.2}}{b_r^2}\right)\sigma_{real}^2(r) \tag{55}$$

relating the variance of the luminosity in real space to what is observed in redshift space. It should be emphasised that this is a *linear theory* result and so we would not want to apply it to scales where σ_l were greater than unity.

[10]In hindsight, it might in fact have been wiser to take a larger scale where linearity is more certain.

Chapter 45

Peculiar Velocity Fields

The point of making a redshift survey is to locate the galaxies in space. This allows a direct determination of the spatial correlations of galaxies and in addition allows us to make a deeper study of the galaxy motions relative to the matter distribution, hopefully pointing a finger at the value of Ω_0.

The first approximation to the spatial distance of a galaxy along the line of sight is simply to use the Hubble Expansion Law. Because galaxies have non-Hubble velocity components, this simple reconstruction of the three-dimensional distribution is distorted by the addition of a velocity component that correlates with the local density. This can be seen in the de Lapparent slice picture shown in figure 1: there is a strong radial pattern in the distribution of the points.

Several techniques have been devised for improving on this. One obvious strategy is to use additional information about the distances to the galaxies, such as a redshift independent distance indicator. That does not solve the problem since the inaccuracies of in distance indicators preclude making a non distorted map directly. The alternative method is to use the fact that peculiar velocities and densities are correlated to reconstruct a map that is dynamically self-consistent.

1 The Velocity-Density relationship

It can be shown (see Peebles, LSSU equations (8.2) and (14.2)) that in linear theory the relationship between the peculiar velocity field $\mathbf{v}$ and the fluctuating gravitational force $\mathbf{g}$ is

$$\mathbf{v} = \frac{2}{3H\Omega^{0.4}}\mathbf{g} \tag{1}$$

where, by virtue of the perturbed Poisson equation, the fluctuating force $\mathbf{g}$ is related to the distribution of relative density fluctuations $\delta(\mathbf{x}) = \delta\rho/\rho$:

$$\mathbf{g}(\mathbf{x}) = Ga(t)\Omega\rho_c \int \frac{\mathbf{x}' - \mathbf{x}}{|\mathbf{x}' - \mathbf{x}|^3}\ \delta(\mathbf{x}', t)\ d^3\mathbf{x}' \tag{2}$$

Note that equation (1) is perfectly simple: if $\Omega_0 = 1$ then $2/3H_0$ is just the age of the Universe, and so this equation simply says $\mathbf{v} = \mathbf{g}t$.

The mass density fluctuations $\delta\rho/\rho$ are supposed to be related to the fluctuations $\delta n/n$ in the observed galaxy density via the bias parameter b:

$$\frac{\delta n}{n} = b\frac{\delta\rho}{\rho} \tag{3}$$

Obviously b could be a function of the local density, $b = b(n)$, or even worse it might not be a universal function. At this first exploratory stage the simplest assumption to make is that $b = constant$, and to try and determine this constant as yet another one of the constants of cosmology. The iteration method decribed below allows b to be one of the parameters involved in making the fit and so b (in fact $b\Omega^{-0.6}$) can be determined self-consistently. If it should turn out that the data analysis gives rise to inconsistencies with prior expectations based on models, then this is obviously the first place to look for a resolution of the problems.

So what we observe is

$$\mathbf{v} = \frac{2}{3H_0}G\rho_c\frac{{\Omega_0}^{0.6}}{b}\int \frac{\mathbf{x}' - \mathbf{x}}{|\mathbf{x}' - \mathbf{x}|^3}\ \frac{\delta n(\mathbf{x}')}{n}\ d^3\mathbf{x}' \tag{4}$$

Note that there is a normalization factor $\Omega_0^{0.6}/b$ to be fitted when relating the variations in the luminosity with the peculiar velocities. Note also that decreasing b increases $\mathbf{v}$, for a given luminosity distribution.

The upshot of this is that methods for determining Ω_0 that compare velocity fields with density fluctuations in fact only determine $\Omega_0 b^{-5/3}$, and we need to get b from somewhere else (usually a theoretical prejudice based on an N- body model!).

It is worth making some comments about applying equation (4) to data. The integral should involve the entire universe, but in practise only the survey volume can be used. There is also a problem that arises when the density field becomes nonlinear, the velocity field can then become triple valued (due to shell crossing). Hence the velocity field prediction will not be as good as the density field prediction in such a method.

The relation (4) between velocity and density fluctuations can be inverted to express the density fluctuations in terms of the density field

$$\Omega^{0.6} H \delta = -\nabla.\mathbf{v} \tag{5}$$

If redshift independent distances are available we have a direct estimate of $\mathbf{v}$ and hence of $\nabla.\mathbf{v}$. These can then be used to produce a consistent map of the density field via a relationship like (5), which in turn can lead to a reassessment of the peculiar velocities and so on. The map can be iterated in just the same way as before, only this time we go the other way around and use the peculiar velocity field to deduce the density field.

2 IRAS and other redshift surveys

If we have no independent distance estimators to individual galaxies we have to use the observed density distribution together with a dynamical model to estimate the peculiar velocities that are consistent with the inferred density. The peculiar velocities can then be subtracted from the observed radial velocities to give a better impression of the density field. The process can then be cycled until convergence is obtained. We can start the process off with a redshift survey to make a first estimate of the local density fluctuations on the assumption the redshift reflects true distance.

The two surveys based on IRAS use slightly different selection criteria for finding galaxies in the IRAS catalogue. The Strauss et al. (1992) survey uses all nonstellar objects having a $60\mu m$ flux greater than 1.9 Jansky, yielding a sample of

over 2500 objects out to a distance corresponding to a redshift of $\simeq 3000$ km. s^{-1}. The QDOT survey (Saunders et al., 1990) selects 1 galaxy randomly out of 6 down to a flux limit of 0.6 Jansky, giving a sample of more than 2000 galaxies out to a distance corresponding to a redshift of $\simeq 7000$ km. s^{-1}.

Because of the far infrared nature of the IRAS survey, elliptical and earlytype galaxies are absent from the surveys, and hence the surveys do not contain most of the galaxies in rich galaxy clusters like Coma. Nonetheless, they do appear to trace the known features in the universe. Accordingly, a correction has to be applied to take account of the missing galaxies when reconstructing the galaxy density field. This correction comes over and above any correction for the bias factor.

3 Surveys with independent distance estimates

If we have redshift independent distance estimates, then we can avoid the step of deducing the peculiar velocity field from the apparent density inhomogeneities. This approach is called the "POTENT" method and has been used taken by Bertschinger and Dekel and their collaborators (Bertschinger et al., 1990). We shall describe this at some length below.

Redshift independent distance estimates can come either from Fisher-Tully type relationships relating the peak rotational velocities of disk galaxies to their absolute magnitude in some waveband, or from the so-called $D_n - \sigma$ relationships relating the central velocity dispersions of elliptical galaxies to the actual diameter of a particular isophote in the galaxy light distribution. The root mean square errors of these techniques are 15% and 21% respectively, and this gives rise to quite large distance errors. The analysis therefore has to be done rather carefully.

This process has a number of advantages. The velocity field divergence is a direct measure of the mass distribution, and so what lies outside the data volume is not relevant. The data sample does not even have to be complete, where we have data we can rebuild the density field. However, there is the serious disadvantage that redshift independent distances are not available for large numbers of galaxies and so the sampling of the universe is necessarily sparser than we would like. Currently, a sample of around 1000 galaxies has been used.

Comparison between the results from these two approaches is very interesting. If the assumptions underlying the methods are correct, there should be

substantial agreement between the reconstructed maps of the universe. In particular, we shall be interested in comparing the bias parameters b (or the bias functions $b(n)$) derived from the two methods.

4 The problem and the POTENT solution

The galaxy redshift surveys for which there are velocity independent distance estimates for the sample galaxies have revealed substantial deviations from uniform Hubble flow. There might be, because of the uncertainty in the distance estimation procedure, some room for scepticism. However, the fact that we already observe a "large" velocity for the Local Group relative to the microwave background radiation and that different samples yield consistent results encourages us to go on and ask the question "what is the cosmological implication of these deviations?".

The first studies of the deviations showed large scale coherence in the peculiar (ie: non-Hubble) component of the velocity field. In particular they showed evidence for the so-called "Great Attractor" in the direction of the Hydra-Centaurus clusters of galaxies. These early studies relied either on the use of the radial component of the peculiar velocity, or on the fitting of a specific model for the Great Attractor and its environment (Lynden-Bell et al. 1988). While such models give an indication of what the Great Attractor is, one is left with a very large parameter space of possible models none of which has an a priori dynamical justification.

This model-fitting situation has been dramatically improved by the discovery of Bertschinger and Dekel (1989) that one could, on the basis of a few reasonable assumptions, reconstruct the entire three dimensional velocity field given only the radial peculiar velocity data for a sample of galaxies. Moreover, the sample does not have to be a complete sample (though where there are most galaxies the reconstruction of the cosmic flow field is obviously most reliable). Bertschinger, Dekel, Dressler and Faber, in a recent series of papers, have applied the technique to a compendium of redshift samples that allow the universe to be mapped out to a distance of 6000 km.s.$^{-1}$.

This discovery has given new impetus to radial velocity surveys and to getting velocity independent distance estimates for individual galaxies.

5 Reconstructing the 3-d Flow

5.1 The comoving coordinate q-space

In Zel'dovich's approximation for the growth of large scale structure [1] the position $\mathbf{r} = a(t)\mathbf{x}$) of a particle that started off at comoving coordinate $\mathbf{q}$ is given by an equation of the form:

$$\begin{aligned} \mathbf{x}(t) &= \mathbf{q} + \beta(t)\nabla S(\mathbf{q}) \\ (\beta &= (t/t_0)^{\frac{2}{3}} \quad \text{for} \quad \Omega_0 = 1) \end{aligned} \tag{6}$$

Here, the function of position $S(\mathbf{q}$ is to be thought of as a function specifying the initial perturbations in the distribution of matter (see below). This equation resembles the familiar equation $\mathbf{x} = \mathbf{x}_0 + \mathbf{u}t$ describing a particle moving with velocity $\mathbf{u}$ under no forces. This resemblance is more than a coincidence and reflects the very nature of the Zel'dovich approximation.

The density fluctuations are given in terms of S by

$$\frac{\delta\rho}{\rho} = \beta\frac{\partial^2 S_0}{\partial \mathbf{q}^2} \tag{7}$$

and in the case $\Omega_0 = 1$ this grows as $t^{2/3}$, the familiar perturbation theory result. From equation (6) it can be shown that the peculiar velocity of a particle that was initially at $\mathbf{q}$ is given by

$$\mathbf{V} = a(t)\dot{\beta}(t)\frac{\partial S_0(\mathbf{q})}{\partial \mathbf{q}} \tag{8}$$

In other words, the present peculiar velocity field $\mathbf{v}$ is expressible as the gradient of a function βS *expressed in comoving coordinates*: $\mathbf{V} = a(t)\nabla_{\mathbf{q}}(\dot{\beta}S)$. Since we do not in fact observe the position of a galaxy in $\mathbf{q}$-space, we would have to make a transformation from $\mathbf{q}$-space to the $\mathbf{r}$- space of our observations. Formally this corresponds to going from a Lagrangian description of the large scale flow to an Eulerian description. It turns out that we should make this transformation iteratively, as we shall see below.

[1] See the lectures of Stephan Gottlöbber in this volume for details.

5.2 The three-dimensional velocity field

In the above approximation the peculiar velocity is the gradient of a velocity potential Φ, and so we can write

$$\begin{aligned} \mathbf{V} &= -\nabla_{\mathbf{q}}\Phi(\mathbf{q}). \\ \Phi(\mathbf{q},t) &= -a\dot{\beta}S(\mathbf{q},t_0). \end{aligned} \tag{9}$$

There is a formal solution to this equation giving Φ in terms of a line integral of $\mathbf{V}$:

$$\Phi(\mathbf{q}) - \Phi(\mathbf{O}) = \int_{\mathbf{O}}^{\mathbf{q}} \mathbf{V}.\mathbf{dl} \tag{10}$$

The integral can be taken over any path from $\mathbf{O}$ to $\mathbf{q}$, and in particular a radial path in the comoving coordinate $\mathbf{q}$-space. This particular choice of path involves only the *radial* component of the velocity. In $\mathbf{q}$-space spherical polar coordinates (q,θ,ϕ):

$$\Phi(\mathbf{q}) = \int_0^q V_r(q',\theta,\phi)dq'. \tag{11}$$

We have set the potential equal to zero at the origin since we don't need its value, only its derivatives. Having got Φ at all points we can then determine the *three-dimensional* velocity field from it by doing

$$\mathbf{V} = -\nabla_{\mathbf{q}}\Phi(\mathbf{q}). \tag{12}$$

The projection of this velocity along the line of sight is the contribution of the peculiar velocity to the observed recession velocity. Thus we can improve our estimate of the true distance to the galaxy.

We seem to have got something for nothing! In fact it was not for free. The price we had to pay was the assumption that the velocity field was derivable from a potential.

5.3 Getting to grips with physical space

Given a galaxy with radial velocity cz and velocity independent distance estimate r, the peculiar radial velocity is

$$V_r = cz - H_0 r. \tag{13}$$

In principle, one could just plug this into the integral on the right hand side of equation for Φ, get Φ and differentiate to get $\mathbf{V}$. This is unfortunately not so easy because this last equation refers to quantities measured in the present physical space, not the comoving coordinate space demanded by the equations (5).

It could of course be argued that we walked into a trap by starting off with the Zel'dovich approximation, which is a Lagrangian description of what goes on, rather than an Eulerian description.

The preceding discussion is that it all takes place in the comoving coordinate q-space. We don't know what this looks like until we know the relation between the present location and velocities of galaxies and the initial conditions. It is just this relationship that is expressed by the Zel'dovich approximation (6). So the situation is somewhat circular, we have to guess what the q-space looks like, calculate where the galaxies ought to be today, and then correct our guess.

5.4 Real Data: sparseness and noise problems

So far, everything has been theoretical, dealing with continuous fields. These fields are, however, sampled at discrete points where observed galaxies happen to lie. The data is also very noisy in the sense that the error bars on the distance estimators are relatively large.

The galaxy sample comes from a number of quite different catalogues. Within a sphere of radius 8000 km.s.$^{-1}$ there are around 500 E/S0 galaxies taken from the "S7" survey, from surveys of individual southern hemisphere clusters and from a survey of the great attractor region. In addition to that there are some 200 S galaxies coming from galaxy cluster surveys. Within a sphere of radius 3000 km.s.$^{-1}$ there are around 200 nearby field spirals distributed over the whole sky.

The distance estimators are different for the various subsamples, but generally have an accuracy of around 20%. This can give rise to errors in the peculiar radial velocity estimate for a single galaxy of 1000 km.s.$^{-1}$ or more.

The way this problem is handled is to smooth the data over large scales, and to use maximum likelihood to estimate the bulk flow within spherical Gaussian

windows.

6 Dipole Motion

We can determine our motion relative to the frame of reference defined by distant galaxies quite simply: the galaxies at a given distance from us should show a dipole distribution of velocities cantered on the apex of our motion. This requires however that we know something about the distance of the galaxies that is independent of the redshift. This raises difficulties in defining the galaxy sample and then getting to the answer: a story that now goes back almost twenty years.

The ultimate measure of the direction of our motion is that given by the dipole component of the cosmic microwave background radiation field (see section 5. In principle, any sample of distant objects that traces the mass distribution fairly should converge to this velocity and direction as the sample gets deeper. This is the issue of *dipole convergence.*

It is also to be expected that different samples should converge on the same values. Thus the dipole motion determined from a sample of optically selected galaxies should be the same as the dipole motion determines from a sample of IRAS selected galaxies. If there were any disagreement this might indicate that the galaxies in these two samples are not equivalent tracers of the mass distribution (Lahav et al, 1988).[2] Of course before jumping to such a conclusion we have to eliminate other possible sources of discrepancy arising from differences in the sample selection. In the case of comparing the dipole determined from an optical sample and from an IRAS sample it has to be remembered that the optical galaxy sample requires a considerable correction for Galactic absorption, whereas the IRAS sample does not.

The requirement that the IRAS dipole agree with the microwave background dipole provides an estimator of the bias factor

$$\beta \equiv \frac{\Omega^{0.6}}{b_{IRAS}} = 0.6 \pm 0.2 \tag{14}$$

(Nusser and Davis, 1993). This value, and the reconstructed velocity field are seen to be in agreement with the POTENT analysis of Dekel et al. (1994), and with

[2]In this regard, it would be interesting to see whether the very rich Hercules cluster complex is better represented in the IRAS survey than the Coma cluster.

values based on the QDOT survey. The general conclusion reached by Freudling et al. (1994) is that to a depth of some 8000 $km.s^{-1}$ the dipole directions for various optical and infrared surveys agree within the errors, and that the bias factor for the optical and infrared catalogues are equal. Within that volume, however, the dipole direction lies some $20^o - 30^o$ away from the microwave background dipole. Convergence has not been achieved within these samples.

Chapter 46

The Microwave Background Spectrum

The job of the FIRAS experiment on board the COBE satellite COBE was to make absolute measurements of the temperature of the sky at inverse wavelengths ranging approximately from 2 $cm.^{-1}$ to 20 $cm.^{-1}$. Because FIRAS was to make an absolute measurement it lived in a liquid Helium cryostat cooled to 1.5 K, and this meant that the lifetime of the experiment was limited to the lifetime of the on-board coolant.

1 The Spectrum

The COBE satellite FIRAS experiment determined that the spectrum of the Cosmic Microwave Background radiation fits a Planck Law with remarkable accuracy (see figure 2). We have already commented (see section 3.1) that this implies that the spectrum must have been set up at very early times. The question now arises as to whether we can use the accuracy of the Planck Law fit to constrain the possible thermal histories of the Cosmic Expansion. This leads us to calculate the *Spectral Distortions* that arise in various models where energy has been injected into the cosmic plasma at various times through various mechanisms such as primordial cosmic turbulence or the decay of exotic unstable elementary particles.

We distinguish two key epochs during the expansion of the universe. The first of these is the time before which any injected energy can be redistributed and

the Planck Law maintained. This occurs at redshift $z_{th} \sim 3 \times 10^6$. After that, we have a period during which thermal equilibrium can be maintained, but not the Planck Law form of the spectrum. This period ends at a redshift that is denoted by z_y after which the there can be no equilibrium: photons can wander around in frequency space, but there are no effective absorption and emission process to drive an equilibrium. Calculations show that $z_y \sim 10^5$.

The history of calculating spectral distortions goes back almost to the discovery of the Cosmic Microwave background Radiation itself with the pioneering papers of Zel'dovich and Sunyaev (1969), Zel'dovich, Illarionov and Sunyaev (1972) and the numerical investigations of Chan and Jones (1975, 1976). In view of the great importance of this subject it is worthwhile going into a little detail explaining how these distortions arise and how they are calculated.

Before going into some details of these distortions, it is worth remembering a problem that arises when we compare observations of a limited wavelength range of a distorted spectrum. The theory asks us to compare the data with what would have been the spectrum had there not been a distortion. We cannot know what would have been, and so the evaluation of the data must be made self-consistently on the basis of the part of the spectrum that is observed. This is non-trivial, especially if we observe only high frequencies (as in the FIRAS experiment). Figure 1 illustrates a distorted spectrum and the way in which the comparison with an undistorted spectrum having the same Rayleigh-Jeans temperature is made.

2 the μ parameter

The equilibrium between photons and free electrons is a solution of the full Kompaneets equation, but as recognised long ago by Zel'dovich and Sunyaev this solution is more general than the Planck Law - it is a Bose-Einstein-like distribution[1]:

[1]Elementary Particles whose spin is an even multiple of $h/2$ (ie: photons and nuclei with even mass numbers) obey Bose-Einstein statistics:

$$n(\epsilon)d\epsilon = \frac{g(\epsilon)d\epsilon}{e^{(\epsilon-\mu)/kT} - 1} \tag{1}$$

where $g(\epsilon)d\epsilon$ is the number of possible particle states in the energy range ϵ to $\epsilon + d\epsilon$. μ is the chemical potential and for photons $\mu = 0$ leading directly to the Planck Law.

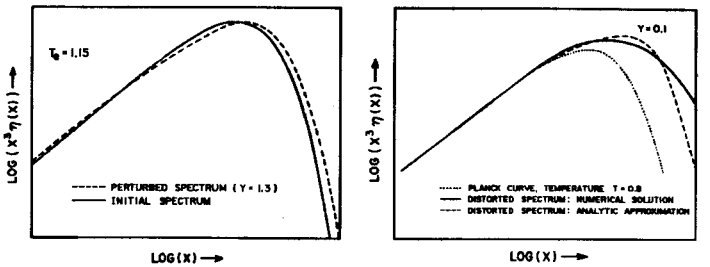

Figure 1: *Photon spectrum interacting with hot electron gas at the time of maximum distortion. The figure on the left shows the distorted spectrum relative to the original Planck spectrum. The figure on the right shows how the Rayleigh-Jeans temperatures are compared (after Chan and Jones, 1975a).*

$$\eta(x) = \left[\exp\left(x\frac{T_0}{T_e} + \mu(x)\right) - 1\right]^{-1} \tag{2}$$

where

$$\mu(x) = \mu_0 \exp\left(-\frac{x_{CB}}{x}\right) \tag{3}$$

and x_{CB} is the frequency where the Compton and Bremsstrahlung processes balance: photons are Compton scattered to higher frequencies as fast as they are created by the free- free process. x_{CB} moves to higher frequencies with time.

What this distribution describes is the competition between the bremsstrahlung process which is efficient at creating photons at low frequencies and the Compton process which causes photons to diffuse to higher frequencies. The resultant spectrum is illustrated in figure 1. At low frequencies the spectrum is Planck-like, but with temperature T_e since the electrons and photons are in equilibrium at those frequencies. At higher frequencies the photon distribution has been shifted and looks like a diluted black body. The detailed shape of the spectrum depends on the function $\mu(x)$, which is itself a consequence of the thermal history of the Universe.

The difficulty in matching this to the observations arises because the "shoulder" appears at very low frequencies where the spectrum is difficult to measure

accurately (figure 2). However, by fitting the data to a Bose- Einstein distribution with μ as a free parameter, we are essentially able to constrain the value of the parameter μ appearing in equation (2).

3 The y-parameter

If the spectrum evolves only through the process of Compton Scattering, the Kompaneets equation (equation 43 for the photon distribution $\eta(\nu)$ becomes quite simple:

$$d\eta t = n_e \sigma_T c \left(\frac{kT_e}{m_e c^2}\right) \frac{1}{x^2} \frac{\partial}{\partial x} \left[x^4 \left(\frac{\partial \eta}{\partial x} + \eta + \eta^2\right)\right] \tag{4}$$

where σ_t is the Thomson cross-section T_e is the electron temperature and where we have nondimensionalised the frequency with the usual substitution

$$x = \frac{h\nu}{kT_e} \tag{5}$$

The important step is to define what is essentially a new time variable y by

$$y = \int_t^{t_0} \frac{k(T_e - T_0)}{m_e c^2} n_e \sigma_T c dt \tag{6}$$

The low-frequency limit of equation (4) then becomes a simple diffusion equation:

$$\frac{\partial \eta}{\partial y} = \frac{1}{x^2} \frac{\partial}{\partial x} \left(x^4 \frac{\partial \eta}{\partial x}\right) \qquad x \ll 1. \tag{7}$$

This has an analytic solution in this low frequency regime which can be expressed in terms of the deviation $\Delta\eta$ in the spectrum at a given frequency relative the unperturbed Planck spectrum η_0 at the same frequency:

$$\frac{\Delta\eta}{\eta_0} = y \quad x \frac{e^x}{e^x - 1} \left[x \frac{e^x + 1}{e^x - 1} - 4\right] \tag{8}$$

$$\eta_0 = (e^x - 1)^{-1} \tag{9}$$

It is in fact better to solve these equations on a computer since then we are not restricted to the small x (low frequency) limit: understanding the COBE FIRAS data requires a better approximation or a numerical solution. This was in fact done a long time ago by Chan and Jones (1975, 1976), and figure 2 shows examples of (highly!) distorted spectra.

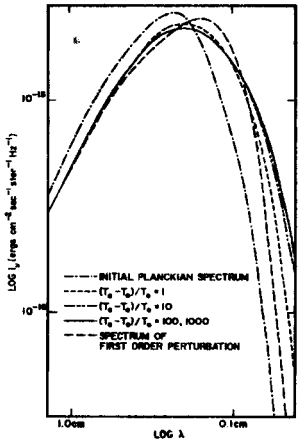

Figure 2: *Simulations of (highly) Compton-distorted Cosmic Microwave background Radiation spectra. Note that most of the effect is in the short-wavelength part of the spectrum and that the simple linear approximation does not work there (after Chan and Jones, 1976).*

4 COBE constraints on y and μ

The COBE limits on these distortions are (Mather et al., 1994)

$$|y| < 2.5 \times 10^{-5}$$
$$|\mu| < 3.3 \times 10^{-4} \tag{10}$$

These are 95% confidence level upper limits. They are apparently derived by fitting the original Zeldovich and Sunyaev formula (equation (8) to the data, rather than a full solution of the Kompaneets equation.

From the point of view of the thermal history of the Universe, these upper limits tell us that there was no great departure from the standard model, at least prior to recombination. However, there are numerous possible sources of distortion away from the Planck Spectrum and there are also possible additional contributions to the radiation flux particularly at the higher frequencies.

In order to improve our understanding of the constraints imposed by the spectral measurements we need two things: we need to go to lower frequencies with greater accuracy (see figure 2) and we need information on the angular variations of the spectrum at different places on the sky. (FIRAS has already provided some information on spatial variations by allowing y and μ to be determined on a pixel-to-pixel basis.

Chapter 47

The Microwave Background Fluctuations

The Differential Microwave Radiometer ("DMR") on board COBE consisted of two identical microwave horns pointing in directions 60° apart on the sky, measuring the temperature difference between two the two horns at each of three frequencies: 31.5 GHz., 53 GHz. and 90 GHz. (9.6, 5.7 and 3.3 mm wavelength). The middle frequency was presumably selected because this is the frequency where the contribution to the signal from the Galaxy is minimised. The satellite rotated about its own axis at 0.8 rpm., and so the entire sky was covered with these difference measurements during the orbital motion of the satellite about the Earth and the Earth about the Sun. The resultant map was broken into 6144 pixels of 2.8° angular size.

Analysis of the data is a highly complex problem because of the need to identify, calibrate and remove a large number of systematic errors that arise in the experiments. In addition to experimental errors, results have to be corrected for the non- cosmic contributions to the radiation field from the plane of the Ecliptic and from our Galaxy. The Galactic radiation has an overall quadrupole distribution, but also has a lot of structure in smaller angular scales. This has to be modelled and subtracted. The fact that the DMR observes at three separate frequencies means that the Galactic contribution can be subtracted by virtue of the fact that the spectrum of emission from the Galaxy is quite different from the Cosmic Background Radiation spectrum at these frequencies. The principle is easy, but the execution is far from straightforward!

1 Measuring Multipoles etc.

The job of the DMR experiment is to look for departures from isotropy on all angular scales. The best way of quantifying these deviations (or putting limits on them) is through spherical harmonic analysis.

If in a direction $\mathbf{q}$ on the sky we measure a temperature ΔT above the mean all-sky temperature $\bar{T}$, we can write the angular dependence of ΔT as

$$\Delta T(\mathbf{q}) = T(\mathbf{q}) - \bar{T} = \sum_{l,m} a_{lm} Y_{lm}(\mathbf{q}). \tag{1}$$

Given a map of the sky $T(\mathbf{q})$, we can find the coefficients a_{lm} by doing spherical harmonic analysis. We have to be careful of the fact that not all of the sky may be mapped: this is a technically complicated process that we cannot go into here. We can then calculate the amplitude of the l^{th} spherical harmonic

$$\Delta T_l^2 = \sum_m \frac{|a_{lm}|^2}{4\pi} \tag{2}$$

The $l = 2$ harmonic is referred to as the RMS quadrupole and is often denoted by

$$Q_{rms} \equiv \Delta T_2 \tag{3}$$

In general it may be more useful to work with the correlation function of the radiation distribution on the sky which can be written in terms of the a_{lm}:

$$C(\theta) = \frac{1}{4\pi} \sum_l (2l+1) C_l P_l(\cos\theta)$$
$$C_l \equiv a_l^2 = \sum_{m=-l}^{l} a_{lm}^2 \tag{4}$$

We will have more to say about $C(\theta)$ below, since this is a quantity that can be predicted directly from theory. One important aspect of the correlation function $C(\theta)$ is that it relates directly to estimates of the temperature fluctuations from beam switching experiments. For 2- and 3-beam experiments:

$$\left(\frac{\Delta T}{T}\right)\Big|_{2B} = 2[C(0) - C(\alpha)]$$
$$\left(\frac{\Delta T}{T}\right)\Big|_{3B} = \frac{1}{2}[3C(0) - 4C(\alpha) + C(2\alpha)] \quad (5)$$

where α is the beam throw. These methods have the advantage of minimising atmospheric contributions to the fluctuations. The 3-beam technique also eliminates the dipole contribution to the fluctuations and so is frequently used.

2 The Sachs-Wolfe Effect

In 1967, Sachs and Wolfe wrote a remarkable paper (Sachs and Wolfe, 1967) predicting that when our instruments were sensitive enough we would observe angular fluctuations in the microwave background radiation. Nobody doubted the importance of their result, but it was to be 25 years for COBE was to detect these fluctuations.

The reason we should see temperature anisotropies is obvious in hindsight: the Universe was probably inhomogeneous on the last scattering surface from which we are receiving the microwave background photons. (If it were not, we would have to find a relatively recent source for the fluctuations that gave rise to galaxies and clusters of galaxies.) The inhomogeneities are of several types. We may have intrinsic temperature fluctuations on this surface due to the presence of initially adiabatic density fluctuations. There will also be fluctuations in the gravitational potential due to the presence of any inhomogeneities. The matter that last scattered the photons in our direction may have had some "peculiar" velocity relative to the cosmic background. Finally, the photons may have passed through some time-dependent potential wells on its way to us: this would give rise to fluctuations in the observed temperature as a consequence of the gravitational redshift.[1]

In general we can write the observed temperature fluctuations as being due to three terms:

$$\frac{\Delta T}{T} = \frac{\delta T}{T}\Big|_{LS} + \frac{1}{c^2}\phi\Big|_{LS} + \frac{2}{c^2}\int_{LS}^{now} \frac{\partial \phi}{\partial t}(\mathbf{x}(t), t)dt \quad (6)$$

[1]Note that stationary potential wells make no contribution since the photons fall into and climb out of the same potential with no net redshift.

The subscript LS implies that these terms are to be evaluated on the last scattering surface. The last term in equation (6) is known as the "Rees-Sciama effect" and is generally small. The other two terms are not necessarily independent, and they depend in detail on the nature of the matter and of the fluctuations in the universe at the time of last scattering. Thus for adiabatic perturbations there would be a close link between the local density fluctuation and the local temperature fluctuations in the sense that the slightly denser regions of the Universe would be slightly hotter.

This last equation is often seen written in the form

$$\frac{\Delta T}{T} = \frac{1}{4}\frac{\delta\rho_\gamma}{\rho_\gamma}\bigg|_{LS} + \frac{1}{3c^2}\phi\bigg|_{LS} - \mathbf{n}.\mathbf{v}|_{LS} + \frac{2}{c^2}\int_{LS}^{now}\frac{\partial\phi}{\partial t}(\mathbf{x}(t),t)dt \qquad (7)$$

where the "Doppler term" $\mathbf{n}.\mathbf{v}|_{LS}$ writes out explicity, in a specific coordinate system at recombination, the contribution to the temperature fluctuation from the fact that the last scatters may be in motion relative to that coordinate system. The vector $\mathbf{n}$ is the direction to the observer. The local temperature fluctuation has been expressed in terms of the local rest-frame radiation density fluctuation $\delta\rho_\gamma/\rho_{gamma}$. A factor $\frac{1}{3}$ has appeared dividing the potential fluctuation, we shall come back to that.

The Sachs-Wolfe effect concerns the contribution from the potential fluctuations, and is the dominant one for lare scales. For the special case of initially adiabatic density fluctuations, the Sachs-Wolfe contribution can be simply written as

$$\frac{\Delta T}{T} = \frac{1}{3c^2}[\phi|_{LS} - \phi|_O] \qquad (8)$$

In other words, the temperature fluctuations are directly proportional the fluctuations in the gravitational potential. The two terms ϕ_{LS} and ϕ_O represent the potential fluctuations at the last scattering surface and at the observer. Thus the effect is the potential difference between the observer and the last scattering surface. However, when it comes to looking at the angular distribution, the contribution from the observer is independent of direction and is absorbed into the isotropic component of the temperature measurement.

There have been several discussions as to where the factor "$\frac{1}{3}$" comes from in this case of adiabatic fluctuations. One's naive expectation may have been simply $\Delta T/T \sim \phi$. Peebles (*LSSU*) explained it as being the "logical" value with a correction of $-\frac{2}{3}\phi$ due to the fact that the cosmic expansion is time-dilated. In

the relativistic treatment of Sachs and Wolfe this factor appears because for very large scale adiabatic perturbations, the fluctuations in the temperature are $-\frac{2}{3}\phi/c^2$. When this is put in equation (6) this gives the $\frac{1}{3}$ factor.

It is worth noting that the gravitational potential fluctuations on super-horizon scales are the solution of the Poisson equation $\nabla^2\phi = 4\pi G\delta\rho$. This implies that for these scales $l > l_H$, the horizon scale at the epoch of last scattering

$$\frac{\Delta T}{T} \sim \left(\frac{l}{l_h}\right)^2 \left(\frac{\delta\rho}{\rho}\right) \tag{9}$$

With a power spectrum of density fluctuations $\mathcal{P}(k) \propto k^n$ we have root mean square density fluctuations varying with scale as $\delta\rho/\rho \propto l^{-(n+3)/2}$ (cf. equation (41). From this

$$\frac{\Delta T}{T} \sim l^{\frac{1}{2}(1-n)} \tag{10}$$

The Harrison Zeldovich spectrum ($n = 1$) thus has temperature fluctuations that are independent of scale. (This is hardly surprising since the potential fluctuations are scale invariant for this spectrum (see section 4.2).

It is interesting to note that if $\Omega \neq 1$, then equation (9) ceases to apply above the curvature scale where gravity is dynamically unimportant. This may provide an important way of directly estimating the density parameter when the large angular scale fluctuations of the microwave background temperature have been mapped out. The actual behaviour on such scales is difficult to calculate and there are some technical problems that remain to be solved.

3 Comparing with theory

The key issue now is to take a cosmogonic theory and predict what, according to that theory, we should observe in the microwave sky. The problem arises because the theory talks in terms of random density and temperature functions, whereas we observe only one realization of such a process.

3.0.1 What a theory can predict

The expected temperature fluctuations can be computed from a theory for the initial perturbations. Given a theory, we can predict the temperature fluctuations over the sky and express this as a sum over independent spherical harmonic components:

$$\Delta T(\mathbf{q}) = T(\mathbf{q}) - \bar{T} = \sum_{l,m} a_{lm} Y_{lm}(\mathbf{q}). \tag{11}$$

In this context, the a_{lm} are random variables taken from some distribution that comes from the model. Because of the definition of $\bar{T}$ being the mean temperature averaged over the sky, the mean of each of the a_{lm} is zero.

Equations (1) and (11) are not the same. In the first equation, the a_{lm} take on particular values that describe our sky and the instruments we used to observe it. In the second case they are a realization of some random process that is a consequence of the particular theory we are looking at.

3.0.2 Expressing it in terms of angles

Theory provides the statistical properties of the a_{lm} appearing in equation (11). The means (ie: the expectation values) of the a_{lm} are zero. Given a theory we can calculate the expectation values of the mean square a_{lm}:

$$C_l \equiv a_l^2 = \langle |a_{lm}|^2 \rangle = \sum_{m=-l}^{l} a_{lm}^2 \tag{12}$$

(Both the notations C_l and a_l^2 are seen in the literature). For a given theory we can calculate the C_l. If we prefer to talk about fluctuations on particular angular scales instead of the spherical harmonic content of fluctuations, we can use the transformation

$$C(\theta) = \frac{1}{4\pi} \sum_l (2l+1) C_l P_l(\cos\theta) \tag{13}$$

where $P_l(\cos\theta)$ is the usual Legendre polynomial of order l.

3.0.3 The instrumental response

In order to use the observations to test a theory we must compute what a given experiment would measure according to this theory: we need to put the detector into the equation. The simplest thing to do is to characterise an experiment by its *instrumental response function*, W_l. The W_l tell us how sensitive the experiment is to each value of l, and in principle we know the W_l if we have the details of the instrumental sensitivity as a function of angular scale.[2] For a simple Gaussian beam of full-width-half-maximum θ_{FWHM}, we need to introduce a window function $W_l \simeq \exp(-(l+\frac{1}{2})^2\theta_s^2/2)$ with $\theta_s = 0.425\theta_{FWHM}$:

$$C(\theta) = \frac{1}{4\pi}\sum_l (2l+1)W_l^2 C_l P_l(\cos\theta) \tag{14}$$

The situation for COBE is a little more complex: we have $W_l(\mathrm{COBE}) \sim 0$ for $l > 20$: COBE is not sensitive to fluctuations on a smaller angular scale than about 2.5°.

The rms temperature fluctuation ($C(0)$) measured by this instrument for the theory whose C_l have been calculated is then:

$$\left\langle \left(\frac{\Delta T}{T}\right)^2 \right\rangle_{expt} = \sum_l \frac{2l+1}{4\pi} W_l^2 C_l \tag{15}$$

There is another important detail to take care of when predicting what a given experiment should measure: the way in which the measurements are made. Most experiments do not map the sky, but aim to measure $C(\theta)$ directly by comparing the temperatures measured at many pairs of spots separated by a distance θ on the sky. Such difference measurements are referred to as beam-switching experiments, and these obviously cannot detect a contribution from the $l = 2$ dipole component of the fluctuations. The theoretical contribution of the $l = 2$ term must therefore be removed from predictions of what this kind of experiment will measure. Some experiments compare points taken three at a time, and the situation is still more complicated.

[2] It is often useful to note that the characteristic angular scale corresponding to a particular value of l is $\theta_l \sim 3500/l$ arc minutes.

3.0.4 Relating density and temperature fluctuations

Since the Sachs-Wolfe effect arises out of potential fluctuations, which are themselves related to density fluctuations, it should be possible to write down directly the spectrum of temperature fluctuations in terms of the spectrum of density fluctuations. This has been done for a large number of theories of initial fluctuations in various cosmological models (see for example Peebles, 1982 for the details of the standard calculation).

If the density fluctuations are characterised by a power spectrum $\mathcal{P}(k)$, it can be shown that on very large scales where the Sachs-Wolfe effect dominates and is not modified by optical depth effects, the coefficients a_{lm} in equation (11) are given by

$$C_l = a_l^2 = 4\pi \left(\frac{\Omega_0 H_0^2}{2c^2}\right)^2 \int \frac{\mathcal{P}(k)}{k^4} j_l^2 \left(\frac{2ck}{\Omega_0 H_0}\right) d^3k. \tag{16}$$

The angular correlation function is[3]

$$C(\theta) = \left(\frac{\Omega_0 H_0^2}{2c^2}\right)^2 \int \frac{\mathcal{P}(k)}{k^4} \frac{\sin kR_H}{kR_H} d^3k, \qquad R_H = \frac{4c}{\Omega_0 H_0} \sin\left(\frac{\theta}{2}\right) \tag{17}$$

Note that R_H is the comoving distance at recombination subtending an angle θ (see equation (6)).

4 Simple theoretical models

The simplest theoretical model is to calculate the fluctuations in the microwave sky arising from a spectrum of adiabatic density fluctuations having a primordial power spectrum

$$\mathcal{P}(k) = Ak^n \tag{18}$$

[3]It should be remembered that, in an open Universe, the equation for $C(\theta)$ only hold for $\theta < \theta_\dagger$, the angle subtended by the curvature radius $R_\dagger$ (see equation (10). This is because the Fourier representation in plane waves becomes invalid on such scales.

where $n = 1$ for the Harrison-Zeldovich initial spectrum. Going through the calculation it is found that

$$|a_l|^2 = \frac{4A}{2^{3-n}} \frac{\Gamma(3-n)\Gamma(l+\frac{n-1}{2})}{\Gamma^2(2-\frac{n}{2})\Gamma(l+\frac{5-n}{2})} \tag{19}$$

This is a somewhat intimidating formula: the Γ-functions are not very intuitive! However, there are some useful and important limiting cases:

$$\begin{aligned} n = 0: \qquad & |a_l|^2 = 8A \frac{1}{(4l^2-1)(2l+3)} \\ n = 1: \qquad & |a_l|^2 = \frac{4A}{\pi} \frac{1}{l(l+1)} \end{aligned} \tag{20}$$

In the large l limit we thus have

$$l^3 C_l \to \text{constant}, \quad l \to \infty, \quad n = 0 \tag{21}$$

$$l^2 C_l \to \text{constant}, \quad l \to \infty, \quad n = 1 \tag{22}$$

Translating from l to angular scales θ using equation 13) we then have that at small angular scales

$$\frac{\Delta T}{T} \propto \theta^{\frac{1}{2}(1-n)} \tag{23}$$

Following common practise, we have used the symbol $\Delta T/T$ to denote the rms value of the temperature fluctuations. We have not folded in an instrumental response, so this represents the measurements from perfect equipment. The interesting thing is that for the $n = 1$ Harrison Zel'dovich Spectrum the amplitude of the temperature fluctuations is scale independent. Conversely, from observational multiple angular scales we can hope to determine n from direct observation, or indeed test the proposed form of the primordial power spectrum.

5 Cosmic Dipole

The first anisotropy to be detected in the microwave background radiation was the Dipole component. This is interpreted as being due to the motion of the Earth

with a velocity v relative to the frame in which the cosmic microwave background radiation is isotropic. The apparent temperature over the sky in a direction making an angle θ with the apex of this motion is then

$$T_{obs} = T_{CBR}\frac{\sqrt{1-(\frac{v}{c})^2}}{1-\frac{v}{c}\cos\theta} \tag{24}$$

$$\simeq T_{CBR}\left[1+\frac{v}{c}\cos\theta\right] \tag{25}$$

where in the second of these equations we have ignored terms in $(v/c)^2$. Two years of DMR data (Bennett et al., 1994) yield a dipole amplitude

$$\Delta T_{dipole} = 3.363 \pm 0.024 \text{ mK} \tag{26}$$

towards Galactic Coordinates

$$\begin{aligned} l &= 264.4^\circ \pm 0.2^\circ \\ b &= +48.1^\circ \pm 0.4^\circ \end{aligned} \tag{27}$$

The uncertainty arises in part from systematic experimental errors and from the need to fit the contributions from the Zodiacal Light and from our Galaxy. The final vector reflects a combination of the motion of the Solar System about the Galaxy, the motion of the Galaxy within the Local Group and the velocity of the Local Group relative to whatever larger structure exist and have an influence on the motion of the Local System of galaxies. We will return to the interpretation of this later.

It is interesting that this dipole component has been detected by FIRAS while measuring the temperature of the Cosmic Microwave Background (Fixsen et al., 1994). FIRAS has sufficient accuracy in determining the spectrum of the radiation field that directional variations in the spectrum can be measured. The result of this analysis gives results that are consistent with the DMR results and have errors of only 0.5° in both l and b.

6 The Quadrupole Component

The quadrupole component of the distribution of the Cosmic background Radiation over the sky is of utmost importance in cosmology. It's value is not contam-

inated, as is the dipole, by uncertainties in our motion. Thus the detection of a quadrupole component is a direct observation of deviations from cosmic homogeneity and isotropy at the early times when the Cosmic Background Radiation was last scattered.

However, there is substantial difficulty in removing the quadrupole contributions from Galactic radiation; this requires an accurate model for Galactic emission. (The details are given in the fascinating paper by Bennett et al., 1994).

The quadrupole is defined by 5 coefficients describing the quadrupole component of temperature distribution on the sky. The values of these coefficients depend on the coordinate system used, and in particular relative to Galactic coordinates:

$$Q(l,b) = Q_1 \frac{1}{2}(3\sin^2 b - 1) + Q_2 \sin 2b \cos l + Q_3 \sin 2b \sin l + Q_4 \cos^2 b \cos 2l + Q_5 \cos^2 b \sin 2l. \quad (28)$$

The RMS quadrupole amplitude (see equation (3)) is independent of the angular coordinates used and is

$$Q_{rms}^2 = \frac{4}{15}\left[\frac{3}{4}Q_1^2 + Q_2^2 + Q_3^2 + Q_4^2 + Q_5^2\right] \quad (29)$$

There is in addition to this a nontrivial contribution arising from the second order Doppler effect (the second order expansion of equation (24). This amounts to a contribution to Q_{rms} of 1.2 μK. The measured cosmic quadrupole from two years of the COBE DMR experiment is

$$Q_{rms} = 6 \pm 3 \ \mu\text{K} \quad (30)$$

where the error bar is a 68% confidence level.

The quadrupole arises out of the Sachs-Wolfe effect and can be in principle be calculated explicitly for an given cosmological model and spectrum of fluctuations. For the standard CDM model with a Harrison-Zel'dovich initial spectrum $\mathcal{P}(k) = Bk$, the quadrupole is

$$Q_{rms} = T_0 \left(\frac{5}{6\pi^2}\right)^{\frac{1}{2}} \left(\frac{H_0}{2c}\right)^2 \Omega_0^{0.77} B^{\frac{1}{2}} \quad (31)$$

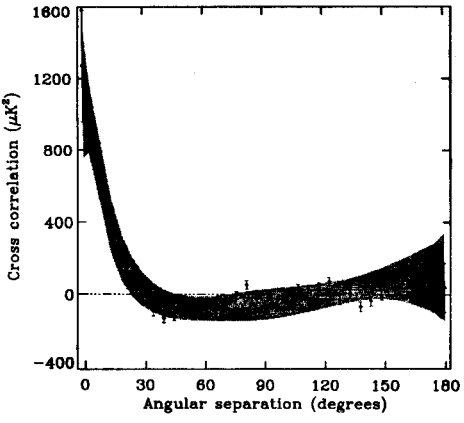

Figure 1: *The correlation function of COBE DMR temperature fluctuations after two years of data (from Bennett et al., 1994). This is in fact the cross-correlation between the dipole subtracted maps at 53 GHz and 90 GHz. The shaded region is an $n = 1$ model normalised to the quadrupole amplitude.*

where $T_0 = 2.736$ K is the background radiation temperature, and H_0 and Ω_0 are the present Hubble constant and cosmic density parameter. Thus the COBE measurement of Q_{rms} provides the normalisation of the power spectrum.

This is a very important point. Once the power spectrum normalisation is known, we can compare the structures that we see on smaller scales ($< 50 - 100h^{-1}$ Mpc.) with the predictions of numerical models using that spectrum. The comparison is, however, not entirely straightforward: when we observe structure in order to make this comparison, we observe the light distribution, not the matter distribution. Our comparison therefore brings in the bias parameter. The situation is shown in figure 1) where we see a direct estimate of the power spectrum from the data, and compare with models having the "COBE normalisation".

7 Degree scale anisotropies

On angular scales of several degrees, the Sachs-Wolfe effect dominates the anisotropies. COBE's angular resolution is around 10°. This means that COBE is seeing features on the last scattering surface which in an $\Omega = 1$ universe correspond to a linear scale today of some $300h^{-1}$ Mpc.. The scale is a factor Ω^{-1} larger in an open universe. The data from the COBE satellite is depicted in figure 1 where wee see direct evidence for structures on scales $> 300(\Omega_0 h)^{-1}$ Mpc..

The expected correlation function of the temperature fluctuations for primeval curvature perturbations is given in terms of the power spectrum of the fluctuations by equation (17). The prediction of the standard CDM scenario (with an initial Harrison Zel'dovich power spectrum and a normalization chosen to fit the measured quadrupole) are shown as the hatched region in the figure. We clearly see evidence of fluctuations: that is one of the triumphs of the COBE experiment. Whether any particular theories are ruled out is a matter for future calculations. Experiments that measure microwave background fluctuations on smaller angular scales than COBE will undoubtedly help the situation, but they are more sensitive to the Doppler terms in equation (7) and so the interpretation becomes more model dependent.

The program from now on, then, is to map the sky at various angular scales and fit the measured correlations to the entire zoo of cosmological models and theories of large scale structure formation. We will be imposing constraints on the power spectrum index, perhaps on the value of Ω, and we may even be able to say whether we live in a Universe dominated by cold dark matter, mixed dark matter, or hot dark matter.

8 The Future of Cosmology?

This article, despite its length, has merely introduced a selection of topics in observational cosmology that are of current interest. The selection is biased by my own interests and many important subjects have been passed over, or simply not been mentioned. There has, for example, been no discussion of nucleosynthesis and how one goes about testing model predictions for the primordial abundances. Nothing has been said about observations of galaxy clusters and the clues they will certainly

provide to the history of structure formation. Nothing has been said about the use of gravitational lenses as probes of the matter distribution and nothing has been said about quasars, the most distant objects we see in our Universe. Cosmology is an large and active branch of theoretical and experimental physics: it is certainly too large to present in one section of a book.

I do hope however that I have demonstrated that observational cosmology is an active field. I hope I have demonstrated its close relationship with theory and its reliance on the latest technology for doing observations. The theory provides a driving force to acquire data, and in turn that data is interpreted in the light of models. That these models are naive is of course a problem, and that is the reason that we see a continual push towards generating ever better models.

The successes we have seen since the discovery of the Microwave background radiation are numerous. We have verified that its spectrum is Planckian, and that it is highly isotropic, but not totally isotropic. The discovery of significant anisotropies is surely one of the great discoveries of twentieth century physics, and the further exploration of these anisotropies will command a lot of effort from experimental teams. Mapping out the anisotropy of the microwave background at a variety of wavelengths and over a substantial range of angular scales will tell us a lot about our Universe and this is evidently among the top priorities for cosmology research.

Measuring distance of galaxies is a complex task that has not been discussed here. The ability to get the distances to individual galaxies with a precision of better than 20% (and hopefully even 10%) will provide an important dynamical map of the Universe. Techniques are available to decode that data and make a map of the spatial distribution of galaxies and their peculiar velocities. This may be the best route to getting at the density parameter. It is certainly important as a tool for evaluating our numerical models and seeing whether we really do understand the formation of large scale structure.

Today, our understanding of large scale structure is predicated on the notion that the inhomogeneities in the matter distribution have been driven by the force of gravity acting on low-amplitude primordial inhomogeneities. Of course that may only be part of the story: gasdynamic processes have certainly played a role on galaxy scales, and probably on cluster scales. It is even conceivable that magnetic fields may have played an important role in shaping galaxies and in controlling the star formation process.

Acknowledgements

Firstly I would like to thank Professor Mario Novello, the organizer of the Brazilian School of Cosmology and Gravitation, for giving me the opportunity of participating in the school. His team of helpers were particularly helpful, especially when it came to translating my copy of the film *"The Meaning of Life"* to the local version of the PAL television system for use in my lectures. It is unfortunate that I cannot incorporate that part of the lectures in this manuscript. Roland Triay suggested that I be invited in the first place. Attending this school was a memorable experience and I am grateful to him for thinking of me.

The Theoretical Astrophysics Center (TAC) is funded by grants from the Danish National ResearchCouncil. Rien van de Weygaert played a role in clarifying the analysis of velocity space data, I am grateful for that.

The diagrams in this article were scanned, "cleaned" and re-edited using ASTRA'S *"ASTRADOC"* Image Documentation Software for the IBM PC. The article was prepared using Word Perfect to edit the text and EMTEX to process it.

A Magnitudes and all that.

Since this is a series of lectures on *Observational* cosmology, it is impossible to avoid discussing the apparent brightness of objects such as stars and galaxies and thereby encountering one of astronomy's major idiosyncrasies - the *magnitude scale.* Ever since the time of Ptolemy, the brightness of stars have been measured relative to one another on a logarithmic scale.

The observed energy flux is always related to some particular waveband where an observation is made. The total brightness of a source integrated over that waveband is measured by optical astronomers in units of ergs.cm.$^{-2}$sec.$^{-1}$ and translated into *magnitudes.* The notion of a magnitude was formalised by Pogson (1856). Two sources of brightness f_1 and f_2 are said to have magnitudes m_1 and m_2 related by

$$m_1 - m_2 = -2.5 \log_{10} \frac{f_1}{f_2} \tag{32}$$

Thus the magnitude scale is established once a standard has been set.

Life is a little more complicated than that: we do not in fact observe the flux integrated over all wavelengths. Observations are always restricted to some specific waveband determined by the observing instrument and its detector. If $f(\lambda)$ denotes the energy flux measured in a filter centred at wavelength λ and having a passband of width $\Delta\lambda$, then the *Flux Density* is given by

$$S(\lambda) = \frac{f(\lambda)}{\Delta\lambda} \text{ergs.cm.}^{-2}\text{sec.}^{-1}\text{Hz}^{-1} \tag{33}$$

The total flux is the integral of this flux density over all wavelengths. The zero points of the magnitude scale has been defined for specific filter sets. For example, in a particular filters known as the "visual band" centred on 5500 A we have

$$\log_{10} S(\lambda) = -0.4 m_V - 8.42. \tag{34}$$

and in this system the Sun has apparent magnitude $m_V(\odot) = -26.77$.

Optical astronomers, then, measure the flux density per unit wavelength in units of ergs.cm.$^{-2}$sec.$^{-1}$Hz^{-1} while radio astronomers measure flux density per unit frequency in measuring units of wattm^{-2}Hz^{-1}. For convenience, radio astronomers translate their flux density measurements into *flux units* (f.u.), where 1f.u. = 10^{-26}wattm^{-2}Hz^{-1}.

B Peculiar velocities - homogeneous background

In section 2.2 we discussed the motion of particles whose motion is driven by the fluctuations in the gravitational potential. A particle moving in an otherwise homogeneous universe moves quite differently and it is instructive to study this case.

The peculiar velocity of a particle is its the velocity relative to an observer whose own motion is precisely comoving in the background. This is depicted in figure 2 where we see the space-time path of a particle relative to the world lines of two observers who are comoving in the background. (This diagram is identical to figure 1 except that the passing particle has a velocity that is less than the speed of light.)

The observer on the world line O looks at the Galaxy G at a time and place when a freely moving particle P passes the same place. The velocity the

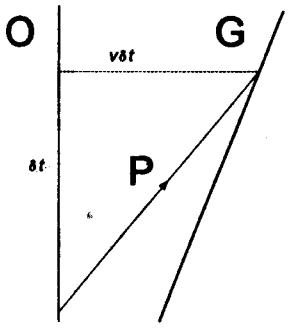

Figure 2: *The Decay of peculiar Velocities. The Observer at O looks at the freely moving particle P moving relative to a (comoving) galaxy G.*

particle has when it passes G is the velocity v it had when it passed O, less the expansion velocity of O relative to P:

$$v(t+\delta t) = v(t) - \frac{\dot{a}}{a} v(t)\delta t. \tag{35}$$

This is simply the expression of the fact that the particle P moves under "no forces" with "constant velocity". The Observer O therefore measures a velocity difference $v(t+\delta t) - v(t)$, whose time dependence is governed by

$$\frac{1}{v}\frac{dv}{dt} = -\frac{\dot{a}}{a}. \tag{36}$$

Thus we have

$$v \propto a^{-1} \tag{37}$$

which is the law for the decay of the peculiar velocity of a freely moving particle. Note that this result is false if any forces act on the particle, which is the case when its peculiar motion is driven by gravitational forces arising from inhomogeneities in the Universe.

To go on to understand motion of a particle against an inhomogeneous background requires that we take account of the acceleration of the particle due

to the inhomogeneities in the mass distribution. To this end we want to rewrite equation (36) as

$$\frac{dV}{dt} + \frac{\dot{a}}{a}v = -\nabla\phi \tag{38}$$

where ϕ is the fluctuating part of the gravitational potential, that is, the part of the potential that is the result of the fluctuations $\delta\rho$ in the mass density.

$$\nabla^2\phi = 4\pi G\rho_b\delta, \quad \delta = \frac{\delta\rho}{\rho}. \tag{39}$$

The solution of this is

$$\phi(\mathbf{x}) = g\rho_b \int \frac{\delta(\mathbf{x})}{|\mathbf{x} - \mathbf{x}'|} d^3\mathbf{x}' \tag{40}$$

where the integral is taken over the whole of space.

We need to solve equation (38) for the peculiar velocity, and to do this we need to know something about the time dependence of the fluctuating potential $\delta\phi$. We notice from equation (39) that $\nabla^2\phi$ scales with time in the same way as $\delta\rho/\rho$, that is as the scale factor a.

References.

Abell, G.O. , 1958, *Astrophys. J. Suppl.*, **70**, 1.

Abell, G.O., Corwin, H.G. and Olowin, R.P. , 1989, *Astrophys. J. Suppl.*, **70**, 1. (ACO)

Bahcall, N. and West, M. , 1992, *Astrophys. J.*, **392**, 419. Bardeen, J.M., Bond, J.R., Kaiser, N. and Szalay, A.S.], 1986, *Astrophys. J.*, **304**, 15.

Barrow, J.D., Henriques, A.B., Lago, M.T.V.T. and Longair, M.S., 1991, *The Physical Universe: The Interface Between Cosmology, Astrophysics and Particle Physics*, Proceedings of the XII Autumn School of Physics, Lisbon, Oct. 1990. (Springer-Verlag, Lecture Notes in Physics 383).

Bennett, C.L., Kogut, A., Hinshaw, G., Banday, A.J., Wright, E.L., Gó rski, K., Wilkinson, D.T., Weiss, R., Smoot, G.F., Meyer, S.S., Mather, J.C., Lubin, P., Loewenstein, K., Lineweaver, C., Keegstra, P., Kaita, E., Jackson, P.D. and Cheng,E.S., 1994, *Astrophys. J.*, **xxx**, xxx.

Bernardeau, F., 1992 , *Astrophys. J.*, **392**, 1.

Bertschinger, E. and Dekel, A. , 1989, *Astrophys. J. Lett.*, **336**, L5.

Bertschinger, E., Dekel, A., Faber, S.M. and Burstein, D. , 1990, *Astrophys. J.*, **364**, 370.

Bond, J.R. and Efstathiou, G., 1984, *Mon. Not. R. astr. Soc.*, **285**, L45.

Bondi, H. and Gold, T., 1948, *Mon. Not. R. astr. Soc.*, **58**, 252.

Broadhurst, T.J., Ellis, R.S., Koo, D. and Szalay, A.S., 1990, *Nature*, **343**, 726.

Chan, K.L. and Jones, B.J.T., 1975a, *Astrophys. J.*, **195**, 1.

Chan, K.L. and Jones, B.J.T., 1975b, *Astrophys. J.*, **198**, 245.

Coles, P, and Jones, B.J.T., 1991 , *Mom. Not. R. astr. Soc.*, **248**, 1.

Collins, C.A., Guzzo, L., Nchol, R.C. and Lumsden, S.L. , 1992, *Observational Cosmology* (Milan September 1992), ed. G. Chincarini, A. Iovino, T. Maccacaro and D. Maccagni, ASP Conference Series.

Da Costa, L.N., Pellegrini, P., Davis, M., Meiksin, A., Sargent, W.L.W, and Tanory, J., 1991 *Astrophys. J. Suppl.*, **75**, 935. (SSRS)

Dalton, G.B., Efstathiou, G., Maddox, S.J. , and Sutherland, W.J., 1992, *Astrophys. J. Lett.*, **390**, L1.

Dekel, A., Faber, S.M., Courteau, S. and Willick, J. , 1994, preprint.

de Lapparent, V., Geller, M.J. and Huchra, J.P. , 1986, *Astrophys. J. Lett.*, **302**, L1. (CfA Slice)

de Vaucouleurs, G. and de Vaucouleurs, A., 1964, *Reference Catalog of Broght Galaxies*, University of Texas, Austin (RC1).

de Vaucouleurs, G., de Vaucouleurs, A. and Corwin, H.G. , 1976, *Second Reference Catalog of Bright Galaxies*, University of Texas. (RC2)

Dressler, A., Faber, S.M. and Burstein, D. , 1991, *Astrophys. J.*, **368**, 54.

Eddington, A.S., 1923, *The Mathematical Theory of Relativity*, Cambridge University Press (reprinted 1965).

Efstathiou, G., Kaiser, N., Saunders, W., Lawrence, A., Rowan-Robinson, M., Ellis, R.S. and Frenk, C.S., 1990, *Mon. Not. R. astr. Soc.*, **247**, 10P.

Fisher, K.B., Davis, M., Strauss, M. , Yahil, A. and Huchra, J.P., 1993, *Astrophys. J.*, **402**, 42.

Fixsen, D.J., Cheng, E.S., Cottingham, D.A., Eplee, R.E., Isaacman, R.B., Mather, J.C., Meyer, S.S., Noerdlinger, P.D., Shafer, R.A., Weiss, R., Wright, E.L., Bennett, C.L., Boggess, N.W., Kelsall, T., Moseley, S.H., Silverberg, R.F., Smoot, G.F. and Wilkinson, D.T., 1994, *Astrophys. J.*, **420**, 445.

Frenk, C.S., White, S.D.M., Efstathiou, G. and Davis, M., 1990, *Astrophys. J.*, **391**, 2.

Freudling,, W., Da Costa, L.N., and Pellegrini, P.S., 1994, *Mon. Not. R. astr. Soc.*, **xxx**, xxx.

Friedmann, A., 1922, *Zs. f. Phys.*, **10**, 337.

Gaztanaga, E., 1994 , *Mon. Not. R. astr. Soc.*, **xxx**, xxx.

Geller, M.J. and Huchra, J.P., 1989, *Science*, **246**, 897.

Giovanelli, R., Haynes, M.P., Myers, S. and Roth, J. , 1986, *Astron. J.*, **92**, 250. (Perseus-Pisces)

Glazebrrok, K., Peacock, J.A., Collins, C.A. and Miller, L. , 1994, *Mon. Not. R. astr. Soc.*, **266**, 65.

Hoyle, F., 1948, *Mon. Not. R. astr. Soc.*, **58**, 372.

Hubble, E.P., 1925, *Publ. Astr. Soc Pacific*, **5**, 261.

Hubble, E.P., 1929, *Proc. Nat. Acad. Sci.*, **15**, 168.

Huchra, J., Davis, M., Latham, D. and Tonry, J. , 1983, *Astrophys. J. Suppl.*, **52**, 89. (CfA1-ZCAT)

Hudson, M.J. , 1994, *Mon. Not. R. astr. Soc.*, **266**, 475.

Humason, M.L., 1929, *Proc. Nat. Acad. Sci.*, **15**, 167.

Humason, M,L., 1931, *Astrophys. J.*, **74**, 35.

Humason, M.L., 1936, *Astrophys. J.*, **83**, 10.

Jones, B.J.T., Coles, P. and Martinez, V.J. , 1992, *Mon. Not. R. astr. Soc.*, **259**, 146.

Juskiewicz, R. and Bouchet, F., 1991 , in *The Distribution of Matter in the Universe*, eds G.Mamon and D.Gerbal (Meudon, Observatoire de Paris).

Kaiser,N., 1984, *Astrophys. J. Lett.* **284**, L9.

Kaiser, N. , 1987, *Mon. Not. R. astr. Soc.*, **227**, 1.

Kofman, L., Bertschinger, E., Gelb, J.M, Nusser, A., and Dekel, A., 1994, *Astrophys. J.* **420**, 44.

Kjærgaard, P., Jørgensen, I., and Moles, M., 1993, *Astrophys. J.*, **418**, 617.

Lahav, O., Rowan-Robinson, M. and Lynden-Bell, D. , 1988, *Mon. Not. R. astr. Soc.*, **234**, 677.

Lemaître, G., 1927, *Ann. Soc. Sci. Bruxelles*, **47**, 49.

Loh, E.D. and Spillar, E.J., 1986, *Astrophys. J. Lett.*, **307**, 1.

Loveday, J., Efstathiou, G., Peterson, B.A. and Maddox, S.J., 1992a, *Astrophys. J. Lett.*, **400**, L43.

Loveday, J., Peterson, B.A. Efstathiou, G. and Maddox, S.J., 1992b, *Astrophys. J.*, **390**, 338. (Stromlo-APM)

Lucchin, F., Matarrese, S., Melott, A.L. and Moscardini, L., 1993, *Astrophys. J.*, **xxx**, xxx.

Lundmark, K., 1924, *Mon. Not. R. astr. Soc.*, **84**, 747.

Lynden-Bell, D., Faber, S.M., Burstein, D., Davies, R.L., Dressler, A., Terlevich, R. and Wegner, G., 1988, *Astrophys. J.*, **326**, 19. (S^7)

Maddox, S.J., Efstathiou, G., Sutherland, W.J. and Loveday, J., 1990, *Mon. Not. R. astr. Soc.*, **242**, 43P.

Maddox, S.J., Sutherland, W.J., Efstathiou, G., and Loveday, J., 1990, *Mon. Not. R. astr. Soc.*, **246**, 433.

Martinez, V.J., Portilla, M. and Saez, D. , 1992, *New Insights into the Universe*, Proceedings of a Summer School held in Valencia, Spain, Sept. 1991 (Springer-Verlag, Lecture Notes in Physics, 408).

Mather, J.C., Cheng, E.S., Cottingham, D.A., Eplee, R.E., Fixsen, D.J., Hewagama, T., Isaacman, R.B., Jensen, K.A., Meyer, S.S., Noerdlinger, P.D., Read, S.M., Rosen, L.P., Shafer, R.A., Wright, E.L., Bennett, C.L., Boggess, N.W., Hauser, M.G., Kelsall, T., Moseley, S.H., Silverberg, R.F., Smoot, G.F., Weiss, R. and Wilkinson, D.T., 1994, *Astrophys. J.*, **420**, 439.

Mattig, W., 1958, *Astron. Nachr.*, **284**, 109.

Metcalfe, N., Fong, R., Shanks, T. and Kilkenny, D. , 1989, *Mon. Not. R. astr. Soc.*, **236**, 207. (DARS)

Nilson, P., 1973, *Uppsala General Catalogue of Galaxies*, *Uppsala Astron. Obs. Ann.*, **6**. (Uppsala)

Padmanabhan, T. , 1993, *Structure Formation in the Universe*, Cambridge University Press.

Peacock, J.A., Heavens, A.F. and Davies, A.T., 1990, *Physics of the Early Universe* (Proceedings of the 36th. Scottish Universities Summer School in Physics: Edinburgh 1989), published by SUSSP (Scottish Universities Summer Schools in Physics).

Peebles, P.J.E., 1970, *Physical Cosmology*, Princeton University Press.

Peebles, P.J.E. , 1974, *Astrophys. J. Lett.*, **189**, L51.

Peebles, P.J.E., 1980, *The Large Scale Structure of the Universe*, Princeton University Press.

Peebles, P.J.E., 1982, *Astrophys. J. Lett.*, **263**, L1.

Peebles, P.J.E., 1993, *Principles of Physical Cosmology*, Princeton University Press.

Petrosian, V., 1976, *Astrophys. J. Lett.* **209**, L1.

Robertson, H.P., 1928, *Phil. Mag.*, **5**, 835.

Sachs, R. and Wolfe, A.M., 1967, *Astrophys. J.*, **147**, 73.

Saha, A., Labhardt, L., Schwengeler, H., Macchetto, F.D., Panagia, N., Sandage, A. and Tammann, G.A., 1994, *Astrophys. J.*, **425**, 14.

Sanchez, F., Collados, M., and Rebolo, R., 1992, *Observational and Physical Cosmology* (Proceedings of the II Canary Islands Winter School of Astrophysics), Cambridge University Press.

Sandage, A., 1961, *The Hubble Atlas of Galaxies*, Carnegie Institute of Washington.

Sandage, A.R. and Cacciari, C., 1990, *Astrophys. J.*, **350**, 645.

Sandage, A. and Perelmutter, J-M., 1991, *Astrophys. J.*, **370**, 455.

Sandage, A. and Tammann, G. , 1981, *The Revised Shapely-Ames Catalog*, Carnegie Institute of Washington. (RSA)

Saslaw, W.C. and Hamilton, A.J.S. , 1984, *Astrophys. J.*, **276**, 13.

Saunders, W., Frenk, C.S.F., Rowan-Robinson, M., Efstathiou, G., Lawrence, A., Kaiser, N., Ellis, R.S., Vrawford, J., Xiaoyang, X. and Parry, I., 1990, *Nature*, **349**, 32. (QDOT)

Shane, C.D. and Wirtanen, C.A. , 1967, *Publ. Lick Obs.*, **22**, part 1.

Sheth.R.K., Mo, H.J. and Saslaw, W.C. , 1994, preprint.

Slipher, V.M., 1915, *Popular Astr.*, **23**, 21.

Strauus, M.A., Davis, M., Yahil, A. and Huchra, J.P. , 1990, *Astrophys. J.*, **361**, 49.

Strauss, M.A., Huchra, J.P., Davis, M. , Yahil, A., Fisher, K. and Tonry, J., 1992, *Astrophys. J. Suppl.*, **83**, 29. (IRAS)

Totsuji, H. and Kihara, T., 1969 , *Pub. Astr. Soc. Japan*, **21**, 221.

Vogely, M.S., Park, C., Geller, M.J. and Huchra, J.P. , 1992, *Astrophys. J.*, **391**, L5.

Wirtz, C., 1922, *Astr. Nachr.*, **216**, 451.

Wright, E.L., Mather, J.C., Fixsen, D.J., Kogut, A., Shafer, R.A., Bennett, C.L., Boggess, N.W., Cheng, E.S., Silverberg, R.F., Smoot, G.F. and Weiss, R., 1994, *Astrophys. J.*, **420**, 450.

Zel'dovich, Ya.B., Illarionov, A.F. and Sunyaev, R.A., 1872, *Sov. Physics: JETP*, **28**, 1287.

Zel'dovich, Ya.B., and Sunyaev, R.A., 1969, *Astrophys. & Sp. Sci.*, **4**, 301.

Zwicky, F., Wild, P., Herzog, E., Karpowicz, M. and Kowal, C.T., 1961-68, *Catalog of Galaxies and Clusters of Galaxies*, California Institute of Technology, Pasadena. (In 6 volumes).